DETERMINING WATER REQUIREMENTS AND SCHEDULING IRRIGATION OF APPLE TREES USING SOIL-BASED, PLANT-BASED AND WEATHER-BASED METHODS

By

YASIN OSROOSH

A dissertation submitted in partial fulfillment of
the requirements for the degree of

DOCTOR OF PHILOSOPHY

WASHINGTON STATE UNIVERSITY
Department of Biological Systems Engineering

AUGUST 2014

To the Faculty of Washington State University:

The members of the committee appointed to examine the dissertation of YASIN OSROOSH find it satisfactory and recommend that it be accepted.

R. Troy Peters, Ph.D., PE, Chair

Colin S. Campbell, Ph.D.

Qin Zhang, Ph.D.

ACKNOWLEDGMENT

I would like to express my deep appreciation to those who generously helped and supported me throughout my research: My supervisor, Dr. Troy Peters for taking the time to pass on valuable knowledge, and my committee members, Dr. Colin Campbell and Dr. Qin Zhang for their constant supervision of my research and valuable suggestions.

I would like to thank those whose help made the completion of my research possible: Professor and Department Chair, Dr. Claudio O. Stöckle. Professor of Agrometeorology and AgWeatherNet director, Dr. Gerrit Hoogenboom. Research Associate, AgWeatherNet, Dr. Mohammad Bannayan. Assistant Research Professor, AgWeatherNet, Dr. Melba Salazar. Research Associate, AgWeatherNet, Dr. Jakarat Anothai. Distinguished Professor in Viticulture, Markus Keller. Assistant Professor at Kansas State University, Dr. Ajay Sharda. I would also like to thank Clint Graf, Sean E. Hill, Robert Dickson, as well as Alan Kawakami and Lynn Mills, Amanda Yager, Frances Bardessono, Linda Root and Patrick Scharf.

I cannot thank my friends enough for their support: Aghil Yari, Dr. Peter Larbi, Jenifer Trap, Dr. Prossie Nakawuka, Mark DeKleine, Mojtaba Chavoshi, Golnaz Badr, Dr. Hassan Mojtahedi, Dr. Yun Zhang, Bikram Adhikari, Suraj Amatya, Dr. Long He, Jianfeng Zhou, Aleana Gongal, Dr. Shaochun Ma and others.

I would also like to acknowledge the assistance and support of the Center for Precision and Automated Agricultural Systems (CPAAS) at Washington State University. This work was funded by the US Department of Agriculture Specialty Crop Research Initiative (USDA SCRI) grant.

Finally, thanks to God for allowing me to successfully take another step in my life, and thanks to my parents for keeping me inspired.

Yasin Osroosh

DETERMINING WATER REQUIREMENTS AND SCHEDULING IRRIGATION OF APPLE TREES USING SOIL-BASED, PLANT-BASED AND WEATHER-BASED METHODS

Abstract

By Yasin Osroosh, Ph.D.
Department of Biological Systems Engineering
Washington State University
AUGUST 2014

Chair: R. Troy Peters

The goal of this work was to estimate water requirements, and to develop precision methods for automating the irrigation of apples. Two models based on the energy balance of a single leaf and infrared thermometry (IRT) were developed to calculate potential (T_p) and actual (T) transpiration from the whole tree. T_p and T were compared with ET_r and ET_c, respectively. The models were evaluated using the canopy temperature (T_c) and air temperature (T_a) data collected in a well-watered orchard and weather data from a nearby weather station during the 2007, 2008 and 2013 growing seasons. In addition, the microclimate of the orchard was investigated using a suite of sensors. Moreover, a wireless data collection network and scheduling algorithms were developed to create a site-specific irrigation control system. The precision methods were compared based on the total irrigation water requirements and water use in 2013. The T_p model was able to reflect the high degree of coupling between the apple trees and the humidity of the surrounding air during cold and humid periods. Both T and T_p were better correlated with ET_c on warm and dry days than during cold and humid periods. Similar results in all of the three growing seasons indicated that ΔT ($T_c - T_a$) could be linearly related to T. The results showed that the transpiration of the trees was intense late

in the morning and afternoon. A high correlation and small difference between daily mean canopy and trunk surface temperatures suggested the potential to use trunk temperature as an alternative for traditional IR measurements. Because of the high discrepancies between the T_a measurements in the orchard and the weather station, it was concluded that T_a should be measured in the vicinity of the IRTs. Within-canopy wind velocities were about 0.1 times the surface wind speeds. In general, the daily means of the measurements in the orchard and weather station were highly correlated while they were not well related at solar noon. The total irrigation water applied by the conventional irrigation (CNTRL) was significantly higher than all of other methods.

TABLE OF CONTENTS

Page

LIST OF ABBREVIATIONS

ET_a	Actual evapotranspiration
ET_r	Reference (alfalfa) evapotranspiration
SWP	Stem water potential
RH	Relative Humidity
TTT	Time Temperature Threshold
NP	Neutron probe
ET	Evapotranspiration
CWSI	Crop water stress index
NWSBL	Non-water stressed base line
WSBL	Water stressed base line
IRT	Infrared thermometer
MAD	Maximum allowable depletion
PWP	Permanent wilting point
FC	Field capacity
P-M	Penman-Monteith
DOY	Day of year
T	Transpiration
P	Precipitation
I	Irrigation
T_c	Canopy temperature
T_a	Air temperature
u	Wind speed
NTBL	Non-transpiring baseline
TDR	Time domain reflectometer
FDR	Frequency domain relectometer

Ψ_{stem}	Stem water potential
CWSI-TT	CWSI with time threshold
g_T	Canopy conductance
SEE	Standard error of estimation
RMSE	Root mean squared error
MAE	Mean absolute error
CV	Coefficient of variation
RE	Relative error
R-Sqr	R^2; R squared; coefficient of determination
COE	Nash and Suttcliffe coefficient of efficiency
STD	Standard deviation

LIST OF TABLES

LIST OF FIGURES

DEDICATION

I dedicate this dissertation to my wonderful mum, and dad…

CHAPTER ONE

GENERAL INTRODUCTION

Background

Irrigation is an integral part of the management package for most of crops. It reduces the danger of drought stress and allows for production in arid areas (Migliaccio et al., 2010). To specify when to irrigate a crop and how much water to apply, irrigation scheduling is needed. The performed irrigation method determines how the required amount of water is applied to the field. However, traditional methods of irrigation scheduling usually lead to over-irrigation resulting in reduced yields, higher energy and water costs and leaching nutrients. To schedule irrigation properly, crop water status, change in yield in response to water stress and irrigation method limitations must be known (Heermann, 1996). The employment of appropriate irrigation scheduling methods can lead to increased profit and water savings for farmers, reduced environmental impacts and sustainable agriculture (Smith et al., 1996). To date, research has offered a large number of agricultural water scheduling tools including procedures to compute crop water needs and to simulate the soil water balance (Pereira, 1999).

Development of technologies that apply the precise amount of water demanded by crops is necessary (Casadesus et al., 2012). Due to advances in irrigation science, new technologies have emerged in the context of agriculture (Wiedenfeld, 2004; Kallestad et al., 2006; Farahani et al., 2007). Weather-based and soil-based irrigation scheduling are examples of such technologies which by considering soil or weather information provide irrigation water to the crop based on actual water requirements (Vellidis et al., 2008; McCready et al., 2009; Migliaccio et al., 2010). A “Precision Irrigation” method, usually referred to as irrigation scheduling in the literature, determines the appropriate timing of irrigations (e.g. “when to irrigate” and/or “how much to irrigate”). Precision irrigation is a concept in the context of irrigation management which controls plant water stress at critical growth stages by applying the necessary amount of water to the crop (O’Shaughnessy and Evett, 2010). In precision irrigation soil and crop sensors are usually used to monitor soil and plant water status and schedule irrigation.

Irrigation scheduling methods are generally categorized into soil-based, and weather-based methods which are carried out by monitoring soil water status, sensing crop stress, and calculating soil water budget and reference ET using weather data, respectively (Al-Kaisi et al., 1997; Orta et al., 2003; Jones, 2004; Ko and Piccinni, 2009). For soil water balance models, soil water in the root zone is the base to decide when to irrigate. Leaf water potential or canopy temperature is monitored as trigger point of irrigation for the methods based on crop status (Stegman et al., 1976; Turner, 1988; Jackson et al., 1977; Wanjura et al., 1995).

A considerable number of scheduling methods have been developed for automatic irrigation. These methods have been widely used by irrigation researchers; however no user-friendly irrigation scheduling model that can be readily used by farmers for single and multiple field cases has been developed (Georgea et al., 2000). In a number of irrigation algorithms a combination of these methods have been used. Best et al. (1986) developed a program called WIF which used soil moisture signal to quantify the present soil moisture content. To predict the earliest irrigation replenishing the root zone to a desired level, it combined soil signal with an estimate of plant water use in the future. Buchleiter et al. (1988) developed an irrigation scheduling program called SCHED based on daily water balance calculations of the present soil moisture depletion and a future estimate of crop ET. To foresee the earliest and latest dates to irrigate a particular field, these two were combined. The SCHED and WIF programs have been successfully used by irrigation consultants (Dockter, 1996; Salazar et al., 1996). Hess (1996) described a real-time software package of irrigation scheduling. The package included almost all of the available algorithms including reference ET, actual ET, soil water balance and a model of irrigation forecast. Their evaluation of these models has shown the performance to be dependent on the accuracy of the input data measured in the field.

The most common irrigation scheduling methods of apples include the conventional method relying on grower's experience and soil moisture monitoring using neuron probe (NP) or time domain reflectometer (TDR). ET estimations combined with a water budget model are also used to schedule irrigation. There are a wide range of plant-based methods for detecting water stress in apple trees and determine when to irrigate apples (Lakso, 2003): 1) visual inspection, 2) midday stem water potential (very good indicator of water status, but too technical for most farmers), 3) canopy temperature monitoring (false signals due to responses of apple stomata to factors like crop load) and 4) trunk and fruit monitoring. Considering the large number of methods available it is very difficult to determine which methods are suited for scheduling irrigation of apple trees, how thermal data can be used for scheduling irrigation of apple trees. It would be interesting to know if inexpensive soil sensors can be used to schedule irrigation of the trees.

Soil-based methods

In these methods, a “soil moisture” or “soil water potential” senor specifies when to irrigate and when to stop irrigating. A wide range of measuring instruments is used for this purpose such as dielectric sensors (TDR, FDR, etc), tensiometers, gypsum blocks, granular matrix sensors, etc. They range from very inexpensive gypsum blocks to fairly expensive TDR sensors. Soil sensors have been used to automate irrigation in a number of plants including bell peppers, tomatos, and onions (Thompson et al., 2007; Enciso et al., 2009; Zotarelli et al., 2009). Vellidis et al. (2008) developed and evaluated a prototype real-time, smart sensor array for scheduling irrigation of cotton which measured soil moisture and temperature as standard inputs. The system was able to successfully monitor soil water status, soil temperature, and air temperature within the canopy during the entire growing season. There are disadvantages associated with use of soil sensors. Plant water stress responds to other factors such as atmospheric conditions, root-zone salinity, availability of nutrients etc. In addition, sampling in heterogeneous soils is difficult and it is difficult to know where the roots are located, thus the spot at which soil moisture is measured might not be a good representative of the entire field. In case of cheap gypsum blocks, they only provide information on when to irrigate but not on how much to irrigate (Fereres et al. 2012).

Weather-based methods

These methods are based on a soil water balance and daily estimations of reference ET from daily weather data and an ET model. Frequently used ET models are the Penman-Monteith (Allen et. al, 1998) and Hargreaves (Hargreaves and Samani, 1985). A complete set of weather parameters from a nearby weather station are required to calculate ET from the Penman-Monteith model while a simple air temperature sensor can provide required information to predict plant water need from the simplified model of Hargreaves. Using a feed-forward ET-based scheduling method can lead to over or under irrigation if the estimates of crop water use are incorrect, the soil water content at the beginning of the season is unknown, or the application efficiency of irrigation system is lower than expected. Casadesus et al. (2012) proposed a method for automated irrigation scheduling by combining a compensating mechanism based on soil or plant sensors readings (feed-back control) and an estimation of water demand by water balance method (feed-forward control). Their system was configurable by the user to support different irrigation strategies. The results suggested that the use of the water balance model allowed for a quick response to weather changes by predicting its effects, while at the same time the feedback mechanism could adapt the amount of water to the requirements of individual orchards by compensating for the bias of the model.

Currently, the P-M equation corrected by a crop-specific coefficient (K_c) is used as the model of transpiration for tree canopies like apples. The P-M model commonly referred to as reference ET (ET_r) is primarily developed for estimating transpiration from dense grass or alfalfa canopies while apple tree leaves are highly coupled to the atmosphere. As a results of this coupling, the water consumption of apple trees is controlled by stomatal regulations, net radiation and vapor pressure deficit (Jarvis, 1985) compared to the transpiration of grass/alfalfa being mainly driven by net radiation (Lakso, 2003). Dragoni et al. (2005) concluded a short dense crop cannot be a proper model for apple trees transpiration leading to overestimation of ET during humid and cold periods. They suggested the P-M model has to be modified to suit different conditions of tall discontinuous apple trees including stomatal and boundary layer conductances, as well as bulk air effect on transpiration.

Plant-based methods

Canopy temperature increases due to stomatal closure which most of the times is associated with water stress. Canopy temperature has shown to be an indicator of plant water stress and been used as an irrigation signal in many crops. Canopy temperature can be easily measured using infrared thermometers (IRTs). Various thermal-based irrigation techniques have been developed including crop water stress index (CWSI; Jackson et al., 1981, 1988), CWSI with a time threshold (CWSI-TT; O'Shaughnessy et al., 2012), stomatal conductance (SC; Blanquicet et al., 2009), time temperature threshold (TTT; Wanjura et al., 1992, 1995; patented) which is only tested on general crops, and IRT-ET_c which calculates actual ET using IR data and is developed for general crops (Ben-Asher et al., 1989).

The use of infrared temperature of plant canopies along with a number of supplemental environmental measurements to standardize canopy temperature is an alternative approach to soil- or weather-based methods in irrigation scheduling of general crops (Cohen et al., 2005). The computation of the CWSI requires two empirically or theoretically determined baselines: the non-water-stressed baseline (NWSBL) or lower boundary (potential) canopy and temperature difference (ΔT_l) representing a fully irrigated crop ideally transpiring at maximum stomatal conductance and the non-transpiring baseline (NTBL). A CWSI value of zero corresponds with a well-watered condition. A CWSI based on empirical baselines was first introduced by Idso et al. (1981) and a theoretical CWSI was first defined by Jackson et al. (1981). The base for derivation of the theoretical baselines has been the P-M ET model (Alves and Pereira, 2000) and the empirical CWSI based on a linear relationship between ΔT and air vapor pressure deficit (Idso et al., 1981). Empirical NWSBLs are climate dependent, site-specific and might change from year to year (Idso et al., 1990; Alves and Pereira, 2000). Thus, a theoretical approach not requiring costly, time-consuming field experiments will be more desirable. Thermal methods in form of empirical CWSI have been studied on pistachios, peaches, olives and grapevines (Testi et al. 2008; Paltineanu et. al. 2013; Berni et al., 2009; Agam et al., 2013; Akkuzu et al., 2013; Wang and Gartung, 2010). Berni et al. (2009) mapped CWSI in Olive orchards using thermal data obtained by remote sensing techniques. To date, no peer-reviewed research has been reported on scheduling the irrigation of apple orchards using a thermal approach.

As discussed before, the grass/alfalfa-based ET is not a suitable model for apple trees transpiration. Estimation of potential transpiration of apple trees requires only NWSBLs which must be developed specifically for apple tree conditions. However, the non-homogeneity of apple tree canopies and highly variable thermal distribution of their surface pose a big challenge in the modeling and required measurements. It might be possible to improve measurements of canopy temperature by trying different installation positions and angles of infrared sensors (IRTs) and averaging readings from a number of sensors to achieve an optimum accuracy.

In practice, the CWSI has shown not to be a reliable signal for irrigation scheduling because instantaneous measurements taken at solar noon or mean CWSI values are affected by impermanent atmospheric conditions such as wind guests or passing clouds (O'Shaughnessy et al., 2012). In a recent research, O'Shaughnessy et al. (2012) tried to overcome some of these issues by assessing the CWSI over daylight hours. In order to improve the performance of the theoretical CWSI as a trigger for automatic irrigation scheduling of grain sorghum, they incorporated a time threshold into the index and named it CWSI-TT (Appendix D: Fig. A.18). The results of their study indicated that this method can be useful for automatically scheduling full or deficit irrigations for grain sorghum in a semi-arid region. However, they expressed a shortcoming of the CWSI-TT as false positive water stress signals leading to over irrigations in the early season because the canopy is under development and thermal sensors partially see the ground.

There is a long history of complaints in the literature on the inefficiencies of the CWSI. People have ignored the fact that the CWSI alone cannot be useful in irrigation scheduling unless used as the core of a well-developed irrigation algorithm. Less attention has been paid to the enhancement of the irrigation algorithms where most of the challenges imposed by the CWSI can be overcome by integrating it into a robust control algorithm. Such an algorithm avoids under or over irrigations by accounting for boundary conditions where the index fails to reflect plant water status. Adding a soil feedback cannot be helpful because it is difficult to determine where to install the soil moisture sensors.

The efforts have been mostly concentrated on improving CWSI calculations by refining the empirical or theoretical methods of estimating the baselines (Blanquicet et al., 2009) while the algorithms available are as simple as comparison of the midday CWSI with a predetermined threshold trying not to exceed it during the season (Jackson et al., 1988). This threshold is crop and site specific and can be determined for a well-watered crop grown on a lysimeter (O'Shaughnessy et al., 2012). Current irrigation scheduling algorithms work with a static threshold (i.e. constant throughout the season) while in reality it is a function of weather and plant conditions. In general, little information is available on the CWSI at which irrigation is needed. In addition, the CWSI value for a crop under no stress is assumed zero and for a severely stressed crop close to one (Fereres et al., 2012). While this assumption might be true in case of homogeneous canopies of major row crops, it might not be applicable to heterogeneous tree canopies. The interference of thermal radiation from the ground with the readings of canopy temperature readings, as well as the rough nature of the tree canopies lead to smaller canopy and air temperature differences and consequently values of greater than zero even for well-watered canopies (Fereres et al., 2012). In case of apple trees, the canopy temperature increases as low crop loads are reached because stomatal conductance is a function of load and reduced as the load decreases (Lakso, 2003). This means non-water stressed baselines are dependent on load and the CWSI might not reach zero in case of well-watered apple trees in an alternate bearing year (little fruit) or postharvest period (no fruit). Therefore, the traditional use of a CWSI reference value as a stress threshold has to be revised.

The TTT method, also called "BIOTIC", is an automatic thermal-based method requiring canopy temperature as feedback. This method is developed by Wanjura et al. (1992, 1995) and requires a "time threshold" and a "temperature threshold". The temperature threshold is the optimal leaf temperature for enzyme activity determined in lab and the time threshold is accumulated time above the temperature threshold for non-stressed crop in specific climate calculated using experiment or simulated data. O'Shaughnessy and Evett (2010) conducted some field experiments using a time temperature threshold (TTT) algorithm in short season cotton. The results indicated that the TTT algorithm was a promising automatic method for irrigation scheduling in arid regions.

Plant-based methods of irrigation scheduling can be more advantageous in detecting plant water stress compared to soil-based methods of replacing water deficit. The tedious nature of soil water measurements using a neutron probe, the difficulty to determine tree root distribution and requirement of numerous field measurements make it inevitable to use plant water status indictors for irrigation scheduling (Naor et al., 1995). However, unlike the soil-based or water budget approaches, plant-based methods of irrigation scheduling lack any direct information on the quantity of water to be applied (Fereres et al. 2012). Thus, plant-based method should be used in combination with soil-based or weather-based methods to determine the required depth of irrigation water.

Stomatal conductance of a leaf can be measured directly using a leaf porometer and scaled up to canopy stomatal conductance. It can also be estimated using an empirical or theoretical model (Blanquicet et al., 2009). As a recent approach, Blanquicet and Bugbee (2007) suggested that real-time stomatal conductance be used as irrigation signal. They proposed to give up the CWSI and replace it with a theoretical method of measuring canopy stomatal conductance. Blanquicet et al. (2009) carried out automated measurement of canopy stomatal conductance for alfalfa and turf grass. They used the energy balance model of plant canopy, canopy temperature and other measurements to calculate the stomatal conductance. They concluded it is possible to use canopy stomatal conductance in irrigation scheduling.

Canopy conductance has been an important part of several modeling efforts for estimating transpiration of tree canopies (Pereira et al., 2006; Green et al., 2003b). It has been directly measured in the field (Green et al., 2003a), alternatively estimated by empirical models (Jarvis, 1976: Thorpe et al., 1980) or as in the original approach of the P-M model assumed constant (Pereira et al., 2006). Apparently, stomatal conductance of apple trees cannot be taken constant because of its relationship with relative humidity (Dragoni et al., 2005) as a result of high coupling between the trees and surrounding bulk air (Jarvis, 1985). The available empirical equations usually demand site specific data on stomatal conductance and microclimate to determine required calibration coefficients. However, measurement of stomatal conductance itself most often is not a feasible option as a large number of field readings are usually required to well represent the tree canopies. If stomata close in response to water deficit, the tree transpiration decreases and canopy temperature increases (Blanquicet et al., 2009). By the use of an energy budget equation, the canopy temperature, along with measurements of meteorological factors affecting conductance, can be therefore replaced with a direct measurement of stomatal conductance required for estimating transpiration of apple trees.

Therefore, as an alternative approach to the direct measurement, canopy conductance can be dealt with indirectly through the measurements of canopy temperature by infrared thermometry.

Accurate knowledge of ET is an important key to maintain well-irrigated crops (Tanny, 2013). Apple trees fall into the category of tall, discontinuous horticultural crops with well-coupled leaves to the surrounding air and atmosphere (Jarvis, 1985). The transpiration of apple trees is controlled by stomatal conductance, net radiation and vapor pressure deficit (Lakso, 2003) all of which can be connected through a simple energy budget equation. Thus, by determining the sensible heat flux from leaf surface and net radiation, apple leaf transpiration can be estimated. The components of the energy budget equation require microclimatic parameters as their inputs while, in many cases, the most feasible data are acquirable from a weather station in the vicinity of the field. Although apple leaves are well-exposed to the air, formation of microclimate around large tree canopies can cause diurnal variations of meteorological variables such as wind speed, relative humidity and air temperature to be notably different than those of obtained from a nearby weather station. The study of the trees microclimate to find relationships between the measurements taken within and outside the field can probably allow for enhancing the estimations of apple trees water use.

An important input to the energy balance equation is canopy temperature. Different modeling approaches have been developed based on the energy budget and thermal temperature of vegetative surfaces to estimate the ET of row crops (Ben-Asher et al., 1989; Taghvaeian et al., 2012). However, direct or indirect application of this method has been challenging in non-homogeneous canopies of tree crops. Tokei and Dunkel (2005) reported a case study on the possible use of canopy temperature in the determination of apple tree transpiration by a theoretical approach. Canopy temperature gives an average temperature value over the top of the surface. In case of a large tree canopy, the leaves range from completely shaded (usually at the lower canopy) to completely sunlit at the top. IR temperature readings have to comply with the assumptions made in the energy budget model of a representative leaf. Mounting position and orientation of the IRT are also of concern. Appropriate mounting position and orientation of the IRT can guarantee the sensor only sees the canopy surface. Any inclusion of soil or sky in the view of the senor can lead to considerable errors in the measurements (Blanquicet et. al, 2009).

Goals and objectives

The overall goal was to develop models to estimate water requirements of apple trees, to identify, refine and develop precision methods for automating irrigation of apple orchards, and to determine which type of irrigation control signal will yield the best results in terms of water use, and applied irrigation water. The specific objectives of this study were to:

1) Develop a theoretical model for estimating potential transpiration of apple trees:

   The goal was to develop an analytical model for estimating potential transpiration of whole apple tree (T) from the energy balance of a single leaf. The effort included a) development of a theoretical NWSBL model, b) a method of estimating net radiation from climatic parameters, and c) a simple model of canopy conductance not relying on field measurements of stomatal conductance. Predicted canopy temperatures and potential transpiration rates in both situations were compared with measured ΔT values and ET calculated using the P-M approach, respectively.

2) Develop a theoretical model for estimation of apple trees actual transpiration based infrared thermometry:

   The goal was to develop an analytical model for estimating real-time transpiration of whole apple tree from the energy balance of a single leaf and thermal measurements. Estimated transpiration rates were compared with those of calculated using the P-M model and adjusted crop coefficient values for the region.

3) Conduct microclimatic measurements and infrared thermometry in apple orchard:

   The objective was to investigate the microclimate formed by apple tree canopies to account for any significant difference between measured variables in the field and a nearby weather station. In addition, surface temperatures of the ground and tree trunk were measured and compared with canopy temperatures. Various position and orientations of infrared temperature sensors were also examined.

4) Develop a wireless central control system and automatic algorithms for precision irrigation of apple trees:

The effort included development of an electronic hardware using infrared temperature sensors, soil moisture sensors and air temperature sensors, monitoring and data logging software (graphical user interface), precision irrigation algorithms including a CWSI-based algorithm, and field experiments.

The off-shoot (secondary) research goal was to simplify growers' lives, decrease water and labor costs, decrease losses of water and nutrients to deep percolation, increase fruit yields and quality.

References

Agam, N., Cohen, Y., Berni, J.A.J., Alchanatis, V., Kool, D., Dag, A., Yermiyahu, U., Ben-Gal, A., 2013. An insight to the performance of crop water stress index for olive trees, Agricultural Water Management, 118: 79–86.

Akkuzu, E., Kaya, Ü., Çamoglu, G., Mengü, G.P., Aşık, Ş., 2013. Determination of crop water stress index (CWSI) and irrigation timing on olive trees using a handheld infrared thermometer. Journal of Irrigation and Drainage Engineering-ASCE, 139: 728–737.

Al-Kaisi, M.M., Berrada, A., Stack, M., 1997. Evaluation of irrigation scheduling program and spring wheat yield response in southwestern Colorado. Agricultural Water Management 34, 137–148.

Alves, I., Pereira, L.S., 2000. Non-water-stressed baselines for irrigation scheduling with infrared thermometers: A new approach. Irrig Sci, 19: 101–106.

Ben-Asher, J., Phene, C.J., 1992. User's guide for estimating crop evapotranspiration (ET_c) using the infrared thermometry (IRT) method. California Agricultural Technology Institute–CATI, Ben Gurion Univ. of the Negev, Israel. Available online at: http://cwi.csufresno.edu/wateright/920701.asp

Best, K.R., James, L.G., Ley, T.W., 1986. An interactive computer model for forecasting irrigations: A project completion report submitted to state of Washington Water Research Center and US Department of the Interior.

Berni, J.A.J., Zarco-Tejada, P.J., Sepulcre-Cantó, G., Fereres, E., Villalobos, F., 2009. Mapping canopy conductance and CWSI in olive orchards using high resolution thermal remote sensing imagery. Remote Sensing of Environment, 113: 2380–2388.

Blanquicet, Jr., J.M., Norman, J.M., Bugbee, B., 2009. Automated measurement of canopy stomatal conductance based on infrared temperature. Agricultural and Forest Meteorology 149, 1931–1945.

Blanquicet, M., Bugbee, B., 2007. Beyond the crop water stress index: Applying biophysical principles to the measurement of canopy stomatal conductance. 99th Annual Meeting of the American Society of Agronomy. November 4-8, 2007, New Orleans, LA.

Burke, J.J., 1993. Thermal kinetic windows of plant enzymes. In Biotechnology for Aridland Plants, Proc. International Symp. IC2 Institute. Mabry, T.J., Nguyen, H.T., Dixon, R.A., Bonness, M.S. (eds.) The University of Texas, Austin, pp. 73–82.

Burke, J.J., Oliver, M.J., 1993. Optimal thermal environments for plant metabolic processes (Cucumis sativus L.): Light-harvesting chlorophyll a/b pigment-protein complex of photosystem II and seedling establishment in cucumber. Plant Phys. 102(1):295–302.

Buchleiter, G.W., Duke, H.R., Heermann, D.F., 1988. User's guide for USDA-ARS irrigation scheduling program SCHED. USDA-Agricultural Research Service Agricultural Engineering Research Center, Colorado State University, Fort Collins, CO.

Casadesus, J., Mata, M., Marsal, J., Girona, J., 2012. A general algorithm for automated scheduling of drip irrigation in tree crops. Computers and Electronics in Agriculture 83, 11–20.

Campbell, G.S., Norman, J.M., 1998. An Introduction to Environmental Biophysics. Springer-Verlag, New York, NY, USA, 286 pp.

Cohen, Y., V. Alchanatis, M. Meron, Y. Saranga, and J. Tsipris. 2005. Estimation of leaf water potential by thermal imagery and spatial analysis. J. Exp. Bot. 56(417):1843–1852.

Dockter, D.T., 1996. AgriMet—The Pacific Northwest Cooperative Agricultural Weather Station Network. In: Camp, C.R., Sadler, E.J., Yoder, R.E. (Eds.), Evapotranspiration and Irrigation Scheduling. Proceedings of the International Conference. ASAE, San Antonio, pp. 75–80.

Dragoni, D., Lakso, A., Piccioni, R., 2005. Transpiration of apple trees in a humid climate using heat pulse sap flow gauges calibrated with whole-canopy gas exchange chambers. Agric. For. Meteorol., 130: 85–94.

Enciso, J., Wiedenfeld, B., Jifon, J., Nelson, S., 2009. Onion yield and quality response to two irrigation scheduling strategies. Scientia Horticulturae 120, 301–305.

Evett, S.R. 2002. Water and energy balances at soil-plant-atmosphere interfaces. In the Soil Physics Companion, 128-188. A.A. Warrick, (Ed), Boca Raton, Fla: CRC Press.

Farahani, H.J., Howell, T.A., Shuttleworth, W.J., Bausch, W.C., 2007. Evapotranspiration: progress in measurement and modeling in agriculture. Trans. ASABE 50, 1627–1638.

Fereres, E., Goldhamer, D., Sadras, V.O., 2012. In Crop yield response to water of fruit trees and vines: guidelines. Steduto, P., Hsiao, T.C., Fereres, E. and Raes, D. (eds.). Ch. 4, pp 246–295.

Georgea, B.A., Shendeb, S.A., Raghuwanshi, N.S., 2000. Development and testing of an irrigation scheduling model. Agricultural Water Management 46, 121–136.

Green, S., Clothier, B., Jardine, B., 2003a. Theory and practical application of heat-pulse to measure sap flow. Agron. J. 95: 1371–1379.

Green, S., McNaughton, K., Wunsche, J., Clothier, B., 2003b. Modeling light interception and transpiration of apple tree canopies. Agron J., 95: 1380–1387.

Hargreaves, G.H., Samani, Z.A., 1985. Reference crop evapotranspiration from temperature. Appl. Eng. Agric. 1(2), 96–99.

Heermann, D.F., 1996. Irrigation scheduling. In: Pereira, L.S., Feddes, R.A., Gilley, J.R., Lesaffre, B. (Eds.), Sustainability of Irrigated Agriculture. Kluwer Academic Publishers, Dordrecht, 233–249.

Hess, T., 1996. A microcomputer scheduling program for supplementary irrigation. Computers and Electronics in Agriculture 15, 233–243.

Idso, S.B., Jackson, R.D., Pinter, P.J., Reginato, R.J., Hatfield, J.L., 1981. Normalizing the stress-degree-day parameter for environmental variability. Agric. Meteorol., 24: 45–55.

Jackson, R.D., Kustas, W.P.E., Choudhury, B.J., 1988. A reexamination of the crop water stress index. Irrigation Science 9, 309–317.

Jackson, R.D., Reginato, R.J., Idso, S.B., 1977. Wheat canopy temperatures: a practical tool for evaluating water requirements. Water Resources Res. 13, 651–656.

Jackson, R.D., Idso, S.B., R.J.E., Reginato, Pinter, P.J., 1981. Canopy temperature as a crop water stress indicator. Water Resources Res. 17, 1133–1138.

Jackson, R.D., Kustas, W.P.E., Choudhury, B.J., 1988. A reexamination of the crop water stress index. Irrigation Science 9, 309–317.

Jarvis, P.G., 1985. Coupling of transpiration to the atmosphere in horticultural crops: the omega factor. Acta Horticulturae 171, 187–205.

Jones, H., 2004. Irrigation scheduling: advantages and pitfalls of plant-based methods. J. Exp. Bot. 55, 2427–2436.

Kallestad, J.C., Sammis, T.W., Mexal, J.G., White, J., 2006. Monitoring and management of pecan orchard irrigation: a case study. HortTechnology 16, 667–673.

Kisekka, I., Migliaccio, K.W., Dukes, M.D., Schaffer, B., Crane, J.H., 2010. Real-time evapotranspiration-based irrigation scheduling and physiological response in a carambola (Averhoha carambola) orchard. Applied Engineering in Agriculture 26, 373–380.

Ko, J., Piccinni, G., 2009. Corn yield responses under crop evapotranspiration-based irrigation management. Agricultural Water Management 96, 799–808.

Lakso, A.N., 2003. In Apples: Botany, production and uses, Water Relations of Apples, eds Ferree D.C., Warrington I.J., CABI Publishing, Wallingford, UK, pp 167–195.

Mitcham, E., Elkins, R., 2007. Pear Production and Handling Manual. 215 pp.

McCutchan, H., Shackel, K.A., 1992. Stem-water potential as a sensitive indicator of water stress in prune trees (Prunus domestica L. cv. French). J. Am. Soc. Hortic. Sci., 117, 607–611.

McCready, M.S., Dukes, M.D., Miller, G.L., 2009. Water conservation potential of smart irrigation controllers on St. Augustine grass. Agricultural Water Management 96, 1623–1632.

Migliaccio, K.W., Schaffer, B., Crane, J.H., Davies, F.S., 2010. Plant response to evapotranspiration and soil water sensor irrigation scheduling methods for papaya production in south Florida. Agricultural Water Management 97, 1452–1460.

Naor, A., Klein, I., Doron., I., 1995. Stem water potential and apple fruit size. J. Am. Soc. Hortic. Sci. 120: 577–582.

Orta, A.H., Erdem, Y., Erdem, T., 2003. Crop water stress index for watermelon. Scientia Horticulturae 98, 121–130.

O'Shaughnessy, S.A., Evett, S.R., 2010. Canopy temperature based system effectively schedules and controls center pivot irrigation of cotton. Agricultural Water Management 97, 1310–1316.

O'Shaughnessy, S.A., Evett, S.R., Colaizzi, P.D., Howell, T.A., 2012. A crop water stress index and time threshold for automatic irrigation scheduling of grain sorghum. Agricultural Water Management 107, 122–132.

Paltineanu, C., Septar, L., Moale, C., 2013. Crop Water Stress in Peach Orchards and Relationships with Soil Moisture Content in a Chernozem of Dobrogea. J. Irrig. Drain Eng., 139(1), 20–25.

Pereira, L.S., 1999. Higher performance through combined improvements in irrigation methods and scheduling: a discussion. Agricultural Water Management 40, 153–169.

Salazar, L.J., Thompson, K.R., Crane, K., 1996. Computerized irrigation scheduling in the San Luis Valley of Colorado. In: Camp, C.R., Sadler, E.J., Yoder, R.E. (Eds.), Evapotranspiration and Irrigation Scheduling. Proceedings of the International Conference. ASAE, San Antonio, pp. 75–80.

Sepulcre-Canto, G., Zarco-Tejada, P.J., Jimenez-Munoz, J.C., Sobrino, J.A., de Miguel, E., Villalobos, F.J., 2006. Detection of water stress in an olive orchard with thermal remote sensing imagery. Agric For Meteorol., 136: 31–44.

Smith, M., Pereira, L.S., Beregena, J., Itier, B., Goussard, J., Ragab, R., Tollefson, L. Van Hoffwegen, P. (Eds.), 1996. Irrigation Scheduling: From Theory to Practice. FAO Water Report 8, ICID and FAO, Rome.

Stegman, E.C., Schiele, L.H., Bauer, A., 1976. Plant water stress criteria for irrigation scheduling. Trans. ASAE 19, 850–855.

Taghvaeian, S., Chávez, J.L., Hansen, N.C., 2012. Infrared thermometry to estimate crop water stress index and water use of irrigated maize in northeastern Colorado. Remote Sens., 4: 3619–3637.

Tanny, J., 2013. Microclimate and evapotranspiration of crops covered by agricultural screens: A review. Biosystems Engineering, 114: 26–43.

Testi, L., Goldhamer, D.A., Iniesta, F. & Salinas, M. 2008. Crop Water Stress Index Is a Sensitive Water Stress Indicator in Pistachio Trees. Irrigation Science, 26: 395–405.

Thompson, R.B., Gallardo, M., Valdez, L.C., Fernandez, M.D., 2007. Using plant water status to define threshold values for irrigation management of vegetable crops using soil moisture sensors. Agricultural Water Management 88, 147–158.

Tokei, L., Dunkel, Z., 2005. Investigation of crop canopy temperature in apple orchard. Physics and Chemistry of the Earth, 30: 249–253.

Turner, N.C., 1988. Measurement of plant water status by the pressure chamber technique. Irrigation Science 9, 289–308.

Vellidis, G., Tucker, M., Perry, C., Kvien, C. Bednarz, C., 2008. A real-time wireless smart sensor array for scheduling irrigation. Computers and Electronics in Agriculture 61, 44–50.

Wang, D., Gartung, J., 2010. Infrared canopy temperature of early-ripening peach trees under postharvest deficit irrigation, Agricultural Water Management, 97(11): 1787–1794.

Wanjura, D.F., Upchurch, D.R., Mahan J.R., 1992. Automated irrigation based on threshold canopy temperature. Trans. ASAE 35(1):153–159

Wanjura, D.F., Upchurch, D.R., Mahan, J.R., 1995. Control irrigation scheduling using temperature-time thresholds. Trans. ASAE 38, 403–409.

Wiedenfeld, B., 2004. Scheduling water application on drip irrigated sugarcane. Agricultural Water Management 64, 169–181.

Zotarelli, L., Scholberg, J.M., Dukes, M.D., Mu˜noz-Carpena, R., 2009. Tomato yield, biomass accumulation, root distribution and irrigation water use efficiency on a sandy soil, as affected by nitrogen rate and irrigation scheduling. Agricultural Water Management 96, 23–34.

CHAPTER TWO

ESTIMATING POTENTIAL TRANSPIRATION OF APPLE TREES USING THEORETICAL NON-WATER-STRESSED BASELINES[1]

2.1 Abstract

To maximize irrigation efficiency, applied water has to be precisely adjusted to the crop water use. We developed a method based on the energy balance of a single apple leaf to calculate potential transpiration (T_p) from the whole apple tree. The T_p model was based on two main sub-models predicting canopy temperature (T_c) and total canopy conductance (g_T). The g_T model was derived by simplifying the energy budget relying on only climatic data and an empirical coefficient. These sub-models were evaluated using the canopy temperature data collected in a Fuji apple orchard during the 2007, 2008 and 2013 growing seasons. The applicability of the T_p model was examined by trying it on a) well-watered, young Fuji apple trees, and b) well-irrigated, older apple trees bearing little fruit (on alternative bearing). Predicted potential transpiration rates at both scenarios were compared with those predicted by the ASCE standardized Penman-Monteith for alfalfa (ET_r). Daily average weather data collected during the three growing seasons provided the inputs to the T_p model and its components. An analysis of the microclimatic data revealed that air temperature must be measured in the vicinity of the infrared thermometers (IRTs). With the exception of air temperature measured in the field, the rest of the meteorological data were obtained from a local weather station. The canopy temperatures of the fully-watered trees were predicted during mid-season with mean absolute errors (MAE) of about 0.41, 0.33 and 0.23 ^{o}C in 2007, 2008 and 2013, respectively. These MAEs were better than the individual IRT accuracy of ±0.6^{o}C. The coefficient of variation of the predictions (CV) averaged 2% over the experiment plots/years being better than that of the measurements (CV = 4.8%) with the exception of one plot in 2007 with little difference (3% vs. 2%). Estimated T_p was fairly correlated with ET_r on warm and dry days ($R^2 = 0.58$, $p<0.001$) with slope and interception of close to 1.0 and 0.0, respectively. The model was able to reflect the high degree of coupling between the apple trees and the humidity of the surrounding air during cold and humid periods as T_p resulted in significantly lower values. The overall results of the experiments with Fuji apple trees showed that when using the crop water stress index (CWSI), the non-water-stressed baselines (NWSBL) and potential transpiration of Fuji apple trees can be estimated using the proposed approach.

Keywords: Infrared thermometry, canopy conductance, reference evapotranspiration, potential transpiration

[1] Submitted to ASCE Journal of Irrigation and Drainage Engineering 6/28/2014

2.2 Introduction

Currently, the Penman–Monteith (P-M) equation (Allen et. al, 1998) corrected by a crop-specific coefficient (K_c) is used as the model of transpiration for tree canopies like apples. The P-M model commonly referred to as reference ET (ET_r) is primarily developed for estimating transpiration from dense grass or alfalfa canopies. Apple tree leaves, however, are highly coupled to the atmosphere. As a result of this coupling, the water consumption of apple trees is controlled by stomatal regulations, radiation and vapor pressure deficit (Jarvis, 1985) compared to the transpiration of grass/alfalfa which are mainly driven by net radiation (Lakso, 2003). Dragoni et al. (2005) concluded a short dense crop cannot be a proper model for apple trees' transpiration leading to an overestimation of ET during humid and cold periods. They suggested that the P-M model be modified to suit different conditions of tall discontinuous apple trees including stomatal and boundary layer conductances, as well as the bulk air effect on transpiration.

Canopy conductance has been an important part of several modeling efforts for estimating transpiration of tree canopies (Pereira et al., 2006; Green et al., 2003b). It has been directly measured in the field (Green et al., 2003a), alternatively estimated by empirical models (Jarvis, 1976: Thorpe et al., 1980), or as in the original approach of the P-M model, assumed constant (Pereira et al., 2006). Apparently, stomatal conductance of apple trees cannot be taken constant because of its relationship with relative humidity (Dragoni et al., 2005) as a result of high coupling between the trees and surrounding bulk air (Jarvis, 1985). The available empirical equations usually demand site specific data on stomatal conductance and microclimate to determine required calibration coefficients. However, measurement of stomatal conductance itself most often is not a feasible option as a large number of field readings are usually required to well represent the tree canopies. If stomata close in response to water deficit the tree transpiration decreases and canopy temperature increases (Blanquicet et al., 2009). Direct measurement of stomatal conductance can be replaced with estimations of a theoretical model based on an energy budget equation, canopy temperature, and measurements of meteorological factors affecting conductance. Therefore, as an alternative approach to the direct measurement, canopy conductance can be dealt with indirectly through the measurement of canopy temperature by infrared thermometry.

A common method of indirect estimation of ET proposed by Jackson et al. (1981) relies on the crop water stress index (CWSI) (Ben-Asher et al., 1989; Taghvaeian et al., 2012). The computation of the CWSI requires two empirically or theoretically determined baselines: the non-water-stressed baseline (NWSBL) or lower boundary (potential) canopy and temperature difference (ΔT_l) representing a fully irrigated crop ideally transpiring at maximum stomatal conductance, and the non-transpiring baseline (NTBL). A CWSI value of zero corresponds with a well-watered condition. A CWSI based on empirical baselines was first introduced by Idso et al. (1981) and a theoretical CWSI was first defined by Jackson et al. (1988). The base for derivation of the theoretical baselines has been the P-M ET model (Alves and Pereira, 2000) and the empirical CWSI based on a linear relationship between ΔT and air vapor pressure deficit (Idso et al., 1981). Empirical NWSBLs are climate dependent, site-specific and might change from year to year (Idso et al., 1990; Alves and Pereira, 2000). Thus, a theoretical approach not requiring costly, time-consuming field experiments will be more desirable.

As discussed before, the grass/alfalfa-based ET is not a suitable model for apple tree transpiration. The estimation of the potential transpiration of apple trees requires only NWSBLs which must be developed specifically for apple tree conditions. However, the non-homogeneity of apple tree canopies and highly variable thermal distribution of their surfaces pose a big challenge in the modeling and required measurements. It might be possible to improve the required canopy temperature as input by trying different installation positions and angles of infrared temperature sensors (IRTs) and averaging readings from a number of sensors to achieve an optimum accuracy.

The goal here was to develop an analytical model for estimating potential transpiration of whole apple tree (T) from the energy balance of a single leaf. The effort included a) development of a theoretical NWSBL model, b) a method of estimating net radiation from, and c) a simple model of canopy conductance not relying on field measurements of stomatal conductance. Predicted canopy temperatures and potential transpiration rates in both situations were compared with measured ΔT values and ET calculated using the P-M approach, respectively.

2.3 Material and methods

2.3.1 Modeling of transpiration

Apple tree leaves were categorized into four main types based on their exposure to long and short wave radiation sources at midday (Fig. 2.1): a) one side exposed to the sky and the other side exposed to the foliage (top leaves), b) both sides mostly exposed to the radiation from the foliage within the canopy (middle or inner leaves), c) one side exposed to radiation from other leaves within the canopy and the other side exposed to the ground surface (bottom leaves), and d) one side exposed to the sky and the other side exposed to the ground surface (side leaves). The top and middle leaves form the upper canopy, and the side and bottom leaves make the lower canopy.

Here we assumed that an infrared sensor (IRT) can only see the upper half of the canopy, thus only leaves falling into the “a” and “b” categories were of importance. The modeling was based on the assumption that the upper half can be treated as a single leaf bearing the characteristics of both upper canopy leaves. This is similar to that of the “big-leaf” approach in the literature (Monteith, 1965; Thorpe, 1978; Caspari et al., 1993) and assumes a representative leaf embraces all of the properties of the whole tree canopy (Jarvis, 1995). Neglecting metabolic heat production and heat storage, the energy balance equation for a single apple leaf is:

$$R_n = R_{abs} - L_{oe} = H + \lambda E \tag{2.1}$$

where R_n is the net radiation, R_{abs} is the absorbed radiation, L_{oe} is the outgoing emitted radiation, λE is the latent heat flux, and H is the sensible heat flux from the leaf (all terms are in Wm^{-2}). Absorbed radiation, for a leaf is the sum of absorbed shortwave and long wave radiations. R_n is the difference between this sum and the emitted long wave radiation from the leaf. The average absorbed radiation for a leaf representative of the upper canopy is then calculated as:

$$R_{abs} = a \times R_{top} + b \times R_{inn} \tag{2.2}$$

where a and b are the percentages of each leaves type and $a + b = 1$. Because apple tree canopies are very sparse, it is very probable that during day all types of the leaves will finally become sunlit for about half of daylight hours. This leads to an assumption of equal numbers of leaves in each category. Therefore, for daily mean values, R_{abs} of the representative leaf can be expressed as:

$$R_{abs} = (R_{top} + R_{inn})/2 \tag{2.3}$$

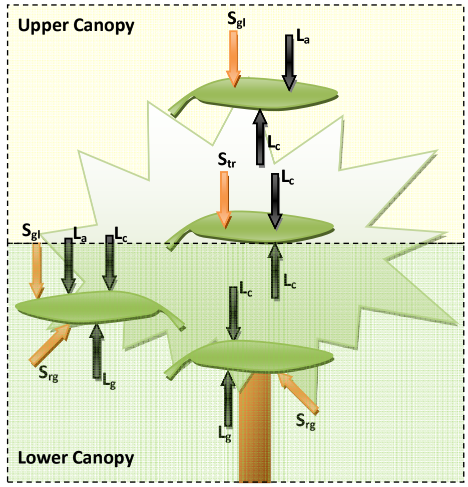

Figure 2.1 Various types of leaves exposure to the long and short wave radiation sources (i.e. incoming and outgoing) at solar noon.

The lower canopy will be still influential by radiating longwave energy at a temperature of T_c (canopy temperature at the border of the two halves) to the upper half. As a simplification, this temperature was assumed to be the same as the canopy temperature measured by the IRT. Total absorbed radiations (long and short waves) for the top and middle leaves were estimated using the following relationships, respectively:

$$R_{top} = \alpha_S\left(F_{gl}S_{gl}\right) + \alpha_L(F_aL_a + F_{c1}L_c) \tag{2.4}$$

$$R_{inn} = \alpha_S(F_{tr}S_{tr}) + \alpha_L(2F_{c1}L_c) \tag{2.5}$$

where S_{gl} is the global solar irradiance (sum of direct beam and diffused: $S_{gl} = S_b + S_d$), and S_{tr} is transmitted shortwave radiation through the apple leaf ($S_{tr} = \tau S_{gl}$). L_a and L_g are longwave flux densities from the atmosphere and the ground computed using the Stefan-Boltzmann equation. All radiations are in W m^{-2}. F_{gl}, F_{tr}, F_a and F_{c1} are view factors between the leaf surface and the various sources of radiation; namely global (0.5) and transmitted (0.5) solar radiations, and atmospheric (0.5) and apple tree canopy (0.5) thermal radiations, respectively. The view factors were calculated according to Campbell and Norman (1998). τ, α_S and α_L are green leaf transmittance, absorptivity in the short and absorptivity in the thermal waveband, respectively. The values of apple leaf and ground optical properties were adapted from the available literature (Green et al., 2003b). The outgoing longwave radiation from the leaf (L_{oe}) was calculated using the Stefan–Boltzmann relationship:

$$L_{oe} = F_e\varepsilon_s\sigma\mathbf{T}_c^4 \tag{2.6}$$

where ε_s is the thermal emissivity of apple leaf ($\varepsilon_s = \alpha$), σ is the Stefan–Boltzmann constant ($5.67 \times 10^{-8}\mathrm{Wm^{-2}K^{-4}}$) $\mathbf{T}_c$ is the canopy temperature (K), and F_e is the view factor between the entire surface of the leaf and the complete sphere of view ($F_e = 1.0$). The emissivity of the sky ($\varepsilon_a(c)$) required to compute the emitted radiation from the atmosphere ($\mathrm{L_a} = \varepsilon_a(c)\sigma\mathbf{T}_\mathrm{a}^4$, $\mathbf{T}_\mathrm{a}$ in Kelvins), was calculated by (Monteith and Unsworth, 1990):

$$\varepsilon_a(c) = (1 - 0.84c)\varepsilon_{ac} + 0.84c \tag{2.7}$$

where c is the fraction of the sky covered by cloud. c was calculated by comparing daylight average of real-time global radiation ($\overline{S_{gl}}$, W m^{-2}) with potential extraterrestrial incoming solar radiation of the same day (R_{ap}, W m^{-2}):

$$c = \left\{\begin{matrix} (1 - \dfrac{\overline{S_{gl}}}{Ra_{Pot}}) & if\ \overline{S_{gl}} \leq R_{ap} \\ 0 & otherwise \end{matrix}\right\} \tag{2.8}$$

R_{ap} was calculated according to the FAO-56 bulletin (Allen et al., 1998). The emissivity of clear sky (ε_{ac}) was estimated using the following empirical relationship (Brutsaert, 1984):

$$\varepsilon_{ac} = 1.72\left(\frac{e_a}{\mathbf{T}_a}\right)^{1/7} \tag{2.9}$$

where e_a is the vapor pressure (kPa) at air temperature ($\mathbf{T}_a$, K).

The term H of the energy balance equation is expressed as (Campbell and Norman, 1998):

$$H = g_H C_P (T_c - T_a) \tag{2.10}$$

where C_P is the heat capacity of air (29.17 J mol^{-1} C^{-1}), T_c is the temperature of the canopy (or the hypothetical leaf, ºC), T_a is air temperature (ºC), g_H is boundary layer conductance to heat (mol m^{-2} s^{-1}). The term H is comprised of two components of H_{ab} and H_{ad} which are sensible heat fluxes from the abaxial and adaxial sides of apple leaf, respectively. This refers to the fact that apple leaves are hypostomatous transpiring mostly through the abaxial side and that there is sensible heat exchange from both sides of the leaf.

The errors in conductance are normally distributed and its direct relationship to the water flux from the leaf makes it a better candidate for use in this case than resistance (Campbell and Norman,1998; Blanquicet et. al, 2009). Thus, conductance here was preferred over the traditional use of resistance in the calculations. The boundary layer conductance of air to heat for laminar forced convection (g_{Hf}) was calculated using the following empirical formula (Campbell and Norman, 1998):

$$g_{Hf} = (1.4)0.135\sqrt{\frac{u}{d}} \tag{2.11}$$

where, u is the wind speed and d is the characteristic dimension defined as 0.72 times the leaf width ($w_l = 5cm$: measured in the field). The factor of 1.4 in Eq. 2.13 is to account for turbulence (Campbell and Norman, 1998).

Assuming equal conductance for both the abaxial and adaxial sides of leaf, the combined air conductance to heat is $g_H = 2g_{Hf}$. Rearranging Eq. 2.1 to solve for E ($= T_p$):

$$T_p = 1555.2\frac{R_n - g_H C_P \Delta T_l}{\lambda} \tag{2.12}$$

where T_p is the canopy potential transpiration (mm day^{-1}), ΔT_l is the potential canopy and air temperature difference ($\Delta T_l = T_c - T_a$) and factor 1555.2 (0.018 kg mol^{-1} × 24 h × 3600 s h^{-1}) converts mol m^{-2} s^{-1} to mm day^{-1}. To estimate T_p, ΔT_l must be determined.

ΔT_l of well-watered apple tree canopies was predicted by the following procedure. First, the latent heat flux (λE) was calculated as (Campbell and Norman, 1998):

$$\lambda E = g_T \lambda \left(\frac{D_c}{P_a}\right) \tag{2.13}$$

where P_a is the atmospheric pressure (kPa), λ is the latent heat of vaporization (J mol^{-1}) and g_T is the total conductance to water vapor (mol m^{-2} s^{-1}) defined by a series combination of air boundary layer conductance (g_v, mol m^{-2} s^{-1}) and stomatal conductance to water vapor (g_s, mol m^{-2} s^{-1}) (Blanquicet et al., 2009). D_c is the canopy-to-air vapor pressure deficit expressed by $D_c = e_s(T_c) - e_a$, where $e_s(T_c)$ is the saturated vapor pressure (kPa) at canopy temperature (T_c, °C), e_a is the vapor pressure (kPa) at air temperature (T_a, °C). Substituting Eq. 2.12 and 2.13 in Eq. 2.1 and rearranging to solve for ΔT_l yields:

$$\Delta T_l = \frac{P_a R_n - g_T \lambda D_c}{g_H C_P P_a} \tag{2.14}$$

In this equation, R_n and D_c are functions of canopy temperature. D_c was linearized as $D_c = \Delta \times \Delta T_l + D_a$, where Δ is the slope of the relationship between saturation vapor pressure (e_s, kPa) and air temperature (T_a, °C). Air vapor pressure deficit (D_a) was calculated as $D_a = e_s - e_a$ (Idso et al., 1981), where e_s is the saturated vapor pressure at the air temperature (T_a) and e_a is the actual vapor pressure of air. To eliminate ΔT_l from the right side of Eq. 2.14, it was then rewritten as:

$$\Delta T_l = \frac{P_a Q - g_T \lambda D_a}{g_H C_P P_a - n P_a + \lambda g_T \Delta} \tag{2.15}$$

where $R_n = Q + n\Delta T$. Q and n are defined by the following equations, respectively:

$$Q = 0.25\left(\alpha_S S_{gl} + \alpha_S S_{t1} + 4(\alpha_L - 1)\mathrm{L_a}\right) \tag{2.16}$$

and:

$$n = (3\alpha_L - 4)\varepsilon_a(c)\sigma\mathbf{T}_a^3 \tag{2.17}$$

By arranging Eq. 2.15, we can linearize ΔT_l in the form $\Delta T_l = a - bD_a$:

$$\Delta T_l = \left(\frac{Q}{g_H C_P - n + \lambda g_T s}\right) - \left(\frac{g_T \lambda / P_a}{g_H C_P - n + \lambda g_T s}\right) D_a \tag{2.18}$$

where $s = \Delta / P_a$. To avoid more sources of uncertainty, g_s and g_v were not analyzed separately, but were dealt with indirectly in form of g_T. Rearranging Eq. 2.14 to solve for g_T yields:

$$g_T = \frac{P_a[R_n - g_H C_P \Delta T_m]}{\lambda D_c} \tag{2.19}$$

where ΔT_m the measured canopy and air temperature difference. D_c and R_n are also computed using measured canopy temperature. A g_T function independent of canopy temperature was also derived after analyzing the field data.

2.3.2 Application of T_p model

Experiment site

The field experiments were conducted in an apple orchard of Fuji in the Roza Farm, at the Washington State University, Irrigated Agriculture Research and Extension Center in Prosser, WA, at the coordinates of latitude 46.26°N, longitude 119.74°W, and 360 m above sea level. The site is located in a semi-arid zone with almost no summer rains and an average annual precipitation of 217 mm. The site's soil is a shallow Warden Silt Loam (Web Soil Survey) of more than 90 cm deep (field observation).

Plot design

The T_p model was initially applied to a field investigation (scenario 1) in 2007 and 2008 where young, well-developed apple trees were fully-irrigated. To investigate the consistency of the results across the orchard during each growing season, 2 rows/blocks of apple trees (42 trees per block) as two replications were marked for conducting the experiment. The rows/blocks were named "N" and "S". The trees were spaced 4 m (row spacing) by 2.5 m (tree spacing) apart in the orchard and irrigated by a micro-sprinkler irrigation system with water emitters of 27 L h^{-1} spaced at 2.5 m intervals. In 2007 and 2008, potential transpiration of apple trees (T_p) was estimated for the two fully irrigated blocks of N and S.

After evaluation and optimization of the T_p model, it was applied to another case in 2013 where the same apple trees that while healthy, for various reasons bore little or no fruit. During the 2013 growing period, the orchard was irrigated this time by two lines of drip tubing laterals per row with in-line 2.0 L h^{-1} drippers, spaced at 91.4 cm intervals along laterals. Six small plots consisting of 18 trees each (6 by 3) were marked for conducting the experiment. Two treatments of N and S were assigned to these plots (3 replications/plots per treatment).

The quantity of irrigation water applied to the trees was controlled to never allow the soil water depletion to exceed the 50% maximum allowed depletion (MAD) for apple trees (Allen et al., 1998). This was assured by taking weekly soil water content readings using a neutron probe (503DR Hydroprobe, Campbell Pacific Nuclear, Concord, CA) to a depth of 90 cm (or deeper) in all of the plots.

Meteorological measurements

Canopy temperature along with meteorological data including relative humidity, solar radiation, wind speed and air temperature were required inputs to the T_p model and its subordinates. The real-time meteorological data of the 2007, 2008 and 2013 growing seasons were obtained from two standard electronic weather stations close to the apple orchard (Roza and WSU HQ, Washington Agricultural Weather Network). During our experiments in the 2007 and 2008 growing seasons, no independent air temperature measurements were taken in the orchard, thus air temperatures recorded in the field using the embedded temperature sensor of a Campbell CR21X datalogger (Campbell Scientific, Logan, UT, USA) were used. The enclosure was shaded by the foliage at all of the times. In addition to these data, in 2013 air temperature was measured using three air temperature sensors (Model 109-L, Campbell Scientific, Logan, UT, USA) installed at a height of 2 m (in-line with the trees) at three locations distant from each other in the orchard. These air temperature sensors were wired to Campbell CR10X dataloggers (Campbell Scientific, Logan, UT, USA). Within-field air temperature was calculated by averaging the readings from the three sensors.

Measurement of canopy temperature

To monitor canopy temperature in 2007 and 2008, a total of 12 IRTs (Exergen model IRt/c.03^{TM}: Type T, Watertown, Mass.) in 6 pairs were mounted above the trees in the N and S plots. The IRTs were pointed downwards at approximately 45 degree angles at both the north and south sides of a tree. The sensors were calibrated using a blackbody calibrator (BB701, Omega Engineering, Inc., Stamford, CT) and wired to a Campbell CR21X datalogger (Campbell Scientific, Logan, UT, USA).

During the 2013 growing season, canopy temperature was measured in real-time using individual IRTs (Excergen model IRt/c.2: Type J, Watertown, Mass.) installed perpendicularly above a tree located at the center of the six plots (small plots of 18 trees). Sepulcre-Canto et al. (2006) and Testi et al. (2008) used similar mounting in Olive and Pistachio trees, respectively. Considering the field view of this model of IRT (35 degrees), this form of orientation and position will decrease the chance of the ground being seen by the IRT. The IRT sensors were wired to a network of Campbell CR10 and CR10X dataloggers (Campbell Scientific, Logan, UT, USA) sending out temperature readings to a central computer through 900 MHz wireless radios (RF401, Campbell Scientific, Logan, UT, USA).

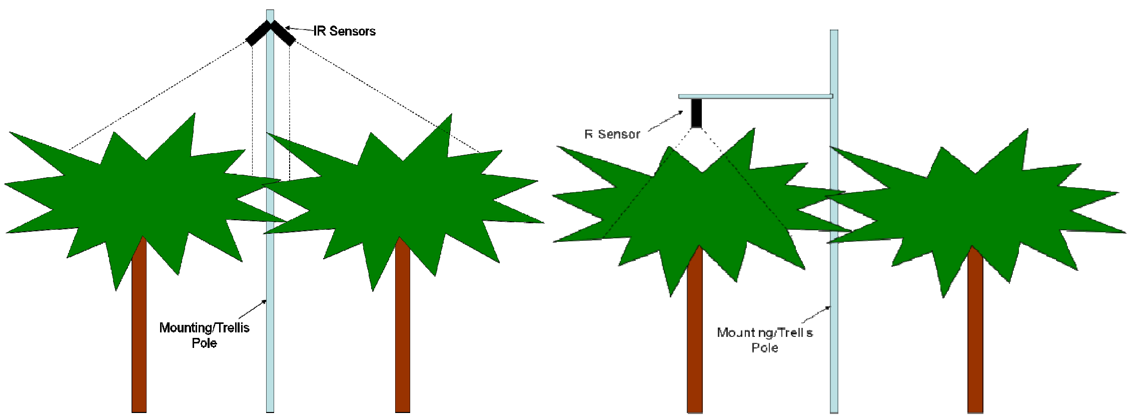

Figure 2.2 IRT sensors setup in the field. In 2007 and 2008, the sensors were pointed downwards at approximately 45 degree angles at both the north and south sides of a tree (left). In 2013, the sensors were installed at the top of trees closer to the crown to avoid any inclusion of the ground in the view.

Estimation of reference ET

To estimate alfalfa reference evapotranspiration (, mm day^{-1}) of the irrigated Fuji apple orchard, the ASCE standardized Penman-Monteith equation (ASCE-EWRI, 2005) was used. The required meteorological data including the daily received solar radiation in (MJ m^{-2} day^{-1}), relative humidity and wind speed were obtained from the nearby weather stations. Air temperature (maximum and minimum) was provided by the in-field sensors.

Model assessment

The performance of the T_p model was evaluated using the estimated values of transpiration from the model and those predicted by the P-M model. The two sub-models of ΔT_l and g_T were assessed using the measured ΔT (ΔT_m). The statistical means used were consisting of: a) the relative error (RE) between total predicted transpiration (T_p) and ET_r, b) the root mean square error ($RMSE$), c) the coefficient of variation of RMSE ($CV\ of\ RMSE$), d) the mean absolute error (MAE), and e) a linear regression between predicted and observed values or two sets of predictions. A satisfactory prediction was assumed when the linear regression yielded slopes close to unity, intercepts close to zero and high correlation (R^2). The accumulated predicted transpiration from the T_p model (D_T) and P-M model (D_{PM}) over a period of time were compared by calculating the relative error (RE):

$$\mathrm{RE} = \frac{D_{PM} - D_T}{D_{PM}} \tag{2.20}$$

The root mean square error (RMSE) was exploited as a measure of the variance between T_p and ET_r:

$$RMSE = \sqrt{\frac{\sum(ET_r - T_p)^2}{n}} \tag{2.21}$$

and as a measure of the variance between predicted canopy and air temperature difference (ΔT_l) and measured canopy and air temperature difference (ΔT_m):

$$RMSE = \sqrt{\frac{\sum(\Delta T_l - \Delta T_m)^2}{n}} \tag{2.22}$$

where n is the number of measurements. The coefficient of variation (CV) of RMSE was calculated by dividing RMSE by the mean of measurements ($\bar{x}$):

$$CV_{RMSE} = \frac{RMSE}{\bar{x}} \tag{2.23}$$

Considering the sensitivity of the RMSE to outliers, the mean absolute error (MAE) was also used as a safer measure of the variance between ΔT_l and ΔT_m:

$$MAE = \frac{\sum|\Delta T_l - \Delta T_m|}{n} \tag{2.24}$$

In addition to the aforementioned statistical means, the coefficient of variation of the standard deviation ($CV\ of\ STD$, the ratio of the standard deviation to the mean) was also employed to calculate canopy temperature variations among the apple trees. The RMSE was also used to measure the average difference between two time series.

2.4 Results and discussions

2.4.1 Microclimatic considerations

The T_p model (Eq. 2.12) and its components required microclimatic parameters including relative humidity, solar radiation, wind speed and air temperature as inputs. We compared air temperature measurements in the orchard in the growing seasons of 2007, 2008 and 2013 with that of obtained from the nearest weather station (i.e. Roza, Washington Agricultural Weather Network). During our experiments in 2007 and 2008, no independent air temperature measurements were taken in the orchard; therefore, the air temperature records by the internal sensor of the datalogger were used. Although this method of air temperature measurement was expected to be associated with errors, our analysis showed that these data were far better than that of obtained from a nearby weather station. A sensitivity analysis and preliminary results revealed that using air temperature data from the weather station could lead to substantial errors making the application of the T_p model impossible.

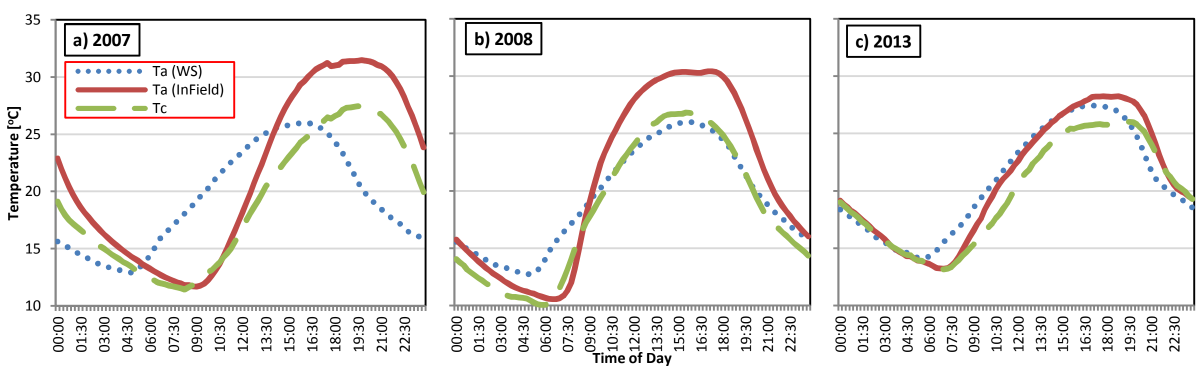

Figure 2.3 Comparison of diurnal changes of air temperature (T_a) obtained from the closest weather station (Roza, Washington Agricultural Weather Network) and those measured in the orchard during the growing seasons of 2007 (a), 2008 (b) and 2013 (c). All graphs (a–c) represent the average of T_a over 118 successive days (DOY=152–270) during mid and late season.

As it can be seen in Fig. 2.3, the two sets of data (i.e. that of obtained from the orchard and nearby weather station) exhibited completely different patterns of air temperature diurnal change in terms of maximum and minimum temperatures and time of their occurrences in the growing seasons of 2007 and 2008. Maximum and minimum of air temperatures measured in the orchard occurred with a few hours of delay after the corresponding air temperatures at the weather station. This resulted in up to 10 ^{o}C of difference between the two time series during some times of day and average difference (RMSE) of 2.8 ^{o}C in 2007 and 1.9 ^{o}C in 2008 for daily mean values.

Regardless of a relatively good method of air temperature measurement that was employed in 2013, similar problem was detected. However, the difference was less pronounced with a RMSE of only 0.44 ^{o}C for daily mean values. This was an expected phenomenon because large tree canopies of apple trees can form local microclimate. This causes diurnal variations of microclimatological variables such as air temperature to be notably different than those of meteorological parameters obtained from a nearby weather station. In 2013, however, the extent of difference in the diurnal changes of air temperature in the field and weather station were less compared to 2007 and 2008 which could be due to lesser degree of canopy growth and consequently lesser impact on the surrounding environment.

ΔT was calculated by averaging over the course of several days for three occasions including early, mid and late in the season with two different series of air temperature data (two scenarios): a) measured within the orchard (Fig. 2.4a2–c2) and b) obtained from the nearby weather station (Fig. 2.4a1–c1). In scenario “a”, maximum stomatal activity of apple trees (e.g. maximum ΔT) occurred late in the morning and late in the afternoon with a shift from early in the season to late in the season. Early in the 2008 and 2013 seasons, ΔT started declining in the morning and reached positive values ($\Delta T \geq 0$) at solar noon. Although similar declining patterns could be seen throughout the seasons, its occurrence at this degree might be partially attributed to the contribution of the ground surface thermal radiation to the canopy temperature. The completion of foliage growth towards the mid season minimized the ground being seen by the IRTs.

A similar pattern of apple trees activity to that of scenario “a” was previously reported by Tokei and Dunkel (2005). This can be explained by the fact that, in addition to R_n, the transpiration of apple trees is controlled by stomatal regulation which is reflected in a lowered or elevated canopy temperature. The observed behavior of the apple trees was different from row crops where the transpiration is mainly driven by net radiation (Lakso, 2003) and is reduced drastically in response to low solar radiation levels (Wanjura and Upchurch, 1997). This will make it very difficult if not impossible to estimate hourly potential transpiration of apple trees as stomatal conductance is controlled by additional factor(s) not included in the energy budget equation. Daily transpiration, however, relies on daily mean values of canopy temperature where only the overall activity is of importance.

Figure 2.4 Average diurnal changes of canopy and air temperature differences (ΔT) during early, mid, and late season in the 2007 (a1, a2), 2008 (b1, b2) and 2013 (c1, c2) growing seasons. Each curve represents the average of ΔT over a few successive days: DOY=152–160 as early, DOY=191–200 as mid and DOY=260–270 as late in the season. Average diurnal variations of ΔT are shown for two situations: air temperature measured in the orchard (a1–c1), and air temperature from the weather station (a2–c2).

In scenario "b" where ΔT was calculated using T_a obtained from the weather station, maximum stomatal activity of apple trees moved to early in the morning with a shift from early in the season to late in the season. This does not comply with the literature as it lacks the activity late in the afternoon reported by Tokei and Dunkel (2005). Our analysis showed daily mean ΔT computed using air temperature obtained from a weather station could not reflect trees stomatal activity being positive or small negative values throughout the season with an average of -0.5 ^{o}C (STD =1.2) in 2007 and -0.6 ^{o}C (STD =1.4) in 2008. We, therefore, only used air temperatures measured in the orchard and focused only on predictions of daily potential transpiration rather than over shorter time scales. All of the other required meteorological parameters were obtained from the weather station assuming that those measurements were reliable enough or of less degree of importance.

2.4.2 Modeling of transpiration Potential ΔT (ΔT_p)

During mid-season, the crop coefficient for converting alfalfa ET_r to apple trees transpiration is almost 1.0 with a peak of 1.06 (Karimi et al., 2013). This is a time when under normal conditions actual transpiration of well-watered apple trees is expected to be close to the alfalfa reference ET (maximum of 6% discrepancy). To avoid uncertainties of canopy temperature measurements especially during early-season (due to incomplete canopy growth), we picked the time period of mid-season (DOY = 155–243) for the purpose of comparisons.

Total conductance to water vapor (g_T) defined by Eq. 2.19 is simply a different arrangement of Eq. 2.18 before linearization and is itself a function of T_c, therefore cannot be directly used to estimate ΔT_l. Considering a high degree of coupling between apple leaves and the surrounding air, daily mean canopy-to-air vapor pressure deficit (D_c) was highly correlated (linearly) with daily bulk air vapor deficit (D_a) during the 2007, 2008 and 2013 growing seasons with R-squared values greater than 0.90 (p <0.001). The slope and intercept of D_c and D_a relationship curves were slightly different across the plots and from year to year. The fully irrigated seasons of 2007 and 2008 had the closest values, while the greatest field variability and difference with the rest of the experimental years was seen in 2013 when the apple trees were on alternate bearing. Considering the good consistency among the field results on the linear relationship between D_c and D_a, further steps were taken to simplify Eq. 2.19 to make it independent of canopy temperature.

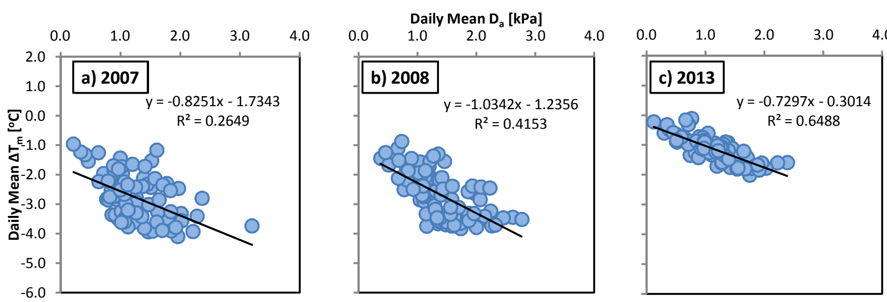

Figure 2.5 Relationship between daily canopy and air temperature difference (ΔT_m) and air vapor pressure deficit (D_a) for mid-season of 2007 (a), 2008 (b) and 2013 (c) (p<0.001).

There was very weak correlation between daily mean D_a and ΔT in the experimental years (Fig. 2.5). To relate D_c to ΔT, D_c was linearized instead as $D_c = \Delta \times \Delta T_l + D_a$. Considering a linear relationship between D_c and D_a, D_c was replaced with $mD_a + b_1$, where m and b_1 are the slope and intercept of D_c and D_a relationship curve, respectively. After some manipulations, Eq. 2.19 was rewritten as:

$$g_T = \frac{Q\Delta + (n - g_H C_P)(\acute{m}D_a + b_1)}{\lambda(mD_a + b_1)s} \tag{2.25}$$

where $\acute{m} = m - 1$. g_T was computed using Eq. 2.25 and coefficients of "m" and "b_1" obtained by a linear regression between D_a and D_c. It was then put in Eq. 2.15 and ΔT_l was estimated for the growing seasons of 2007, 2008 and 2013. The statistical results are presented in Table 2.1. The correlation was not satisfactory which could be due to different reasons including field variability, linearization error, temperature measurement error etc. We tried determining the empirical coefficients by fitting Eq. 2.25 to Eq. 2.19. The values obtained for coefficient "m" were very close to unity. We, therefore, omitted "m" ($m = 1$), added two new empirical coefficients of b_0 and b_2 and modified the model to the following form:

$$g_T = b_2 \left[\frac{Q\Delta + b_1(n - g_H C_P)}{\lambda(D_a + b_1)s} \right] + b_0 \tag{2.26}$$

Among the remaining coefficients, b_1 had a minimum effect on the results (an improvement of about 0.1°C if included). Therefore, with minimal compromising of the prediction's accuracy, Eq. 2.26 was further optimized to the following equation:

$$g_T = b_2 \left[\frac{P_a Q}{\lambda D_a} \right] + b_0 \tag{2.27}$$

This equation, without the calibration coefficients, is very similar to the inverse of the climatic resistance defined by Rana et al. (2005). Eq. 2.27 is only dependent on air vapor pressure deficit and Q which is a function of global radiation (S_{gl}) and air temperature. We used this relationship for the rest of total canopy conductance estimations required for determining NWSBLs.

Table 2.1 Comparison of predicted potential canopy and air temperature difference (ΔT_l) and observed ΔT (ΔT_m). The coefficients are obtained by linear regression between D_a and D_c (b_o = 0.0 and b_2 = 1.0).

Year	Plot	b_1	m	R^2	ΔT_m	CV of STD	ΔT_l	MAE (°C)	CV of RMSE
2007	S	0.07	0.69	0.39	-3.00	0.04	-1.91	1.12	0.07
	N	0.07	0.71	0.33	-2.80	0.02	-1.73	1.11	0.06
2008	S	0.01	0.64	0.56	-2.77	0.07	-3.15	0.52	0.03
	N	0.02	0.69	0.55	-2.69	0.03	-2.56	0.46	0.03
2013	S	0.06	0.92	0.14	-1.06	0.08	-0.23	0.89	0.05
	N	0.00	0.84	0.43	-1.18	0.05	-1.20	0.24	0.02

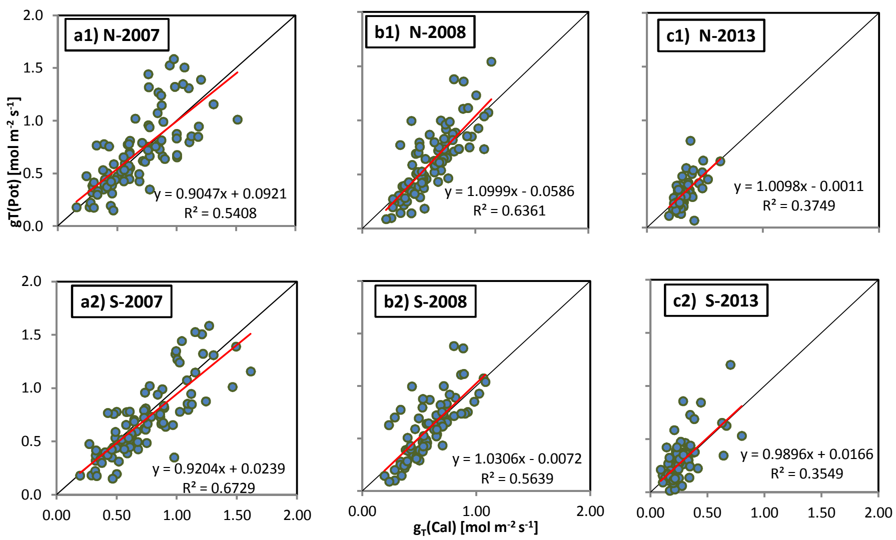

Figure 2.6 Comparison of average daily potential conductance (g_T(Pot), mol m^{-2} s^{-1}) estimated by Eq. 2.27, and that calculated by Eq. 2.19 (g_T(Cal), mol m^{-2} s^{-1}) ($p<0.001$).

By fitting the average daily potential conductance estimated by Eq. 2.27 to that calculated by Eq. 2.19 (linear regression), the values of b_2 for the 2007 and 2008 seasons were obtained as 11.5 and 9.5, respectively. For the same period, b_0 values were found to be -0.30 and -0.15, respectively. Due to the high non-uniformity of the canopies in 2013, the coefficients calculated for the N and S plots were quite different with $b_2 = 4.3$ and $b_0 = -0.05$ for the N plot, and $b_2 = 8.0$ and $b_0 = -0.4$ for the S plot. The results of linear regression between the simplified g_T model (Eq. 2.27) and the original model (Eq. 2.19) for the N and S plots are illustrated in Fig. 2.6 (a–c). The average of b_2 and b_o in 2007 and 2008 ($\overline{b_2} = 10.5$, $\overline{b_0} = -0.23$) were applied to both years to investigate the repeatability of the results. The linear regression yielded slopes of close unity and intercepts of close to zero in 2007, 2008 and 2013. However, the R^2 value in 2013 (R^2=0.38, $p<0.001$) was less desirable compared to 2007 (R^2=0.67, $p<0.001$) and 2008 (R^2=0.64, $p<0.001$).

The empirical coefficients of b_0 and b_2 were determined for each season separately by fitting ΔT_l to the measured values of ΔT (ΔT_m). The results are presented in Table 2.2. As it can be seen, the values of b_2 in 2007 and 2008, and for the N and S plots were almost the same, and b_0 was zero. In 2013, however, the coefficients were different from the rest of the years. In 2013, the field also showed a high degree of non-uniformity among the tree canopies of the N and S plots which is reflected in the statistical results of Table 2. The plots of $g_T(Pot)$, $g_T(N)$ and

$g_T(S)$ are illustrated in Fig. 2.7. The difference between $g_T(N)$ and $g_T(S)$ resulted from a difference in the measured canopy temperatures which is itself due to the non-uniformity of the apple tree canopies.

Table 2.2 Comparison of predicted potential canopy and air temperature difference (ΔT_l) and observed ΔT (ΔT_m). The coefficients were obtained by linear regression between ΔT_l and ΔT_m (b_1 = 0.0 and m = 1.0).

Year	Plot	b_0	b_2	R^2	ΔT_m	CV of STD	ΔT_l	MAE (°C)	CV of RMSE
2007	S	0.00	8.47	0.67	-3.00	0.04	-2.98	0.38	0.02
	N	0.00	7.63	0.53	-2.80	0.02	-2.77	0.43	0.03
2008	S	0.00	8.12	0.76	-2.77	0.07	-2.80	0.34	0.02
	N	0.00	8.14	0.76	-2.69	0.03	-2.71	0.32	0.02
2013	S	0.16	1.58	0.25	-1.06	0.08	-1.09	0.27	0.02
	N	0.22	1.06	0.74	-1.18	0.05	-1.16	0.18	0.01

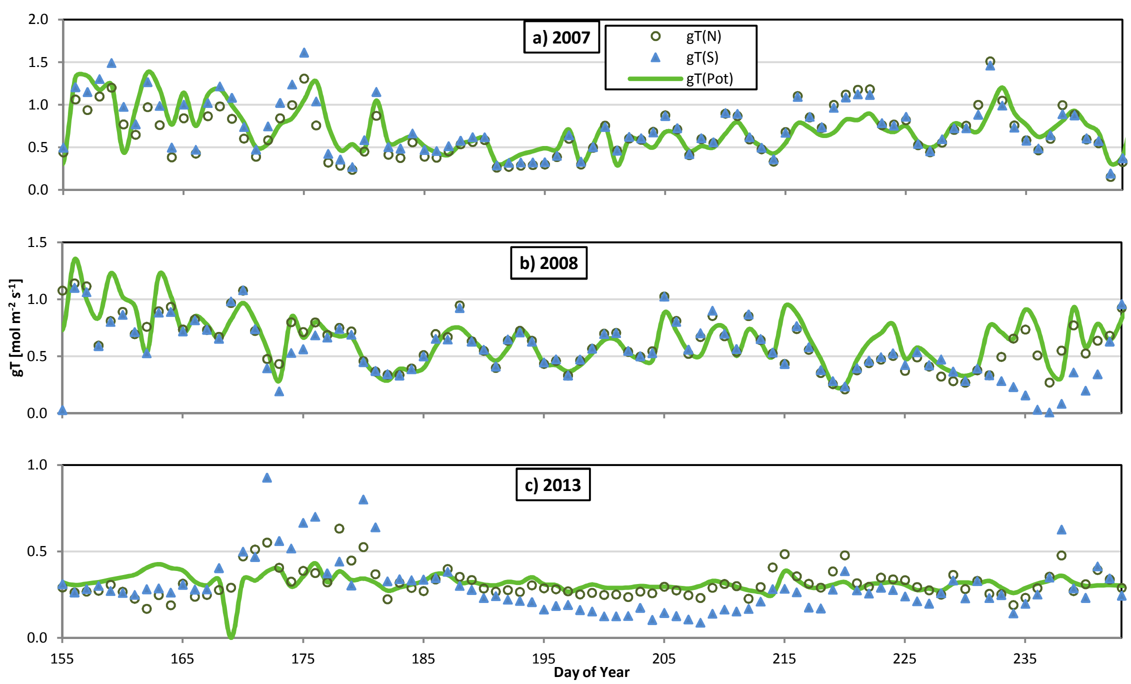

Figure 2.7 Plots of average daily potential conductance (g_T(Pot), mol m^{-2} s^{-1}) estimated by Eq. 2.27, and that of calculated by Eq. 2.19 (g_T(Cal), mol m^{-2} s^{-1}) for the N and S plots (in 2007 and 2008, b_o = 0.0 and b_2 = 8.0; in 2013, b_o = 0.22 and b_2 = 1.06).

The weak correlation between $g_T(Pot)$ and $g_T(Cal)$ in 2013 can be explained by the fact that the apples trees were on alternate bearing. This means that although variations of stomatal conductance were dependent on weather conditions, the average level of stomatal conductance was maintained low in response to the small fruits on them (Palmer et. al., 1997). In 2013, the trees played the main role in controlling the average canopy conductance rather than climatic factors, while in 2007 and 2008 stomatal regulations were more affected by radiation and vapor pressure deficit.

Measured and predicted canopy and air temperature differences (daily average) for the three years of field investigations are plotted in Fig 2.8. Linear regression between ΔT_l and ΔT_m using the data of mid-season in 2007 yielded a slope, intercept and R^2 of 0.92, -0.26 and 0.67 for the S plot (Fig. 2.9a), and 0.83, -0.49 and 0.53 for the N plot, respectively. For the same period in 2008, a linear regression between ΔT_l and ΔT_m resulted in a slope, intercept and R^2 of 1.19, 0.56 and 0.76 for the S plot, and 1.05, 0.15 and 0.76 for the N plot (Fig. 2.9b), respectively.

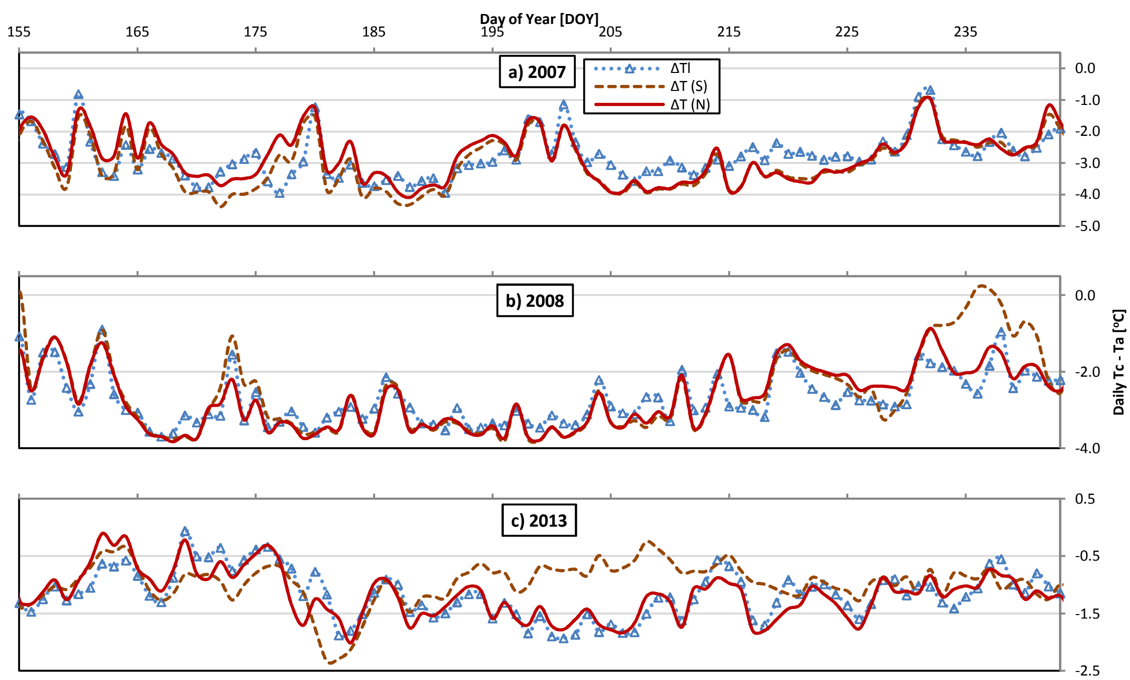

Figure 2.8 Plots of measured (ΔT_N and ΔT_S) and predicted (ΔT_l) canopy and air temperature difference (daily average) for the three years of field investigations (N and S plots, mid-season in 2007, 2008 and 2013).

In 2013, the results from the N and S plots were quite different with no correlation between ΔT_l and ΔT_m in the S plot with slope, intercept and R^2 of 0.56, -0.45 and 0.25, respectively, and a relatively high correlation between the predicted and measured ΔT in the N plot with slope, intercept and R^2 of 0.85, -0.19 and 0.74 (Fig. 2.9c), respectively. The ΔT predictions were all satisfactory in the experimental years with average MAEs of 0.41, 0.33

and 0.23 °C in 2007, 2008 and 2013, respectively. Moreover, as presented in Table 2.2, variation of predictions (CV of RMSE) in all of the experiment plots/years was better than that of measurements (CV of STD) with the exception of the N plot in 2007 with small difference (3% vs. 2%).

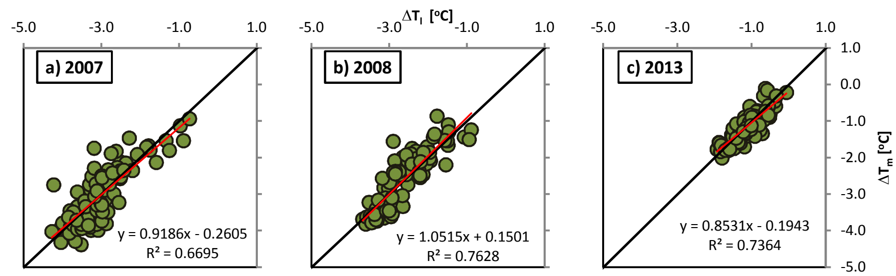

Figure 2.9 Correlation between measured and predicted canopy and air temperature difference (daily average of ΔT) for the three years of field investigations (mid-season in 2007, 2008 and 2013).

The variation of canopy temperature measurements among the plots and from year to year was about 4.8%. This small variation indicates that the number of IRT sensors used per plot and canopy surface viewed by the IRTs were good enough. In addition, this could be an indication that, as planned, all of the trees were well-irrigated (Testi et al., 2008). As the linear regression resulted in good correlations and ΔT was accurately predicted (Table 2.2), as well as similar results in the N and S plots, it was concluded that the performance of the ΔT_l model was satisfactory.

2.4.3 Potential transpiration (T_p)

In all of the three years, T_p showed a good correlation with ET_r, with T_p being overall more than P-M reference ET (Fig. 2.10a1–c1). Based on the results presented in Table in 2.2, the best match between the predicted and observed ΔT in the 2007 and 2008 growing seasons were achieved by only adjusting b_2. The rounded average of b_2 in these years (b_2=8.0) was used to estimate ΔT_l and potential transpiration rates of the apple trees in 2007, 2008 and 2013. Except for the air temperature which was measured in the orchard, all of the meteorological parameters required to compute T_p and ET_r were obtained from the weather station.

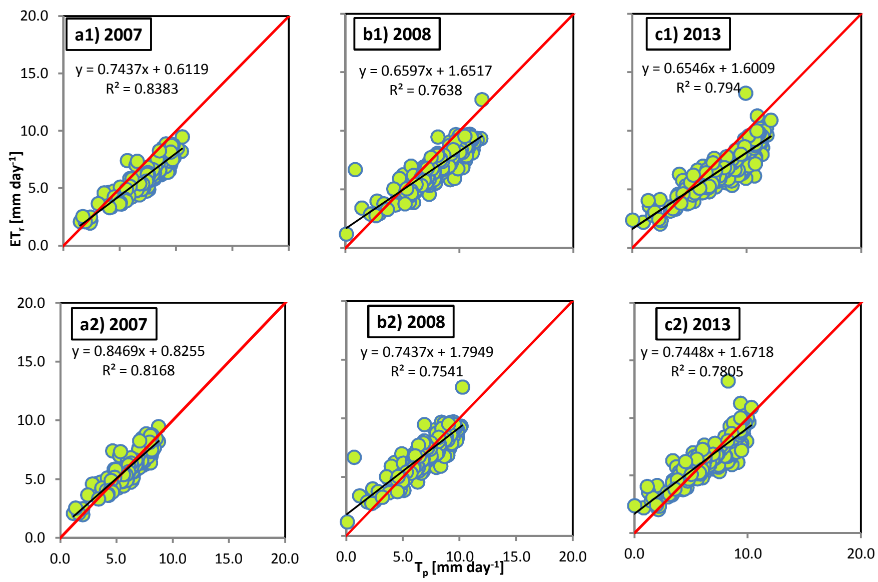

Figure 2.10 Correlation of daily potential transpiration (mm day^{-1}) estimated by the T_p model for two apple tree rows (N and S) with that of predicted by the P-M model (ET_r) for the 2007, 2008 and 2013 growing seasons (p<0.001).

Linear regression between daily T_p and ET_r (Fig. 2.10a1–c1) yielded good correlations with R^2 of 0.84, 0.76 and 0.89 ($p < 0.001$) for mid-season in 2007, 2008 and 2013, respectively. However, non-zero interception values and line slopes of about 0.7 pointed out at the fact that the T_p model overestimated transpiration compared to the P-M method. Due to this overestimation, total T_p was higher, yielding relative errors (RE) of -18%, -0.13% and -0.14% during mid-season in 2007, 2008 and 2013, respectively (Table 2.3).

Table 2.3 Comparison of predicted potential transpiration rates by the P-M model (ET_r) and the T_p model in the growing seasons of 2007, 2008 and 2013 (b_o = 0.0, b_1 = 0.0, b_2 = 8.0, and m = 1.0).

Year	R^2	RMSE (mm)	RE
2007	0.78	1.45	-0.18
2008	0.70	1.64	-0.13
2013	0.81	1.52	-0.14

For the purpose of comparing the T_p and ET_r behaviors, two boundary conditions of warm and dry ($D_a > 1.4kPa$, $S_{gl} = 330 \pm 30$), as well as cold and humid ($D_a < 0.4kPa$, $S_{gl} = 150 \pm 50$) were assumed. T_p was fitted to ET_r to minimize their difference (Fig. 2.10a2–c2). This resulted in b_2 values of 6.13, 6.51 and 6.50 (b_0=0) for the

2007, 2008 and 2013 seasons, respectively. As it can be seen, no significant change in the R^2 values occurred as T_p estimations were already fairly close to those of the ET_r estimations. Similar to the reference alfalfa/grass, during warm and dry days the transpiration of apple trees was expected to be mainly driven by net radiation (Dragoni et al., 2005). As it was anticipated, the estimated T_p was well correlated with ET_r (R^2 = 0.58, p<0.001) on warm and dry days with a slope of close to unity (≈0.99) and interception of close to zero (≈0.10) (Fig. 2.11a). However, because of a high coupling between the apple trees and the humidity of the surrounding air (Jarvis, 1985) T_p resulted in significantly lower values (Fig. 2.11b) during cold and humid periods showing a very week correlation with ET_r (R^2 = 0.42, p<0.001).

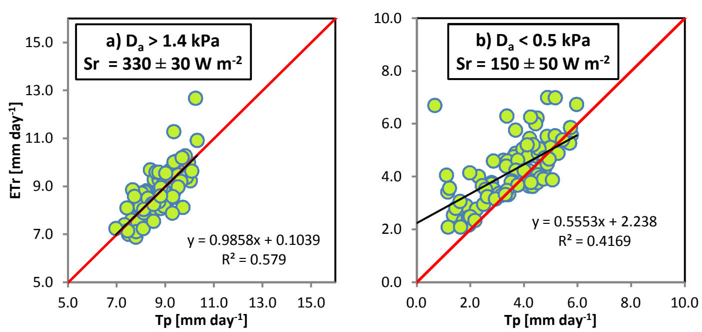

Figure 2.11 Correlation between T_p and ET_r during warm and dry periods (a; p<0.001), and during cold and humid days (b; p<0.001) for the 2007, 2008 and 2013 growing seasons (combined). In each category, days with similar average daily solar radiation were used.

Total crop water use predictions from the T_p model and P-M approach calculated for mid-season in 2007, 2008 and 2013 are depicted in Fig. 2.12. Although the accumulated T_p of the N and S plots were very close, their values were averaged to obtain one single value. Calculation of T_p using the coefficients presented in Table 2.3 (b_0 = 0.0 and b_2 = 8.0) resulted in a small difference of about 100 mm between the total T_p and ET_r during all of the experimental years (Fig. 2.12a). Accumulated T_p was also computed by assuming b_0 = 0.0 and b_2 ≈ 6.5 (Fig. 2.12b). The difference between the predicted values from the two models was very trivial.

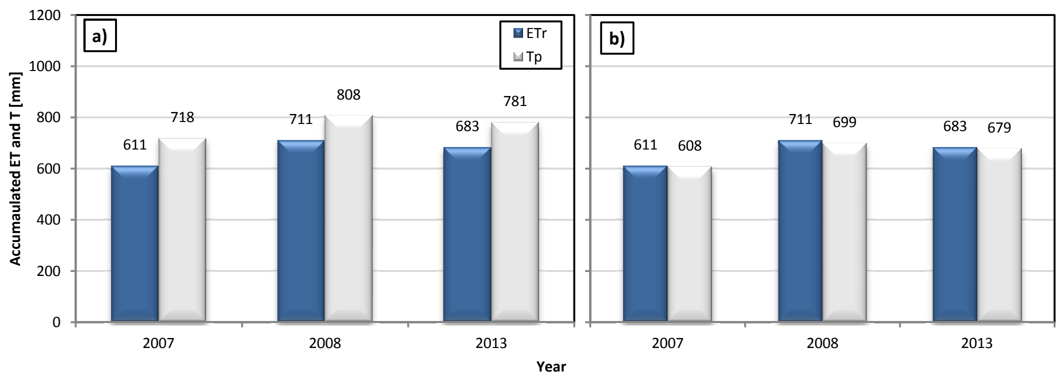

Figure 2.12 Accumulated water use predicted by the T_p and P-M ET_r models at mid-season in 2007, 2008 and 2013 (averages of the N and S plots). T_p was calculated using the coefficients presented in Table 2.3 (a) and using the values of $b_0 = 0.0$ and $b_2 \approx 6.5$ (b).

According to Dragoni et al. (2005), during warm and dry days the crop coefficients (K_c) are expected to be similar to the published K_c for arid climates like Washington State. Considering the dominance of dry and warm periods during mid-season in Eastern Washington and a difference of about 3% (average) between accumulated ET_r and ET_c, the total predicted transpirations seemed logical. In the studied area with an arid climate (high D_a), there does not seem to be any advantages in using T_p over the P-M model for the estimation of apple trees potential water use. However, in more humid climates (smaller D_a) ET_r seems to be minimally correlated with T_p. In more humid climates, using ET_r is expected to lead to significant overestimation of apple trees transpiration rates.

2.5 Conclusions

During the 2007 and 2008 growing seasons canopy temperatures of apple trees were measured using IRTs pointed downwards at approximately 45 degree angles at both the north and south sides of a tree and in 2013 using those of installed perpendicularly above a tree, respectively. A transpiration model along with these IR measurements, in-field air temperature sensors, and local meteorological data from a nearby weather station were used to estimate potential transpiration of apple trees. The T_p model presented here adequately described the transpiration of apple trees under real field conditions.

Since alfalfa/grass mainly respond to net radiation, in the P-M approach a constant value of 0.6 mol m^{-2} s^{-1} is assumed for the "big leaf" stomatal conductance (Allen et al., 1998). To account for the response of apple leaves stomas to the bulk air relative humidity, in the present approach, a simple model with theoretical basis dependent merely on radiation and vapor pressure deficit was developed. Under normal conditions (well-irrigated, young apple trees), this model only requires the determination of one empirical coefficient. In the studied orchard, this empirical coefficient showed to be fairly constant with slight variations from plot to plot and from year to year. In 2013, the average stomatal conductance was maintained low by the trees in response to low fruit loads which resulted in the empirical coefficients being different than the other years. This has to be accounted for in estimations of transpiration at post harvest times because a reduction in crop loads can decrease the stomatal conductance and consequently transpiration of apple trees (Auzmendi et al., 2011; Girona et al., 2011). To formulate this phenomenon, the relationship between the conductance and apple fruit loads needs to be established.

The canopy temperatures of the fully-watered trees were well predicted, with an average MAE of about 0.32^{o}C. These MAEs were better than the accuracy of an individual IRT indicated in the manual (±0.6^{o}C). Climatic parameters and canopy conductance (g_T) were the only required inputs to the ΔT_p model. Once used to calculate the CWSI, the present NWSBL model can be used for fully automating of apple orchards. Considering the response of apple trees to the bulk air relative humidity, the advantages of the NWSBL and T_p models will be more pronounced if used in more humid areas compared to Eastern Washington.

The components of the T_p model required microclimatic parameters as their input while, in many cases, the most feasible data are acquired from a weather station in the vicinity of the field. Our analysis revealed that, although apple leaves were well-exposed to the air, formation of microclimate around large tree canopies caused diurnal variations of a meteorological variable like air temperature to be notably different than those of obtained from a nearby weather station. All of the other required meteorological parameters were obtained from the weather station assuming those measurements were reliable, however, study of the microclimate to find relationships between the measurements taken within and outside the field can probably allow for enhancing the estimations of crop water use from the model.

Apple trees transpiration was modeled based on the energy budget of a single leaf. There were some sources of uncertainty in the modeling of light and thermal energy interceptions by apple trees. A tree canopy is comprised of an unknown number of shaded and sunlit leaves, and shoot growth constantly changes light interception patterns. Apple trees, which have discontinuous canopies, can have various forms of architecture and their leaves are of different shapes, sizes and orientations. Moreover, the T_p model was basically derived for light interception conditions at midday. This introduced some errors in estimations of transpiration when used for times other than solar noon in hourly or smaller time scales. Another approximation was introduced into the model by the temperature across the upper half of the canopy being assumed uniform and equal to the average temperature measured with the IRTs. Here we compared our approach against the P-M model. The performance of the T_p model and its components can be further investigated using lysimeter (Auzmendi et al., 2011) or sap flow measurements (Dragoni et al., 2005; Nicolasa et al., 2005).

Acknowledgments

This work was funded by the US Department of Agriculture Specialty Crop Research Initiative (USDA SCRI) grant. The authors would like to thank Clint Graf for his help in establishing the irrigation system, weed control, and pesticide applications. The authors thank Sean E. Hill and Robert Dickson for helping out in a number of computer related issues, as well as Evan Zumini for his assistance with dataloggers. The authors also acknowledge the great help of Dr. Mohammad Bannayan with the statistical analysis.

References

Allen, R.G., Pereira, L.S., Raes, D., Smith, M., 1998. Crop evapotranspiration: guidelines for computing crop water requirements. Irrigation and Drainage Paper No. 56. FAO, Rome, Italy, 300 pp.

Alves, I., Pereira, L.S., 2000. Non-water-stressed baselines for irrigation scheduling with infrared thermometers: A new approach. Irrig Sci, 19: 101–106.

ASCE-EWRI, 2005. The ASCE standardized reference evapotranspiration equation. Technical Committee Report to the Environmental and Water Resources Institute of the American Society of Civil Engineers from the Task Committee on Standardization of Reference Evapotranspiration. ASCE-EWRI, 1801 Alexander Bell Drive, Reston, VA 20191–4400, 173 pp.

Auzmendi, I., Mata, M., Lopez, G., Girona, J., Marsal, J., 2011. Intercepted radiation by apple canopy can be used as a basis for irrigation scheduling. Agricultural Water Management, 98: 886–892.

Ben-Asher, J., Phene, C.J., 1992. User's guide for estimating crop evapotranspiration (ET_c) using the infrared thermometry (IRT) method. California Agricultural Technology Institute–CATI, Ben Gurion Univ. of the Negev, Israel. Available online at: http://cwi.csufresno.edu/wateright/920701.asp

Blanquicet, Jr., J.M., Norman, J.M., Bugbee, B., 2009. Automated measurement of canopy stomatal conductance based on infrared temperature. Agricultural and Forest Meteorology 149, 1931–1945.

Brutsaert, W., 1984, Evaporation into the Atmosphere: Theory, History, and Applications. Boston: D: Reidel.

Campbell, G.S., Norman, J.M., 1998. An Introduction to Environmental Biophysics. Springer-Verlag, New York, NY, USA, 286 pp.

Caspari, H.W., Green, S.R., Edwards, W.R.N., 1993. Transpiration of well-watered and water-stressed Asian pear trees as determined by lysimetry, heat-pulse, and estimated by a Penman-Monteith model. Agricultural & Forest Meteorology, 67(1-2): 13–27.

Dragoni, D., Lakso, A., Piccioni, R., 2005. Transpiration of apple trees in a humid climate using heat pulse sap flow gauges calibrated with whole-canopy gas exchange chambers. Agric. For. Meteorol., 130: 85–94.

Girona, J., Del Campo, J., Mata, M., Lopez, G., Marsal, J., 2011. A comparative study of apple and pear tree water consumption measured with two weighing lysimeters. Irrig. Sci., 29: 55–63.

Green, S., Clothier, B., Jardine, B., 2003a. Theory and practical application of heat-pulse to measure sap flow. Agron. J. 95: 1371–1379.

Green, S., McNaughton, K., Wunsche, J., Clothier, B., 2003b. Modeling light interception and transpiration of apple tree canopies. Agron J., 95: 1380–1387.

Idso, S.B., Jackson, R.D., Pinter, P.J., Reginato, R.J., Hatfield, J.L., 1981. Normalizing the stress-degree-day parameter for environmental variability. Agric. Meteorol., 24: 45–55.

Idso, S.B., Pinter Jr., P.J., Reginato, R.J., 1990. Non-water-stressed baselines: the importance of site selection for air temperature and air vapour pressure deficit measurements. Agricultural and Forest Meteorology, 53(1/2): 73–80.

Jackson, R.D., Idso, S.B., Reginato, R.J., 1981. Canopy temperature as a crop water stress indicator. Water Resour. Res., 17: 1133–1138.

Jarvis, P.G., 1976. The interpretation of the variation in the leaf water potential and stomatal conductances found in canopies in the field. Philos. Trans. R. Soc. London, Ser. B 273: 293–310.

Jarvis, P.G., 1985. Coupling of transpiration to the atmosphere in horticultural crops: the omega factor. Acta Horticulturae, 171: 187–205.

Jarvis, P.G., 1995. Scaling Processes and Problems, Plant Cell and Environment, 18 (10), 1079–1089.

Karimi, T., Peters, T., Stockle, C.O., 2013. Revising Crop Coefficient for Washington State. ASABE Annual International Meeting, Kansas City, Missouri. Available online at: http://elibrary.asabe.org/azdez.asp?JID=5&AID=43715&CID=miss2013&T=2

Lakso, A.N., 2003. Water relations of apples. In: Ferree D.C., Warrington I.J. (Eds.), Apples: Botany, Production and Uses. CABI Publishing, pp. 167–194.

Monteith, J.L., 1965. Evaporation and environment: the state and movement of water in living organisms. Symp. Soc. Exp. Biol., 19: 205–234.

Monteith, J.L., Unsworth, M.H., 1990. Principles of Environmental Physics, 2nd Ed., Edward Arnold, New York, p. 53–54.

Nicolasa, E., Torrecillasa, A., Ortuno, M.F., Domingo, R., Alarco, J.J., 2005. Evaluation of transpiration in adult apricot trees from sap flow measurements. Agricultural Water Management, 72: 131–145.

Palmer, J.W., Giuliani, R., Adams, H.M., 1997. Effect of crop load on fruiting and leaf photosynthesis of 'Braeburn'/M.26 apple trees. Tree Physiology, 17: 741–746.

Pereira, A.R., Green, S.R., Villa Nova, N.A., 2007. Penman-Monteith reference evapotranspiration adapted to estimate irrigated tree transpiration. Agric. Water Manage., 83: 153–161.

Rana, G., Katerji, N., Lorenzi, F., 2005. Measurement and modeling of evapotranspiration of irrigated citrus orchard under Mediterranean conditions. Agric. For. Meteorol. 128: 199–209.

Sepulcre-Canto, G., Zarco-Tejada, P.J., Jimenez-Munoz, J.C., Sobrino, J.A., de Miguel, E., Villalobos, F.J., 2006. Detection of water stress in an olive orchard with thermal remote sensing imagery. Agric For Meteorol., 136: 31–44.

Testi, L., Goldhamer, D.A., Iniesta, F. & Salinas, M. 2008. Crop Water Stress Index Is a Sensitive Water Stress Indicator in Pistachio Trees. Irrigation Science, 26: 395–405.

Taghvaeian, S., Chávez, J.L., Hansen, N.C., 2012. Infrared thermometry to estimate crop water stress index and water use of irrigated maize in northeastern Colorado. Remote Sens., 4: 3619–3637.

Thorpe, M.R., 1978. Net radiation and transpiration of apple trees in rows. Agric. Meteorol., 19: 41–57.

Thorpe, M.R., Warrit, B., Landsberg, J.J., 1980. Responses of apple leaf stomata: a model for single leaves and a whole canopy. Plant Cell Environ. 3: 23–27.

Tokei, L., Dunkel, Z., 2005. Investigation of crop canopy temperature in apple orchard. Physics and Chemistry of the Earth, 30: 249–253.

Wanjura, D.F., Upchurch, D.R., 1997. Accounting for humidity in canopy-temperature-controlled irrigation scheduling. Agricultural Water Management, 34: 217–231.

CHAPTER THREE

ESTIMATING ACTUAL TRANSPIRATION OF APPLE TREES BASED ON INFRARED THERMOMETRY[2]

3.1 Abstract

To maximize irrigation efficiency, applied water has to be precisely adjusted to the crop water use. We developed a method based on the energy balance of a single apple leaf to calculate transpiration (T) from the whole tree. The model uses canopy and air temperatures measured in the orchard, and other meteorological data from a local weather station as inputs. Two scenarios were examined to support the application of this model: a) well-watered, young Fuji apple trees, and b) older apple trees bearing little fruit. Estimated transpiration rates at both scenarios were compared with those of predicted using the Penman-Monteith model corrected by regionally adjusted crop coefficients (ET_c). The model was evaluated using the temperature data collected in an apple orchard during the growing seasons of 2007, 2008 and 2013. During the mid- and late-seasons of 2007 and 2008, T were better related to ET_c on warm and dry days (R^2 = 0.57, slope = 1.16, Intercept = 0.4) than during cold and humid periods (R^2 = 0.48, slope = 0.69, Intercept = 2.3). Combining the results of the two seasons, the T-model estimations were well correlated with ET_c (R^2 = 0.77) with relationship slope and intercept of 1.0 and 1.08, respectively. In 2013, the mean actual water use as calculated by a soil water budget was significantly less than ET_c while there was no significant difference between the mean total T and the actual water use. In 2013, a linear regression analysis of the T and solar noon stem water potential (Ψ_{stem}) showed they were highly correlated (solar noon T: R^2 = 0.85; daily T: R^2 = 0.87). While our experiments presented varied results on a linear relationship between air vapor pressure deficit (D_a) and T from year to year, similar results in all of the three growing seasons indicated that the canopy and air temperature difference (ΔT_m) could be linearly related to T. According to the T-model, maximum transpiration of the apple trees occurred in the morning. As a basis for a fully automated system of irrigating apple orchards, the present model can provide real-time water use in any time scale.

Keywords: Infrared thermometry, stem water potential, crop coefficient, evapotranspiration

[2] Submitted to ASCE Journal of Irrigation and Drainage Engineering on 7/6/2014

3.2 Introduction

To maximize irrigation efficiency, applied water has to be precisely adjusted to the crop water use (Casadesús et al., 2011). To estimate the water use of apple trees (ET_c), the evapotranspiration (ET) calculated using the Penman–Monteith equation (Allen et. al, 1998) and corrected by a crop-specific coefficient (K_c) is often used (Lakso, 2003). Due to various approximations and assumptions in the determination of K_c, ET_c estimations can be inaccurate (Auzmendi et al., 2011). To eliminate the need for using a crop coefficient, some researchers have related the transpiration of apple trees to the field measurements of the daily or solar noon radiation interception (Auzmendi et al., 2011; Girona et al., 2011; Casadesús et al., 2011). However, these relationships are empirical and most of the times site-specific data are required (Pereira et al., 2006).

Apple trees fall into the category of tall, discontinuous horticultural crops with well-coupled leaves to the atmosphere (Jarvis, 1985). The transpiration of apple trees is controlled by stomatal conductance, net radiation and vapor pressure deficit (Lakso, 2003; Dragoni et al., 2005). In addition to responding to environmental factors like solar radiation and vapor pressure deficit (Jarvis, 1985; Lakso, 2003), the stomatal conductance of apple leaves changes in response to changes in crop loads (Palmer et. al., 1997). The latter is not directly accounted for in available empirical relationships (Jarvis, 1976: Thorpe et al., 1980), thus satisfactory estimations are dependent upon local adjustments and empirical coefficients.

If stomata close in response to a water deficit the tree transpiration decreases and canopy temperature increases (Blanquicet et al., 2009). As an alternative approach, stomatal conductance and therefore transpiration can be possibly estimated through the measurements of canopy temperature by infrared thermometry. Rather than being a relative indicator of water stress, the canopy temperature along with measurements of metrological factors affecting stomatal conductance can be possibly used to estimate transpiration of apple trees by the use of an energy budget equation. There is fairly good literature available on the applications of infrared thermometry in ET estimations of homogenous row crops. Jackson et al. (1981) proposed a method to calculate crop ET indirectly from the crop water stress index (CWSI) measurements. Following the same approach, Taghvaeian et al. (2012) used CWSI values to estimate maize transpiration. Ben-Asher et al., (1989) used infrared thermometry to estimate aerodynamic and canopy resistance required for the computation of transpiration from a Penman ET equation in tomatoes.

However, the non-homogeneity of the tree canopies poses a big challenge in the use of infrared thermometry, the modeling of the transpiration process, and in the required measurements. Considering the high cost of thermal cameras, complicated image processing requirement and inadequate resolution of satellite images (Testi et al. 2008), it is still beneficial to try different installation positions and angles of infrared sensors (IRTs) and averaging readings from a number of sensors to achieve an optimum accuracy. Thermal methods in the form of the empirical CWSI have been studied on some fruit trees including pistachios, peaches, olives and grapevines (Testi et al. 2008; Paltineanu et. al. 2013; Berni et al., 2009; Agam et al., 2013; Akkuzu et al., 2013; Wang and Gartung, 2010). Tokei and Dunkel (2005) reported a case study on the possible use of canopy temperature in the determination of apple tree transpiration by a theoretical approach. Their study focused primarily on the interactions of the canopy temperature and some environmental factors (i.e. radiation and relative humidity) measured in the vicinity of the tree canopies with some specialized instruments.

The goal here was to develop an analytical model for estimating the real-time transpiration of whole apple trees from the energy balance of a single leaf similar to that of the big leaf approach (Monteith, 1965; Thorpe, 1978; Caspari et al., 1993). This effort included a method of estimating net radiation from climatic parameters to eliminate a need for net radiation measurements in the field. Estimated transpiration rates were compared with those calculated using the P-M model and adjusted crop coefficient values for the region.

3.3 Materials and methods

3.3.1 Modeling of transpiration

It was assumed that the infrared temperature sensors (IRTs) could only see the upper half of the canopy (Fig. 3.1). Based on this assumption, the top tree leaves were categorized into two main types based on their exposure to long and short wave radiation sources at solar noon: a) one side exposed to the sky and the other side exposed to the foliage (top leaves) and b) both sides mostly exposed to the radiation from the foliage within the canopy (middle or inner leaves). The modeling was based on the assumption that the upper half can be treated as a single leaf bearing the characteristics of both upper canopy leaf types. Neglecting metabolic heat production and heat storage, the energy balance equation for a single apple leaf is:

$$R_n = R_{abs} - L_{oe} = H + \lambda E \tag{3.1}$$

where R_n is the net radiation, R_{abs} is the absorbed radiation, λE is the latent heat flux, L_{oe} is the outgoing emitted radiation, H is the sensible heat flux from the leaf (all terms are in Wm^{-2}). Absorbed radiation for a leaf is the sum of absorbed shortwave and long wave radiations and net radiation. R_n is the difference between this sum and emitted long wave radiation from the leaf. Assuming equal numbers of leaves in each category, R_{abs} of a leaf from the upper canopy can be expressed as:

$$R_{abs} = (R_{top} + R_{inn})/2 \tag{3.2}$$

The lower canopy will be influential by radiating longwave energy at a temperature of T_c (canopy temperature at the border of the two halves) to the upper half. This temperature is assumed to be the same as the canopy temperature measured by the IRT. The total absorbed radiation (long and short wave) for the top and middle leaves were estimated using the following relationships, respectively:

$$R_{top} = \alpha_S\left(F_{gl}S_{gl}\right) + \alpha_L(F_aL_a + F_cL_c) \tag{3.3}$$

$$R_{inn} = \alpha_S(F_{tr}S_{tr}) + \alpha_L(2F_cL_c) \tag{3.4}$$

where S_{gl} is the global solar irradiance (sum of the direct beam and diffused: $S_{gl} = S_b + S_d$), and S_{tr} is transmitted shortwave radiation through apple leaves ($S_{tr} = \tau S_{gl}$). L_a, L_c and L_g are the longwave flux densities from the atmosphere, apple tree canopies, and the ground computed using the Stefan-Boltzmann equation. All radiation is measured in W m^{-2}. F_{gl}, F_{tr}, F_a and F_c are view factors between the leaf surface and the various sources of radiation; namely global (0.5) and transmitted (0.5) solar radiation, and atmospheric (0.5) and apple tree canopy (0.5) thermal radiation, respectively. The view factors were calculated according to Campbell and Norman (1998). τ, α_S and α_L are green leaf transmittance, absorptivity in the short, and absorptivity in the thermal waveband, respectively. The values of apple leaf and ground optical properties were adapted from the available literature (Green et al., 2003b). The outgoing longwave radiation from the leaf/canopy (L_{oe}) was calculated using the Stefan–Boltzmann relationship:

$$\mathrm{L_{oe}} = \mathrm{F_e}\varepsilon_\mathrm{s}\sigma\mathbf{T}_\mathrm{c}^4 \tag{3.5}$$

where ε_s is the thermal emissivity of apple leaf ($\varepsilon_s = \alpha$), σ is the Stefan–Boltzmann constant ($5.67 \times 10^{-8}\mathrm{Wm^{-2}K^{-4}}$) $\mathbf{T}_\mathrm{c}$ is the canopy temperature (K), and F_e is the view factor between the entire surface of the leaf and the complete sphere of view ($F_e = 1.0$). The emissivity of the sky ($\varepsilon_a(c)$) that is required to compute the emitted radiation from the atmosphere ($\mathrm{L_a} = \varepsilon_a(c)\sigma\mathbf{T}_\mathrm{a}^4$, $\mathbf{T}_\mathrm{a}$ in Kelvins), was calculated by (Monteith and Unsworth, 1990):

$$\varepsilon_a(c) = (1 - 0.84c)\varepsilon_{ac} + 0.84c \tag{3.6}$$

where c is the fraction of the sky covered by clouds. c was calculated by comparing the daylight average of real-time global radiation ($\overline{S_{gl}}$, W m^{-2}) with the potential extraterrestrial incoming solar radiation of the same day (R_{ap}, W m^{-2}):

$$c = \begin{Bmatrix} (1 - \frac{\overline{S_{gl}}}{Ra_{Pot}}) & if\ \overline{S_{gl}} \le R_{ap} \\ 0 & otherwise \end{Bmatrix} \tag{3.7}$$

R_{ap} was calculated according to the FAO-56 bulletin (Allen et al., 1998). The emissivity of a clear sky (ε_{ac}) was estimated using the following empirical relationship (Brutsaert, 1984):

$$\varepsilon_{ac} = 1.72 \left(\frac{e_a}{\mathbf{T}_a}\right)^{1/7} \tag{3.8}$$

where e_a is the vapor pressure (kPa) at air temperature ($\mathbf{T}_a$, K). The term H in the energy balance equation is expressed as (Campbell and Norman, 1998):

$$H = g_H C_P \Delta T_m \tag{3.9}$$

where C_P is the heat capacity of air (29.17 J mol^{-1} C^{-1}), ΔT_m is the measured canopy and air temperature difference ($\Delta T_m = T_c - T_a$), T_c is the canopy temperature (or the hypothetical leaf, ºC), T_a is the air temperature (ºC), and g_H is the boundary layer conductance to heat (mol m^{-2} s^{-1}). The term H is comprised of two components of H_{ab} and H_{ad} which are sensible heat fluxes from the abaxial and adaxial sides of apple leaf, respectively. This refers to the fact that apple leaves are hypostomatous transpiring mostly through the abaxial side and that sensible heat exchange occurs from both sides of the leaf. Following Campbell and Norman (1998) and Blanquicet et al. (2009), conductance here was preferred over the traditional use of resistance in the calculations. The boundary layer conductance of air to heat for laminar forced convection (g_{Hf}) was calculated using the following empirical formula (Campbell and Norman, 1998):

$$g_{Hf} = (1.4)0.135\sqrt{\frac{u}{d}} \tag{3.10}$$

where, u is the wind speed and d is the characteristic dimension defined as 0.72 times the leaf width ($w_l = 5cm$: measured in the field). Assuming equal conductance for both abaxial and adaxial sides of leaf, the combined air conductance to heat is $g_H = 2g_{Hf}$. Rearranging Eq. 3.1 to solve for E ($= T$) yields:

$$T = 1555.2\frac{R_n - g_H C_P \Delta T_m}{\lambda} \tag{3.11}$$

where T is the actual transpiration (mm day^{-1}) and the factor 1555.2 (0.018 kg mol^{-1} × 24 h × 3600 s h^{-1}) converts mol m^{-2} s^{-1} to mm day^{-1}. Considering that T is a function of ΔT_m, the slope and intercept of the line fitted to the data set can be described by rearranging Eq. 3.11 in a linearized form ($T = c + b\Delta T_m$) as the following:

$$T = \left(\frac{Q}{\lambda}\right) - \left(\frac{g_H C_P - n}{\lambda}\right)\Delta T_m \tag{3.12}$$

where $R_n = Q + n\Delta T_m$. Q and n are defined by the following equations, respectively:

$$Q = 0.25\left(\alpha_S S_{gl} + \alpha_S S_{t1} + 4(\alpha_L - 1)\mathrm{L_a}\right) \tag{3.13}$$

and:

$$n = (3\alpha_L - 4)\varepsilon_a(c)\sigma\mathbf{T}_\mathrm{a}^3 \tag{3.14}$$

3.3.2 Application of T-model

Experimental site

The field experiments were conducted in a Fuji apple orchard on the Roza Farm of the Washignton State University Irrigated Agriculture Research and Extension Center near Prosser, WA, at the coordinates of latitude 46.26°N, longitude 119.74°W, and 360 m above sea level. The site was located in a semi-arid zone with almost no summer rains and an average annual precipitation of 217 mm. The site's soil was a shallow Warden Silt Loam soil (Web Soil Survey) of more than 90 cm deep (field observation). Using 3 dielectric soil moisture sensors (10HS, Decagon Devices Inc., Pullman, WA), soil moisture readings were taken from 3 different locations in the orchard after heavy irrigations to determine the field capacity. From these measurements, the volumetric water content at field capacity was found to be 32.5%.

Plot design

Two scenarios were examined to support the application of this model. The T-model was initially applied to field investigations (scenario 1) in 2007 and 2008 where young, well developed apple trees were fully-irrigated throughout the growing seasons. Once the model had been evaluated and optimized, it was applied to another case (scenario 2) in 2013 where the same apple trees were older and were bearing little or no fruit. During the 2007 and 2008 growing seasons, 2 rows/plots of apple trees (42 trees per plot) were marked for conducting the experiment.

The rows were named “N” and “S”. The trees were spaced 4 m (row spacing) by 2.5 m (tree spacing) apart in the orchard and irrigated by a micro-sprinkler irrigation system with water emitters of 27 L h^{-1} spaced at 2.5 m intervals (in-row between each tree). The transpiration of apple trees was estimated in the two fully-irrigated plots of N and S.

During the 2013 growing period, the same orchard was irrigated by two lines of drip tubing laterals of in-line 2.0 L h^{-1} drippers, spaced at 91.4 cm intervals along laterals. This time three plots, each consisting of 48 trees (3 sub-plots of 6 by 3 per plot), were marked for conducting the experiment. In addition to the “N” and “S” plots, the scientifically-based irrigation method using a neutron probe (NP) soil moisture meter was assigned to a new plot. Manual irrigation was scheduled in the plots of the NP treatment based on weekly readings of the soil water content using a neutron probe (503DR Hydroprobe, Campbell Pacific Nuclear, Concord, CA). Throughout growing season, the quantity of irrigation water applied to the trees was controlled to not allow the soil water depletion to exceed the 50% maximum allowed depletion (MAD = 0.96 m) for apple trees (Allen et al., 1998). This was assured by taking weekly soil water content readings using a neutron probe in all of the plots.

Meteorological measurements

Canopy temperature along with meteorological data including relative humidity, solar radiation, wind speed and air temperature were required inputs to the T-moel. The real-time meteorological data of the 2007, 2008 and 2013 growing seasons were obtained from two standard electronic weather stations close to the apple orchard (Roza and WSU HQ, Washington Agricultural Weather Network). In 2007 and 2008, air temperature was recorded in the field using the embedded temperature sensor of a Campbell CR21X datalogger (Campbell Scientific, Logan, UT, USA). In addition to these data, in 2013 air temperature was measured using three air temperature sensors (Model 109-L, Campbell Scientific, Logan, UT, USA) installed at a height of 2 m (in-line with the trees) at three locations distant from each other in the orchard. The air temperature sensors were shielded (41303-5A, Campbell Scientific, Logan, UT, USA). These air temperature sensors were wired to Campbell CR10X dataloggers (Campbell Scientific, Logan, UT, USA). Air temperature was calculated by averaging readings from the three sensors. Vapor pressure deficit was calculated using the following equation (Idso et al., 1981):

$$D_a = e_s(T_a) - e_a \tag{3.15}$$

where $e_s(T_a)$ is the saturated vapor pressure at the air temperature (T_a) and e_a is the actual vapor pressure of air.

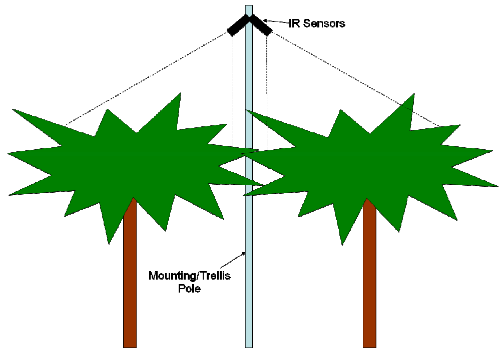

Figure 3.1 IRT sensors setup in the field. In 2007 and 2008, the sensors were pointed downwards at approximately 45 degree angles at both the north and south sides of a tree.

Measurement of canopy temperature

To monitor canopy temperature in 2007 and 2008, a total of 12 IRTs (Exergen model IRt/c.03™: Type T, Watertown, Mass.) in 6 pairs were mounted above the trees in the 2 rows. The IRTs were pointed downwards at approximately 45 degree angles at both the north and south sides of a tree (Fig 3.1). The sensors were calibrated using a blackbody calibrator (BB701, Omega Engineering, Inc., Stamford, CT) and wired to a Campbell CR21X datalogger (Campbell Scientific, Logan, UT, USA). In 2013, canopy temperature was measured using individual IRTs (Excergen model IRt/c.2: Type J, Watertown, Mass.) installed perpendicularly above a tree pointed straight down and located at the center of the six sub-plots (3 per plot). Sepulcre-Canto et al. (2006) and Testi et al. (2008) used similar mounting in Olive and Pistachio trees, respectively. Considering the field view of this model of IRT (35 degrees), this form of orientation and position will decrease the chance of the ground being seen by the IR sensor and the number of sensors being used. The IRT sensors were wired to a network of Campbell CR10 and CR10X dataloggers (Campbell Scientific, Logan, UT, USA) sending out temperature readings to a central computer wirelessly.

Estimation of transpiration

To estimate daily transpiration (T, mm d^{-1}) of apple trees during the growing season, two approaches were examined: a) the daily averages of the meteorological data and canopy temperatures were used, and b) the 15 min time interval transpiration (T_{15}) was calculated and the 24 h total was obtained by accumulation ($\sum_{i=1}^{96} T_{15}$). Solar noon and noon transpiration rates were also estimated using the average values of the variables around solar noon (i.e. from 11:00AM to 1:00PM) and solar noon (i.e. from 1:00PM to 3:00PM), respectively. To estimate the daily crop evapotranspiration (ET_c , mm d^{-1}) of the irrigated Fuji apple orchard, the ASCE standardized Penman-Monteith equation (ASCE-EWRI, 2005) was used in combination with the crop coefficient values adjusted for the local climate (Karimi et. al, 2013):

$$ET_c = K_c \times ET_r \tag{3.16}$$

where ET_r is the alfalfa reference evapotranspiration. To estimate daily ET_r, the meteorological data of the 2007, 2008 and 2013 growing season including daily received solar radiation (MJ m^{-2} d^{-1}), maximum and minimum temperatures, relative humidity and wind speed were obtained from the nearby weather stations.

Crop water use

A water budget equation was used to estimate irrigation water use by apple trees in 2013 (Evett, 2002):

$$ET_{wb} = P + I + F - \Delta S \pm D - R \tag{3.17}$$

where ET_{wb} is the actual crop water use (mm), P is precipitation (mm), I is the applied irrigation depth (mm), F is lateral flux of water entering the control volume (positive) or exiting it (negative), D_p is deep percolation (mm) and R is runoff (mm). D and R were assumed to be negligible. In addition, there was no shallow water table below the root zone, thus upward flow was not a concern. F was also assumed to be zero because soil moisture readings were taken at the center of the plots where the effect of horizontal fluxes are negligible. ΔS is the change in soil water content (mm) and was calculated using the neuron probe readings:

$$\Delta S = \theta_f - \theta_i \tag{3.18}$$

where θ_f is the final soil water content (mm) in the end of the measuring period (week or growing season) and θ_i is the initial soil water content (mm; week or season).

Measurements of stem water potential

During the growing season of 2013, the stem water potential (Ψ_{stem}) at solar noon was measured once per week from mid to late summer (July 31 to October 2). Solar noon Ψ_{stem} measurements were taken near solar noon within a 2-hour time window (between 1:00PM and 3:00PM) and on the same day as the neutron probe measurements. For each measurement six shaded leaves (per plot) from the inner, lower part of each tree canopy close to the trunk of the apple trees (where an IRT was mounted) were selected, enclosed in aluminum foil covered plastic envelopes, and left attached to the tree for a period of time between 15 min and 60 min. The Ψ_{stem} of the leaves was then measured with a pressure bomb (Model 615, PMS Instrument Co., Albany, OR). The Ψ_{stem} measurements were made under different weather conditions including cold, humid and overcast days.

Model assessment

The performance of the T-model was evaluated using the estimated values of transpiration from the model and those predicted by the P-M model and corrected by local K_c values. The statistical measures used were: a) the relative error (RE) between predicted transpiration (T) and predicted crop ET (ET_c), b) the root mean square error ($RMSE$), c) the coefficient of variation of the RMSE ($CV\ of\ RMSE$), d) the Nash and Suttcliffe Coefficient of Efficiency (COE) (Nash and Suttcliffe, 1970) and e) a linear regression between the transpiration model and ET_c. A satisfactory prediction was assumed when the linear regression yielded slopes close to unity, intercepts close to zero and high correlation (R^2). The COE gives an account of the deviation from unity of the observations variance and the ratio of the mean squared errors. Therefore, the closer the COE to one is, the better the performance of the model is. The total amount of predicted transpiration (D_T) and crop ET (D_{ET}) at the end of the growing season were compared by calculating the relative error (RE):

$$\mathrm{RE} = \frac{D_{ET} - D_T}{D_{ET}} \tag{3.19}$$

The root mean square error (RMSE) was exploited as a measure of the variance between predicted transpiration and crop ET:

$$RMSE = \sqrt{\frac{\sum(ET_c - T)^2}{n}} \tag{3.20}$$

where n is the number of measurements. The CV of the RMSE was calculated by dividing the RMSE by the mean of the T-model predictions ($\bar{T}$):

$$CV_{RMSE} = \frac{RMSE}{\bar{T}} \tag{3.21}$$

In 2013, the correlation between the solar noon Ψ_{stem}, as widely accepted indicator of apple trees water status (Lakso, 2003), and the solar noon and daily T was investigated. The statistical analysis also included an analysis of variance (at $p = 0.05$) using the SigmaPlot 11.0 (Systat Software Inc., San Jose, CA) to conduct multiple comparisons of crop water use means of the irrigation treatments (i.e T, ET_c, ET_{WB} and ET_{NP}).

3.4 Results and discussions

3.4.1 Daily transpiration

T-model and Penman-Monteith method

During mid-season, the crop coefficient for converting alfalfa ET_r to apple trees transpiration is nearly 1.0 with a peak of 1.06 (Karimi et al., 2013). This is a time when, under dry and warm conditions, actual transpiration of well-watered apple trees is expected to be close to the alfalfa reference ET (Dragoni et al., 2005) with a maximum of a 6% discrepancy. To avoid uncertainties of canopy temperature measurements especially during the early-season due to incomplete canopy growth, we picked a mid- and late-season time period for the purpose of comparisons but mainly focused on mid-season.

Estimations of daily transpiration (mm day^{-1}) using the T-model required input parameters that included the daily average air temperature, relative humidity, solar radiation and wind speed. The model also required simultaneous canopy temperature measurements which were recorded every 15 min throughout the season. Daily transpiration estimated by the T-model, and that predicted by the crop ET equation (ET_c) are plotted in Fig. 3.2. ET_c was calculated as the product of the ET_r and K_c values adjusted for the local climate. All of the meteorological parameters were obtained from the nearby weather stations except for air temperature which was measured in the field.

Discrepancies in the estimations of daily T in the fully-irrigated plots N and S can be seen in Fig 3.2 and Fig 3.3. The difference in transpiration was caused by difference in canopy temperature measurements which was a result of field/canopy variability and/or the canopy temperature measurement errors. Statistical analysis showed there was no significant difference between the means of daily average (P = 0.699) and solar noon transpirations of the two tree rows (P = 0.787); however, there were random occasions when there was a significant difference between the N and S (data not shown).

Compared to ET predictions of the P-M method, the T-model seemed to have overestimated transpiration during the mid-seasons of 2007 and 2008 and underestimated it in 2013. In 2007 and 2008, the apple orchard was young and well-watered during the entire growing season (DOI=110–278). Linear regression between T and ET_c for mid and late seasons combined (DOI=155–270) in 2007 yielded a slope, intercept and R^2 of 0.99, 1.07 and 0.72, respectively for the N plot. The results for the S plot were almost the same with slope, intercept and R^2 of 1.05, 1.08 and 0.77, respectively. Transpiration was relatively well estimated with COEs of 0.86 (N-plot) and 0.80 (S-plot);

however average T for the mid season when the transpiration of apple trees was expected to be almost the same rate as reference ET was overestimated; 7.9 mm d^{-1} and 8.4 mm d^{-1} estimated by the T-model compared to 6.9 mm by the P-M (RMSE = 1.6 and 2.0 mm).

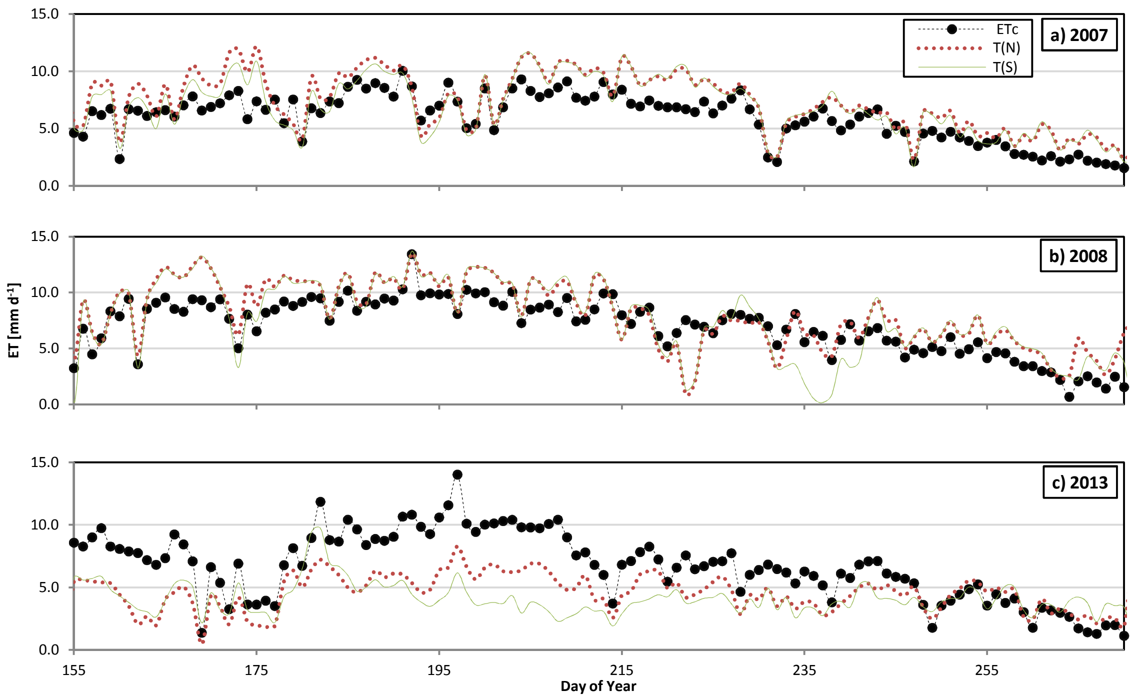

Figure 3.2 Comparison of the daily transpiration (T, mm d^{-1}) estimated by the T-model for the N and S plots, and that predicted by the crop ET (ET_c) for the growing seasons of 2007 (a), 2008 (b) and 2013 (c). ET_c was calculated as the product of the P-M reference ET (ET_r, ASCE-EWRI, 2005) and the crop coefficient values adjusted for the local climate (Karimi et. al, 2013).

Linear regression between T and ET_c for mid- and late-seasons (combined) in 2008 yielded slope, intercept and R^2 of 1.0, 1.19 and 0.78 for the N plot, and 1.11, -0.02 and 0.69 for the S tree row, respectively. Similar to 2007, transpiration was relatively well predicted with COEs of 0.88 (N-plot) and 0.83 (S-plot) and the average transpiration of the mid-season was overestimated, 8.9 mm d^{-1} and 8.4 mm d^{-1} estimated by the T-model compared to 7.8 mm by the P-M (RMSE = 1.7 and 2.1 mm). Comparing the results from Fig. 3.4 and Table 3.1 suggests that the T predictions of mid-season in 2007 and 2008 were less correlated with ET_c (weaker correlations during mid-season compared to mid- and late-seasons combined).

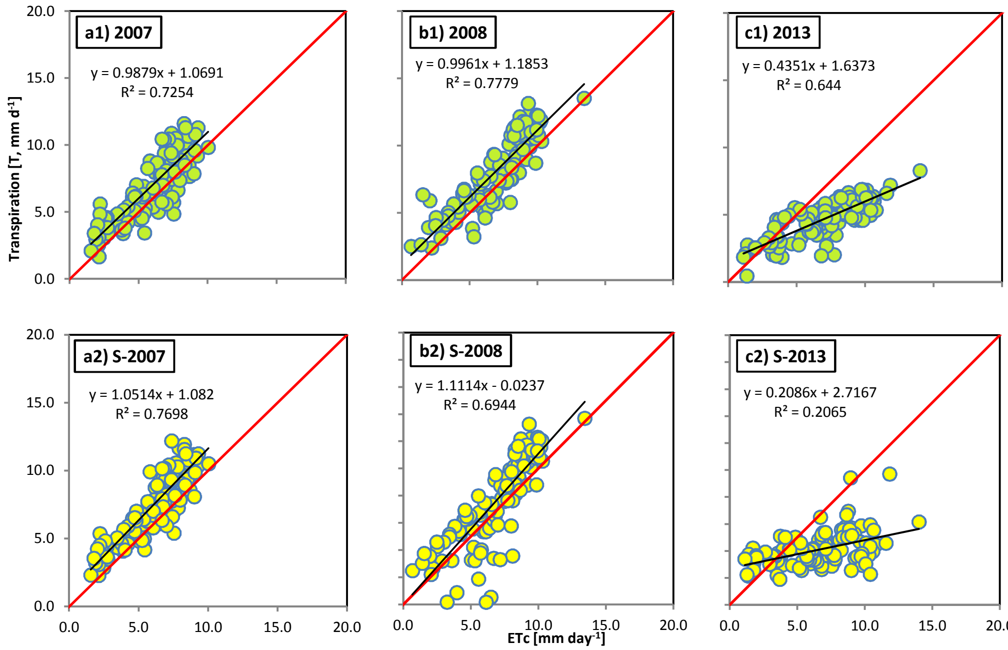

Figure 3.3 Comparison of daily transpiration (T, mm d^{-1}) estimated by the T-model for two apple tree rows (N and S), and that predicted by the crop ET (ET_c) equation for the 2007 (a1, a2), 2008 (b1, b2) and 2013 (c1, c2) growing seasons (DOY=155–270). ET_c was calculated as the product of the P-M reference ET (ET_r, ASCE-EWRI, 2005) and the crop coefficient values adjusted for the local climate (Karimi et. al, 2013).

Table 3.1 Comparison of predicted transpiration from the T-model and ET_c for mid-season of 2007, 2008 and 2013.

					Total ET (mm)			Average ET (mm d^{-1})				
Year	Plot	R^2	Slope	Intercept	ET_c	T-Model	RE (%)	ET_c	T-Model	RMSE	CV of RMSE	COE
2007	N	0.59	1.07	0.47	628	716	-14	6.9	7.9	1.6	0.24	0.86
	S	0.63	1.12	0.58		758	-22		8.4	2.0	0.29	0.80
2008	N	0.73	1.25	-0.96	731	827	-13	7.8	8.9	1.7	0.22	0.88
	S	0.72	1.60	-4.28		786	-8		8.4	2.1	0.26	0.83
2013	N	0.68	0.55	0.58	702	427	37	7.7	4.8	3.1	0.41	0.84
	S	0.23	0.30	1.93		374	45		4.2	4.0	0.52	0.75

In 2013, linear regression between T and ET_c yielded an R^2 of 0.64 (p <0.001) and 0.21 (p =0.002) for the N and S plots, respectively. Transpiration was well predicted with COEs of 0.85 and 0.75 for the N and S plots, respectively. However, over the experiment period average T was under estimated, 4.8 mm d^{-1} and 4.2 mm d^{-1} predicted by the T-model compared to 7.7 mm by the P-M (CV_{RMSE} = 41% and 52%). Considering that the apple trees were experiencing an alternate bearing year, a decrease in transpiration in response to less fruit loads on the trees was expected (Palmer et. al., 1997). This is illustrated in Fig. 3.2 where transpiration rate remained relatively constant throughout the mid- and late-seasons.

Total water use

Total crop water use of apple trees was calculated by the accumulation of daily T (T_{avg}) and ET_c over mid-season in 2007, 2008 and 2013. In 2007, the total transpiration was predicted to be slightly higher by the T-model (716 mm and 758 mm compared to 628 by the P-M) yielding REs of -14% and 22% in the N and S plots, respectively. In 2008, the errors of estimating total transpiration during the mid-season were relatively small with REs of -13% and -8% in the N and S plots, respectively. In 2013, the estimations of total transpiration using the P-M and T-model were also different with T being significantly smaller than ET_c with 427 mm and 374 mm predicted by the T-model compared to 702 mm by the P-M. Although the values were very close, the total T of the N and S plots was averaged to obtain one T_{avg} value (Fig. 3.4a). There was a trivial difference between averaged total T_{avg} and ET_c with T_{avg} being 18% and 11% more in 2007 and 2008, respectively. In, 2013, however, the difference was significant with T_{avg} being 47% less than total mid-season ET_c.

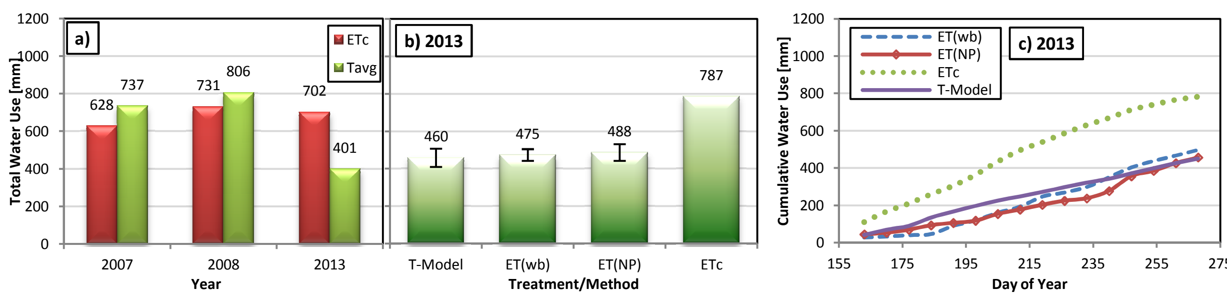

Figure 3.4 Total water use estimated by the T-model (accumulated T_{avg}) and the P-M ET corrected by crop coefficient (accumulated ET_c) in the growing seasons of 2007, 2008 and 2013 (a) (only mid-season: DOY=155–240). Comparison of apple trees water use estimated by the T-model (accumulated T), water budget approach (ET_{WB}), accumulated ET_c and water use of fully-irrigated trees under the NP treatment (ET_{NP}) during the 2013 growing season (b) (DOY=155–270). The soil moisture readings at the beginning and end of the season were used to calculate total water use. The error bars show the standard error of the mean. Cumulative water use estimated by the T-model, water budget approach (ET_{WB}), ET_c and water use under the NP treatment (ET_{NP}) during the 2013 growing season (c). The weekly soil moisture readings were used to calculate weekly and cumulative water use.

In order to determine which method correctly estimated water use during the irrigation period of the 2013 growing season (DOY=155–270), actual water use of the apple trees was estimated using a water budget approach (ET_{wb}, Eq. 3.17) and compared with the total T_{avg} (average of the N and S plots). A comparison was also made with the accumulated water use of the trees under the NP treatment for the same period (Fig 3.4b). It was expected that the water use of the trees under the NP treatment to reflect the actual amount of water consumed by well-watered apple trees. On the other hand, ET_c was meant to predict the water use of well-watered orchard trees correctly. However, the accumulated ET_c ($\sum ET_c$ = 787 mm) was significantly greater than that of the NP treatment water use ($\sum ET_{NP}$ = 488±45 mm). There was no significant difference between the water use calculated by the energy budget equation ($\sum ET_{WB}$ = 475±31 mm) and accumulated T_{avg} ($\sum T_{avg}$ = 460±49 mm) with a P-value of 0.667. Similarly, the differences in the mean values of accumulated T from the T-model, water budget and NP methods were not statistically significant (P = 0.885). Therefore, while ET_c failed to predict the total transpiration of apple trees correctly during the growing season of 2013 (Fig. 3.4b, c), the performance of the T-model was quite satisfactory.

T and solar noon Ψ_{stem}

In the 2013 growing season, trees within a specific plot (i.e. N or S) did not necessarily receive irrigation water on the same day as the other plot. However, statistical analysis revealed there was no significant difference among the plots on solar noon Ψ_{stem} (P = 0.110) over the period of measurements (DOY=212–275). In addition, soil water depletion in the N and S plots never exceeded the 50% MAD recommended for apple trees (Allen et al., 1998). This can be translated into the fact that the fluctuations of both solar noon Ψ_{stem} and T were not related to a soil water deficit, but caused by other factors. In addition to a non-limiting soil water status, the non-stressed solar noon Ψ_{stem} values (Naor et al., 1997; Naor, 2000; Naor and Cohen, 2003) indicated that the irrigation treatments maintained the trees well-watered.

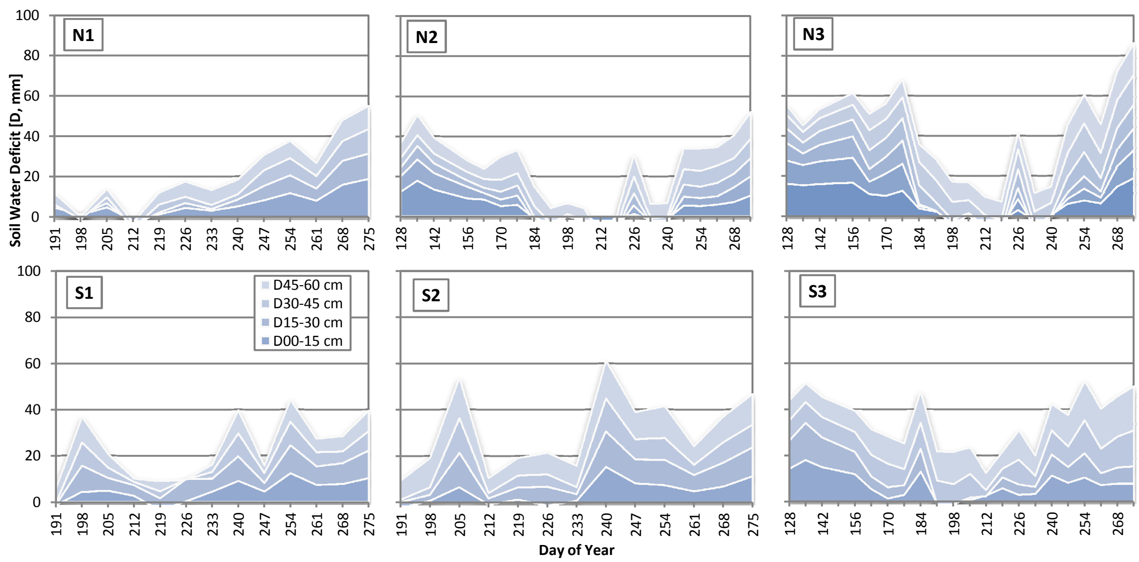

Figure 3.5 Soil water deficit (depletion) in 2013 at the root zoone down to the depth of 60cm in the sub-plots under N (N1, N2, and N3) and S (S1, S2, and S3). The soil moisture was monitored using a neutron probe.

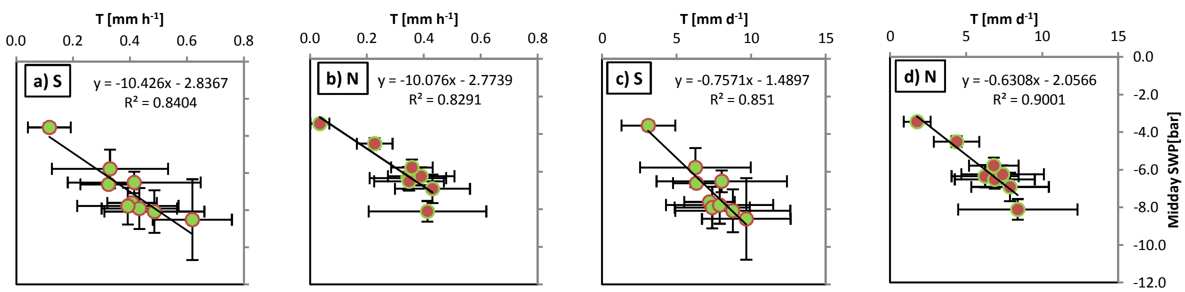

Figure 3.6 Linear relationship between solar noon (SWP) and solar noon transpiration (mm h-1) estimated by the T-model in the N and S irrigation plots in 2013 (a, b). Linear relationship between solar noon and daily transpiration (mm d-1) estimated by the T-model in the N and S irrigation plots in 2013 (c, d). Each value represents the average of up to six measurements per plot. The error bars show the standard error of the mean.

To quantify the tension status of the apple trees, up to six readings (per plot per measurement day) were averaged to calculate the of each plot (N and S). The apple trees of both plots had similar solar noon fluctuations (Fig. 3.6). The trees maintained relatively high solar noon over the period of the experiment with fluctuations mainly driven by the weather conditions. During this period, solar noon values were higher (less negative) than -1.0 bar. There was an increasing trend in the towards the end of the season with a minimum of -11.0 bar and maximum of -3.5 bar. Although Ψ_{stem} measurements were taken in different weather conditions, both solar noon T (mm h^{-1}) and daily T (mm day^{-1}) were highly linearly correlated with Ψ_{stem} with $R^2 = 0.92$ and $R^2 = 0.87$ (p<0.001), respectively (Fig. 3.6). Considering there was no water stress, Ψ_{stem} was mainly dependent on solar radiation, air temperature and relative humidity, thus the lower the Ψ_{stem}, the lower the transpiration rate was.

Accumulated T and average T

To estimate the accumulated daily transpiration (T_{acc}) from the T-model, 15 min time interval transpiration (T_{15}) was calculated and the 24 h total was obtained by accumulation ($\sum_{i=1}^{96} T_{15}$). Accumulated transpiration was highly correlated with daily average T (T_{avg}) in 2007 (Fig. 3.7a; y = 0.93x + 0.19, $R^2 = 0.93$, $p < 0.001$), 2008 (Fig. 3.7b; y = 1.02x + 0.53, $R^2 = 0.95$, $p < 0.001$) and 2013 (Fig. 3.7c; y = 0.95x + 0.15, $R^2 = 0.92$, $p < 0.001$). Compared with the use of average meteorological data, accumulated T did not show any significant advantage in estimations of daily transpiration.

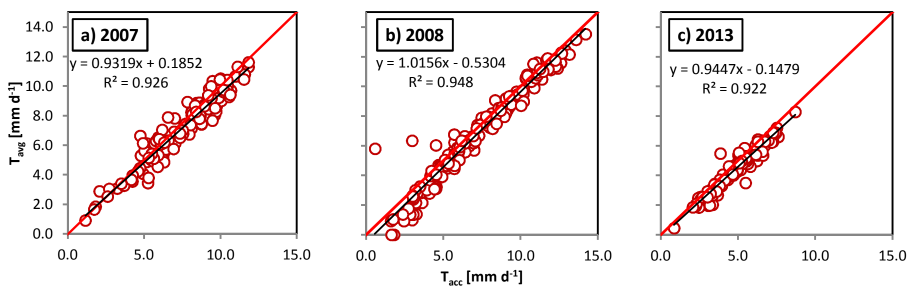

Figure 3.7 Relationship between daily transpiration estimated by accumulation of 15min transpiration over 24h (T_{acc}, mm d^{-1}) and by using daily average data (T_{avg}, mm d^{-1}).

3.4.2 Diurnal changes of transpiration

Solar noon (T_{mid}) and noon (T_{noon}) transpiration rates were estimated using the average values of meteorological data measured around noon (11:00AM to 1:00PM) and solar noon (1:00PM to 3:00PM), respectively. The relationships between T_{mid} and T_{avg}, as well as T_{noon} and T_{avg} during mid- and late-seasons of 2007, 2008 and 2013 are illustrated in Fig. 3.8.

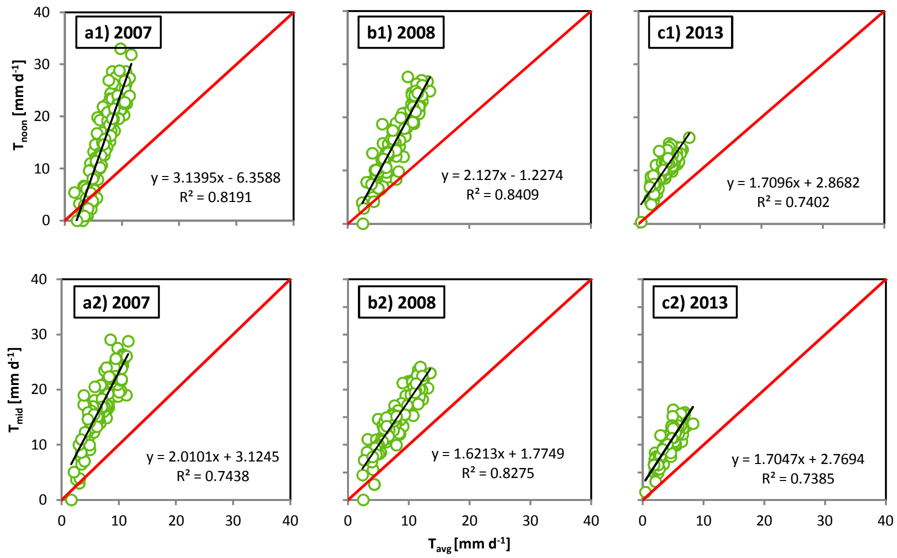

Figure 3.8 Relationship between noon transpiration (T_{noon}, mm d^{-1}) and daily T (T_{avg}) (a1–c1), as well as relationship between solar noon transpiration (T_{mid}, mm d^{-1}) and T_{avg} (a2–c2), estimated by the T-model during the growing periods of 2007 (a1 and a2), 2008 (b1 and b2) and 2013 (c1 and c2). T_{noon} and T_{mid} were calculated using the average meteorological data of 11:00AM to 1:00PM and 1:00PM to 3:00PM, respectively.

In all of the seasons, transpiration rates at both noon and solar noon were highly correlated with T_{avg} with R-squared values of 0.82 and 0.74, respectively, in 2007, values of 0.84 and 0.83, respectively, in 2008, and similar value of 0.74 for both noon and solar noon, in 2013. Establishing a relationship between T_{avg} and estimations of transpiration at other times of day (before 11:00AM and after 3:00PM) resulted in significantly lower R^2 values (data not shown). The slopes of the relationships indicated a higher rate of T_{noon} than T_{mid} in 2007 and 2008 with values of about 3.1 and 2.1 times T_{avg}, respectively for T_{noon} compared to 2.0 and 1.6 times T_{avg}, respectively for T_{mid}. In 2013, the slope at noon was the same as that at solar noon with a value of 1.70 exhibiting no decrease from noon to solar noon as it was observed in 2007 and 2008.

Considering that T_{noon} was greater than or equal to T_{mid}, the maximum T must have occurred at a time other than solar noon. To find an answer to this we explored diurnal patterns of the apple tree's transpiration predicted by the T-model. Transpiration rates for 15 min time intervals were calculated during early-, mid- and late-seasons of 2007, 2008 and 2013 using the average values of air temperature, relative humidity, solar radiation and canopy temperature over the course of several successive days (Fig. 3.9).

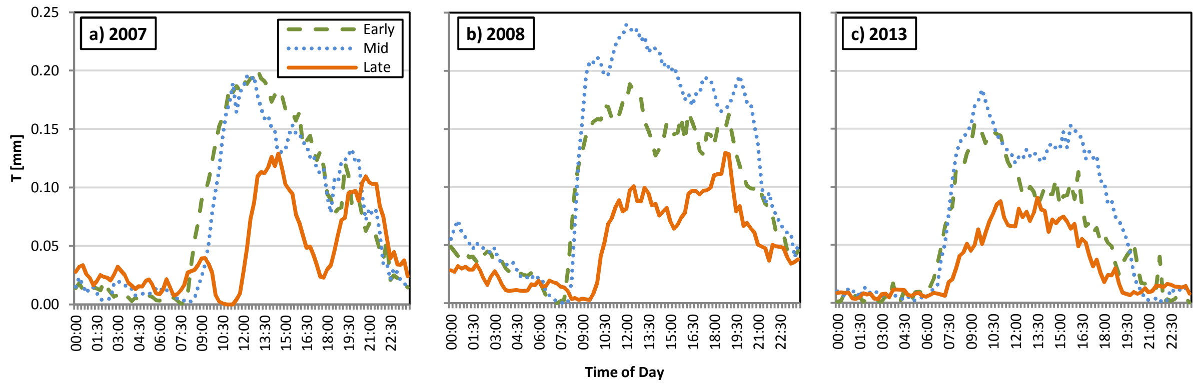

Figure 3.9 Diurnal changes (average) of T estimated by the T-model during the 2007 (a), 2008 (b) and 2013 (c) growing seasons. Each curve represents the average of T over a few successive days: DOY=152–160 as early, DOY=191–200 as mid and DOY=260–270 as late in the season.

As depicted in Fig. 3.9, the maximum transpiration of apple trees happened sometime in the morning and in the afternoon with a shift from early to late in the season. A similar pattern of the hourly transpiration rates of apple trees was previously reported by Tokei and Dunkel (2005). The time of peak transpiration coincided with a peak in canopy and air temperature difference which can be explained by the fact that, in addition to R_n, the transpiration of apple trees was controlled by stomatal regulation reflected in a lowered or elevated canopy temperature.

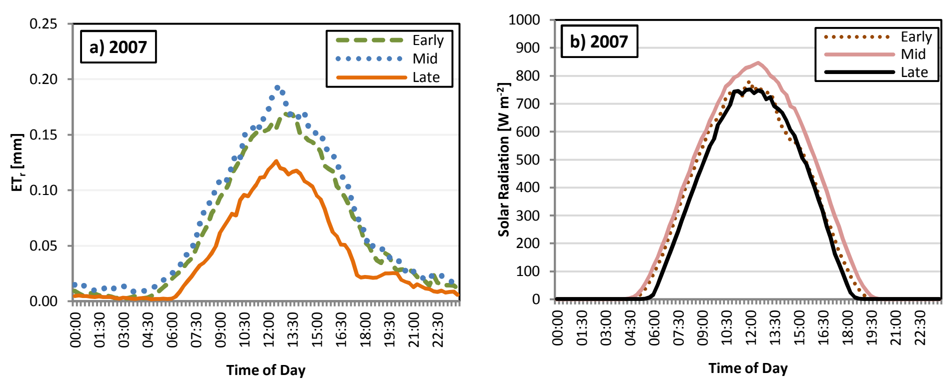

Figure 3.10 Hourly changes of ET_r (a) and incoming solar radiation (b) averaged over the course of several successive days during (DOY=152–160), mid (DOY=191–200) and late (DOY=260–270) in the 2007 growing season.

The hourly transpiration (averaged over several days) estimated by the P-M model (ET_r) for three different occasions of early, mid and late in the 2007 growing season is depicted in Fig. 3.10. As it can be seen, the peak ET_r

has coincided with a peak in incoming solar radiation. The observed behavior of the apple trees was different than row crops where the transpiration is mainly driven by net radiation (Lakso, 2003) and is reduced drastically in response to low solar radiation levels (Wanjura and Upchurch, 1997).

3.4.3 Transpiration and humidity

The relationship between the whole canopy transpiration of apple trees and the air vapor pressure deficit (D_a) was previously studied. Dragoni et al. (2005) demonstrated that in a humid climate, transpiration of the trees was highly related to D_a. Auzmendi et al. (2011) also showed that T was dependent on D_a at different weather conditions. To conduct a comparison of T and ET_c behaviors on different days, two arbitrarily defined conditions of "warm and dry" ($D_a > 1.5kPa$, $S_{gl} > 320$), as well as "cold and humid" ($D_a < 1.0kPa$, $S_{gl} < 230$) were assumed. The predicted values of transpiration by the models were grouped into these two categories and separately fitted by a linear regression (Fig. 3.11). The transpiration of apple trees was expected to be mainly driven by net radiation during warm and dry days similar to that of the reference alfalfa/grass (Dragoni et al., 2005).

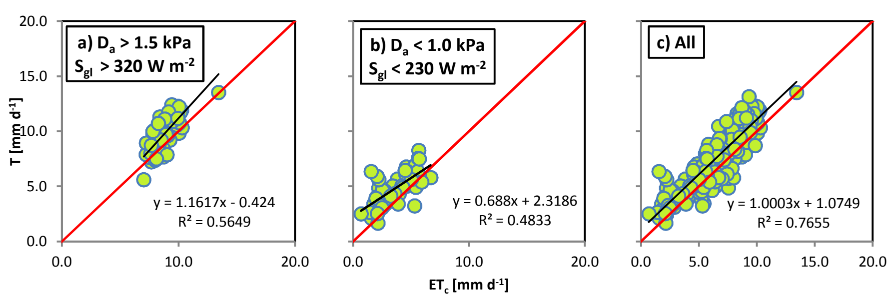

Figure 3.11 Correlation between T_p and ET_r during warm and dry periods (a; p<0.001), during cold and humid days (b; p<0.001) and for all of the days during the growing seasons of 2007 and 2008 (c).

As anticipated, estimated T was better correlated with ET_c (R^2 = 0.57, p<0.001) on warm and dry days with a slope of 1.16 and interception of 0.42 (Fig. 3.11a). Because of a high coupling between the apple trees and the humidity of the surrounding air (Jarvis, 1985) T resulted in lower values compared to ET_c during cold and humid periods showing a weak correlation with ET_r (R^2 = 0.48, p<0.001) with a slope of 0.69 and interception of 2.32 (Fig.

3.11b). Combining the results from the growing seasons of 2007 and 2008 (all days included) yielded a fairly good correlation between T and ET_c ($R^2 = 0.77$, $p<0.001$) with a slope of 1.00 and intercept of 1.08 (Fig. 3.11c).

The overall results confirmed the idea that the transpiration of apple trees changes significantly in response to air vapor pressure deficit. While the relationship between solar radiation and T is theoretically established in Eq. 3.12, D_a is not explicitly available in this equation. How D_a relates to T can be explained through its impact on stomata (Rana et al., 2005; Dragoni et al., 2005) and consequently ΔT_m as any change in stomatal conductance has a direct effect on canopy temperature (Blanquicet et al., 2009). Thus, D_a is expected to be integrated into the canopy temperature component of the T-model.

An empirical linear relationship between D_a and ΔT_m was first established by Idso et al. (1981) in row crops. Testi et al. (2008) were also able to develop a similar empirical relationship in Pistachio trees. However, such a relationship has not been properly established in apple trees. Here, following the same principals as in the original approach of Jackson et al. (1981), we tried to theoretically relate D_a to ΔT_m and transpiration. Using the latent heat flux formula (Campbell and Norman, 1998), T (mol m^{-2} s^{-1}) may be defined as:

$$T = g_T\left(\frac{D_c}{P_a}\right) \tag{3.22}$$

where g_T is the canopy conductance (a series combination of boundary layer conductance to water vapor, g_v, and stomatal conductance, g_s, all in mol m^{-2} s^{-1}) and D_c is the canopy to air vapor pressure deficit (kPa). Linearizing D_c to $\Delta(\Delta T_m) + D_a$ (Δ, in kPa C^{-1}, is the slope of the relationship between saturation vapor pressure and air temperature) and substituting it in Eq. 3.22, T can then be defined as a function of ΔT_m and D_a:

$$T = (g_T s)\Delta T_m + \left(\frac{g_T}{P_a}\right) D_a \tag{3.23}$$

where $s = \Delta/P_a$ (C^{-1}). Combining Eqs. 3.12 and 3.22 and rearranging in the form of $\Delta T_m = a - mD_a$ to solve for ΔT_m gives:

$$\Delta T_m = \left(\frac{1}{\gamma^* + s}\right) Q - \left(\frac{1}{P_a}\right)\left(\frac{1}{\gamma^* + s}\right) D_a \tag{3.24}$$

where $\gamma^* = (g_H C_P - n)/\lambda g_T$, that is, γ^* is similar to the psychrometric constant defined by Campbell and Norman (1998). Having ΔT_m from Eq. 3.24, substituting it in Eq. 3.12 and doing some manipulation, T can be expressed in a linear form, ($T = a + bD_a$), as the following:

$$T = \frac{(1-\beta)}{\lambda} Q + \frac{\lambda g_T \beta}{P_a} D_a \tag{3.25}$$

where $\beta = 1/(1 + \frac{s}{\gamma^*})$. Making an assumption of constant stomatal conductance, a linear relationship between T and D_a will be imaginable where an increase in air vapor pressure deficit leads to an increment in T. This cannot be necessarily a valid assumption as the stomata of apple leaves respond to factors such as bulk air relative humidity (Jarvis, 1985; Dragoni et al., 2005) and net radiation (Rana et al., 2005). Thus, γ^* is not constant under normal conditions.

Eq. 3.25 relates transpiration to D_a and presents a theoretical method for estimating potential transpiration of apple trees. As it was previously discussed, canopy/stomatal conductance is not constant and needs to be measured or estimated. Empirical models of Jarvis (1976) and Thorpe et al. (1980) defined the stomatal conductance of apple leaves as a function of the vapor pressure deficit and radiation. A reduction in crop loads after harvest or an alternate bearing condition (little fruit) like in the growing period of 2013, however, can cause stomatal closure and consequently a reduction in transpiration rates (Auzmendi et al., 2011; Girona et al., 2011; Lakso, 2003). This makes the use of an empirical model of stomatal conductance very limited.

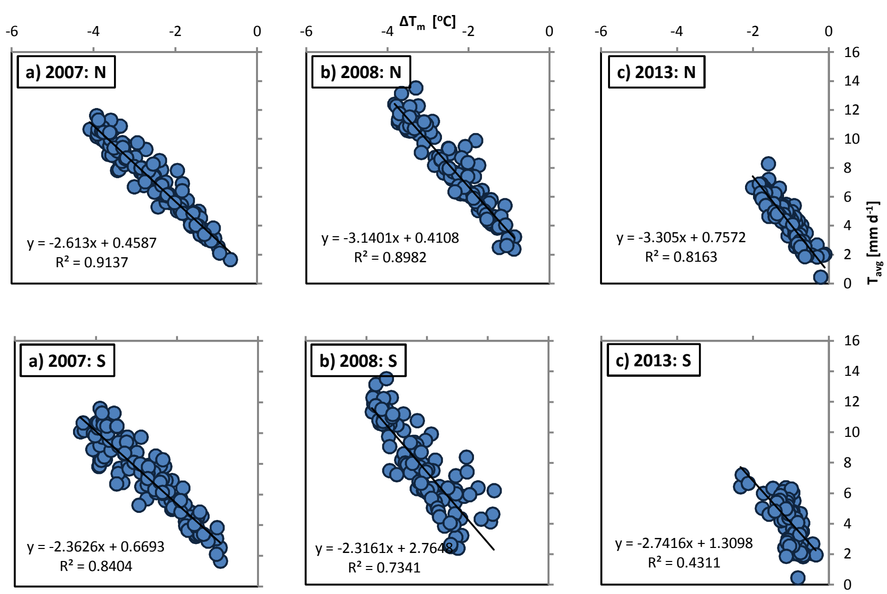

Figure 3.12 Daily mean T (T_{avg}) versus daily mean canopy and air temperature difference (ΔT_m) in the growing seasons of 2007 (a1, a2), 2008 (b1, b2) and 2013 (c1, c2).

In the linear version of the T-model (Eq. 3.12), the intercept (c) is a function of net radiation (Q component) while the slope of the T and ΔT_m relationship is mainly controlled by the air conductance to heat (g_H). Being climate dependent, Q and g_H are functions of solar radiation and wind speed, respectively, and air temperature affects both. As depicted in Fig. 3.12, the fitted lines to the data had similar slopes and intercepts across the field and from year to year. This included the growing season of 2013 when the alternate bearing condition caused a significant decrease in the transpiration rate of the apple trees. Although transpiration rate dropped from about 14 mm in 2008 to 8 mm in 2013, a linear relationship with a similar constant was maintained between T and ΔT_m.

3.5 Conclusions

During the growing periods of 2007 and 2008, canopy temperatures of apple trees were measured using IRTs pointed downwards at approximately 45 degree angles at both the north and south sides of a tree. In 2013, IRTs were installed perpendicularly above the trees. A transpiration model along with IR and air temperatures measured in the orchard, and local meteorological data from a nearby weather station were used to estimate transpiration of apple trees. The T-model presented here adequately described the transpiration of apple trees under real field conditions.

In 2007, 2008 the transpiration of the trees predicted by the T-model was slightly higher than that of ET_c with relative errors of 18% and 11% in mid-season. In 2007 and 2008 it was assumed that the apple trees were well watered (non-limiting amount of water in the soil) and that the P-M ET_c model predictions exactly reflected the crop water use of apple trees during the season. The apple trees had a mean crop level of above 100 fruit per tree in 2007. The same assumption was made for 2013; however, as a result of alternate bearing the orchard yielded less than 15 fruit per tree with no fruits on some of the trees. This provided a good opportunity to evaluate the T-model when the P-M model failed to predict the decreased transpiration rate of apple trees in response to lower crop loads. Both D_a and stomatal conductance effects on transpiration were integrated into the canopy temperature component of the T-model.

In 2013, the trees received less water compared with the conventional calendar-based method. In 2013, T estimations were very close to the actual water use of the trees. The calculated water consumptions by the trees using the water budget approach were not significantly different than the total estimated transpiration by the T-model or the plots irrigated by neutron probe. Furthermore, T-model estimations were highly correlated with solar noon stem water potential, ψ_{stem}, which was logically anticipated.

Although the overall performance of the T-model was satisfactory, net radiation (daylight average) estimations on some days were sometimes small negative values close to zero, while net radiation is expected to be positive during the daytime (Allen et al., 1998). A source of error was the simplicity of the approach used here to calculate cloud cover and sky emissivity. More advanced approaches for estimating incoming longwave radiation can be found in Flerchinger et al. (2009). Another reason for this error could be due to the fact that using the average value of incident solar radiation as in the case of using accumulated S_{lg} estimations on cloudy days were much better.

Apple tree transpiration was modeled based on the energy budget of a single leaf. There were some sources of uncertainty in modeling light and thermal energy interception by apple trees. A tree canopy is comprised of an unknown number of shaded and sunlit leaves, and shoot growth constantly changes the light interception pattern. Apple trees have discontinuous canopies. They can have various forms of architecture and their leaves are of different shapes, sizes, and orientations. Moreover, the T-model was basically derived for light interception conditions at solar noon. This introduced some errors in the estimations of T when used for times other than solar noon as in hourly or smaller time scales. Another approximation was introduced into the model by the temperature across the upper half of the canopy being assumed uniform and equal to the average temperature measured with the IRTs.

One interesting finding of this study was that the peak transpiration in apple trees occurred in the morning. Considering this fact, maybe morning hours are to be considered a better time for monitoring the water status of apple trees and for the purpose of irrigation scheduling rather than solar noon. It was also shown that the accumulated transpiration of apple trees was close to the average daily transpiration.

The overall results of the experiments with Fuji apple trees showed that actual canopy transpiration can be reliably estimated using infrared thermometery. The estimations of the T-model were highly correlated with midday Ψ_{stem} which is the best known indicator of water stress in apple trees. Their relationship can be used to determine when to irrigate. In addition, real-time water use can be computed in any time scale which determines how much water should be applied. Therefore, the present approach can provide a basis for a fully automated system of irrigating apple orchards. The possibility of precision irrigation scheduling of small areas within larger fields or even individual trees is another advantage. There may also be a hope for replacing IRT sensors with satellite IR pictures for estimating transpiration of larger orchards. The conventional use of a crop coefficient and reference ET can be then replaced by the present approach. Here we compared our approach against the P-M model. Using the noncalibrated T-model for the calculation of crop water use resulted in small errors. Further improvement can be achieved by calibrating the model using lysimeter data (Auzmendi et al., 2011) or sap flow measurements (Dragoni et al., 2005; Nicolasa et al., 2005).

Acknowledgments

This work was funded by the US Department of Agriculture Specialty Crop Research Initiative (USDA SCRI) grant. The authors would like to thank Clint Graf for his help in establishing the irrigation system, weed control, and pesticide applications. The authors thank Sean E. Hill, Evan Zumini and Robert Dickson for helping out in a number of computer related issues, as well as Alan Kawakami and Lynn Mills for their assistance with the pressure bomb. The authors also acknowledge the great help of Dr. Mohammad Bannayan with the statistical analysis. We also acknowledge the assistance and support of the Center for Precision and Automated Agricultural Systems (CPAAS) at Washington State University.

References

Agam, N., Cohen, Y., Berni, J.A.J., Alchanatis, V., Kool, D., Dag, A., Yermiyahu, U., Ben-Gal, A., 2013. An insight to the performance of crop water stress index for olive trees, Agricultural Water Management, 118: 79–86.

Akkuzu, E., Kaya, Ü., Çamoglu, G., Mengü, G.P., Aşık, Ş., 2013. Determination of crop water stress index (CWSI) and irrigation timing on olive trees using a handheld infrared thermometer. Journal of Irrigation and Drainage Engineering-ASCE, 139: 728–737.

Allen, R.G., Pereira, L.S., Raes, D., Smith, M., 1998. Crop evapotranspiration: guidelines for computing crop water requirements. Irrigation and Drainage Paper No. 56. FAO, Rome, Italy, 300 pp.

ASCE-EWRI, 2005. The ASCE standardized reference evapotranspiration equation. Technical Committee Report to the Environmental and Water Resources Institute of the American Society of Civil Engineers from the Task Committee on Standardization of Reference Evapotranspiration. ASCE-EWRI, 1801 Alexander Bell Drive, Reston, VA 20191–4400, 173 pp.

Auzmendi, I., Mata, M., Lopez, G., Girona, J., Marsal, J., 2011. Intercepted radiation by apple canopy can be used as a basis for irrigation scheduling. Agricultural Water Management, 98: 886–892.

Ben-Asher, J., Phene, C.J., 1992. User's guide for estimating crop evapotranspiration (ET_c) using the infrared thermometry (IRT) method. California Agricultural Technology Institute–CATI, Ben Gurion Univ. of the Negev, Israel. Available online at:

http://cwi.csufresno.edu/wateright/920701.asp

Berni, J.A.J., Zarco-Tejada, P.J., Sepulcre-Cantó, G., Fereres, E., Villalobos, F., 2009. Mapping canopy conductance and CWSI in olive orchards using high resolution thermal remote sensing imagery. Remote Sensing of Environment, 113: 2380–2388.

Blanquicet, Jr., J.M., Norman, J.M., Bugbee, B., 2009. Automated measurement of canopy stomatal conductance based on infrared temperature. Agricultural and Forest Meteorology 149, 1931–1945.

Brutsaert, W., 1984, Evaporation into the Atmosphere: Theory, History, and Applications. Boston: D: Reidel.

Campbell, G.S., Norman, J.M., 1998. An Introduction to Environmental Biophysics. Springer-Verlag, New York, NY, USA, 286 pp.

Casadesús, J., Mata, M., Marsal, J., and Girona, J., 2011. Automated irrigation of apple trees based on measurements of light interception by the canopy. Biosystems Engineering, 108(3): 220–226.

Caspari, H.W., Green, S.R., Edwards, W.R.N., 1993. Transpiration of well-watered and water-stressed Asian pear trees as determined by lysimetry, heat-pulse, and estimated by a Penman-Monteith model. Agricultural & Forest Meteorology, 67(1-2): 13–27.

Cohen, Y., V. Alchanatis, M. Meron, Y. Saranga, and J. Tsipris. 2005. Estimation of leaf water potential by thermal imagery and spatial analysis. J. Exp. Bot., 56(417): 1843–1852.

Dragoni, D., Lakso, A., Piccioni, R., 2005. Transpiration of apple trees in a humid climate using heat pulse sap flow gauges calibrated with whole-canopy gas exchange chambers. Agric. For. Meteorol., 130: 85–94.

Flerchinger, G.N., Xaio, W., Marks, D., Sauer, T.J., Yu, Q., 2009. Comparison of algorithms for incoming atmospheric long-wave radiation. Water Resour. Res., 45(3): W03423.

Girona, J., Del Campo, J., Mata, M., Lopez, G., Marsal, J., 2011. A comparative study of apple and pear tree water consumption measured with two weighing lysimeters. Irrig. Sci., 29: 55–63.

Green, S., McNaughton, K., Wunsche, J., Clothier, B., 2003. Modeling light interception and transpiration of apple tree canopies. Agron J., 95: 1380–1387.

Idso, S.B., Jackson, R.D., Pinter, P.J., Reginato, R.J., Hatfield, J.L., 1981. Normalizing the stress-degree-day parameter for environmental variability. Agric. Meteorol., 24: 45–55.

Jackson, R.D., Idso, S.B., Reginato, R.J., 1981. Canopy temperature as a crop water stress indicator. Water Resour. Res., 17: 1133–1138.

Jarvis, P.G., 1976. The interpretation of the variation in the leaf water potential and stomatal conductances found in canopies in the field. Philos. Trans. R. Soc. London, Ser. B 273: 293–310.

Jarvis, P.G., 1985. Coupling of transpiration to the atmosphere in horticultural crops: the omega factor. Acta Horticulturae, 171: 187–205.

Karimi, T., Peters, T., Stockle, C.O., 2013. Revising Crop Coefficient for Washington State. ASABE Annual International Meeting, Kansas City, Missouri. Available online at:
http://elibrary.asabe.org/azdez.asp?JID=5&AID=43715&CID=miss2013&T=2

Lakso, A.N., 2003. In Apples: Botany, production and uses, Water Relations of Apples, eds Ferree D.C., Warrington I.J., CABI Publishing, Wallingford, UK, pp 167–195.

Monteith, J.L., 1965. Evaporation and environment: the state and movement of water in living organisms. Symp. Soc. Exp. Biol., 19: 205–234.

Monteith, J.L., Unsworth, M.H., 1990. Principles of Environmental Physics, 2nd Ed., Edward Arnold, New York, p. 53–54.

Naor, A., 2000. Solar noon stem water potential as a plant water stress indicator for irrigation scheduling in fruit trees. Acta Horticulturae 537:447–454.

Naor, A., Cohen, S., 2003. Sensitivity and variability of maximum trunk shrinkage, solar noon stem water potential, and transpiration rate in response to withholding irrigation from field grown apple trees. HortScience, 38: 547–551.

Naor, A., Klein, I., Doron, I., Gal, Y., Ben David, Z., Bravdo, B., 1997. The effect of irrigation and crop load on stem water potential and apple fruit size. Journal of Horticultural Science., 72(5): 765–771.

Nash, J.E., Sutcliffe, J.V., 1970. River flow forecasting through conceptual models part I – A discussion of principles, Journal of Hydrology, 10(3): 282–290.

Nicolasa, E., Torrecillasa, A., Ortuno, M.F., Domingo, R., Alarco, J.J., 2005. Evaluation of transpiration in adult apricot trees from sap flow measurements. Agricultural Water Management, 72: 131–145.

O'Shaughnessy, S.A., Evett, S.R., Colaizzi, P.D., Howell, T.A., 2012. A crop water stress index and time threshold for automatic irrigation scheduling of grain sorghum. Agricultural Water Management, 107: 122– 132.

Palmer, J.W., Giuliani, R., Adams, H.M., 1997. Effect of crop load on fruiting and leaf photosynthesis of 'Braeburn'/M.26 apple trees. Tree Physiology, 17: 741–746.

Paltineanu, C., Septar, L., Moale, C., 2013. Crop Water Stress in Peach Orchards and Relationships with Soil Moisture Content in a Chernozem of Dobrogea. J. Irrig. Drain Eng., 139(1): 20–25.

Pereira, A.R., Green, S.R., Villa Nova, N.A., 2007. Penman-Monteith reference evapotranspiration adapted to estimate irrigated tree transpiration. Agric. Water Manage., 83: 153–161.

Rana, G., Katerji, N., Lorenzi, F., 2005. Measurement and modeling of evapotranspiration of irrigated citrus orchard under Mediterranean conditions. Agric. For. Meteorol. 128: 199–209.

Sepulcre-Canto, G., Zarco-Tejada, P.J., Jimenez-Munoz, J.C., Sobrino, J.A., de Miguel, E., Villalobos, F.J., 2006. Detection of water stress in an olive orchard with thermal remote sensing imagery. Agric For Meteorol., 136: 31–44.

Taghvaeian, S., Chávez, J.L., Hansen, N.C., 2012. Infrared thermometry to estimate crop water stress index and water use of irrigated maize in northeastern Colorado. Remote Sens., 4: 3619–3637.

Testi, L., Goldhamer, D.A., Iniesta, F. & Salinas, M. 2008. Crop Water Stress Index Is a Sensitive Water Stress Indicator in Pistachio Trees. Irrigation Science, 26: 395–405.

Thorpe, M.R., 1978. Net radiation and transpiration of apple trees in rows. Agric. Meteorol., 19: 41–57.

Thorpe, M.R., Warrit, B., Landsberg, J.J., 1980. Responses of apple leaf stomata: a model for single leaves and a whole canopy. Plant Cell Environ. 3: 23–27.

Tokei, L., Dunkel, Z., 2005. Investigation of crop canopy temperature in apple orchard. Physics and Chemistry of the Earth, 30: 249–253.

Wang, D., Gartung, J., 2010. Infrared canopy temperature of early-ripening peach trees under postharvest deficit irrigation, Agricultural Water Management, 97(11): 1787–1794.

Wanjura, D.F., Upchurch, D.R., 1997. Accounting for humidity in canopy-temperature-controlled irrigation scheduling. Agricultural Water Management, 34: 217–231.

CHAPTER FOUR

INFRARED THERMOMETRY AND MICROCLIMATIC MEASUREMENTS IN A FULLY-IRRIGATED APPLE ORCHARD[3]

4.1 Abstract

Apple tree transportation can be estimated using an energy budget model, but it requires knowledge of microclimatic parameters. These data are usually acquired from a nearby weather station while diurnal variations of meteorological variables in the field might be considerably different. A case study was conducted in an apple orchard to investigate possible discrepancies among the measurements within the canopies, in the orchard and those obtained from an adjacent weather station. The measurements of air temperature, relative humidity, and wind speed were taken using a suite of different sensors. Canopy, tree trunk and ground surface under the trees were also monitored using infrared thermometers (IRTs). An exponential model was used to formulate in-depth change of wind speed inside the tree canopies. The relationship between canopy and air temperature difference (ΔT) and vapor pressure deficit (D_a) was also investigated. The IRTs mounted at a 45^{o} angle in 2007 and 2008, resulted in better thermal readings than those mounted perpendicularly or with a nadir view of the canopies in 2013. In addition to a high correlation (R^2 = 0.88), there was a small difference of about 0.7^{o}C between daily mean canopy and trunk surface temperatures suggesting the potential for using trunk temperature as an alternative for traditional IR measurements. Air temperature (T_a) measurements showed high discrepancies between within-orchard and weather station measurements reaching an average difference of 6.3^{o}C at solar noon in 2007. Within-canopy wind velocities were about 0.1 times the surface wind speeds meaning transpiration rates of inner canopy leaves were much lower compared to the leaves at the canopy surface. ΔT was fairly well correlated with D_a for the daylight values in all of the experimental years. Linear regressions yielded better correlation between ΔT and stem water potential (Ψ_{stem}) ($R^2 = 0.76$) once in-field air temperature data was used. In general, the daily means of the measurements from different locations were highly correlated while they were not well related at solar noon (average of 1:00PM–3:00PM). It was concluded that air temperature data should be measured in the field in the vicinity of other plant and microclimate measurements. All other required meteorological parameters can be obtained from a nearby weather station. The results of this study can be a base for later estimations of actual transpiration of apple trees using an analytical model.

Keywords: Microclimate, Air temperature, Wind speed, Infrared thermometry, Vapor pressure deficit

[3] Submitted to ASCE Journal of Irrigation and Drainage Engineering on 7/6/2014

4.2 Introduction

Accurate knowledge of evapotranspiration (ET) is an important key to maintain well-irrigated crops (Tanny, 2013). Apple trees fall into the category of tall, discontinuous horticultural crops with a canopy that is well-coupled to the surrounding air (Jarvis, 1985). The transpiration of apple trees is controlled by stomatal conductance, net radiation and vapor pressure deficit (Lakso, 2003) all of which can be connected through a simple energy budget equation. Thus, by determining the sensible heat flux from leaf surfaces and net radiation, apple leaf transpiration can be estimated. The components of the energy budget equation require microclimatic parameters as their inputs while, in many cases, the most feasible data are acquirable from a weather station in the vicinity of the field. Although apple leaves are well-exposed to the air, the formation of a microclimate around large tree canopies can cause diurnal variations of meteorological variables such as wind speed, relative humidity and air temperature to be notably different than those obtained from a nearby weather station. The study of the trees' microclimate to find relationships between the measurements taken within and outside the field can probably allow for enhancing the estimations of apple trees water use.

An important variable in the energy balance equation is canopy temperature. Different modeling approaches have been developed based on the energy budget and thermal temperature of vegetative surfaces to estimate the ET (Ben-Asher et al., 1989; Taghvaeian et al., 2012) and for irrigation scheduling of row crops (Cohen et al., 2005). However, direct or indirect application of this method has been challenging in non-homogeneous canopies of tree crops. Tokei and Dunkel (2005) reported a case study on the possible use of canopy temperature in the determination of apple tree transpiration by a theoretical approach.

Canopy temperature is measured using an infrared thermometer (IRT) which gives an average temperature value over the top of the surface. In case of a large tree canopy, the leaves range from completely shaded (usually at the lower canopy) to completely sunlit at the top. IR temperature readings have to comply with the assumptions made in the energy budget model of a representative leaf. Mounting position and orientation of the IRT are also of concern. Appropriate mounting position and orientation of the IRT can guarantee the sensor only sees the canopy surface. Any inclusion of soil or sky in the view of the senor can lead to considerable errors in the measurements (Blanquicet et. al, 2009).

The goal here was to investigate the microclimate formed by apple tree canopies to account for any significant difference between measured variables in the field and those at a nearby weather station. In addition, surface temperatures of the ground and tree trunk were measured and compared with canopy temperatures. The effects of various positions and orientations of infrared temperature sensors were also examined.

4.3 Materials and methods

4.3.1 Theoretical considerations

Transpiration model

Neglecting metabolic heat production and heat storage, the energy balance equation for an evaporating apple leaf is:

$$R_n = R_{abs} - L_{oe} = H + \lambda E \tag{4.1}$$

where R_n is the net radiation, R_{abs} is the absorbed radiation by the leaf, λE is the latent heat flux, L_{oe} is the outgoing emitted radiation, H is the sensible heat flux from the leaf, and all terms are in Wm^{-2}. R_n is the difference between the sum of absorbed shortwave and long wave radiations and net radiation (for the leaf), and emitted long wave radiation from the leaf. The term H can be expressed as (Campbell and Norman, 1998):

$$H = g_H C_P (T_l - T_a) \tag{4.2}$$

where C_P is heat capacity of air (29.17 J mol^{-1} C^{-1}), T_l is the leaf temperature (ºC), T_a is air temperature (ºC), g_H is the boundary layer heat conductance (mol m^{-2} s^{-1}). The boundary layer conductance of air to heat for laminar forced (g_H) convection was calculated using the following empirical formulas (Campbell and Norman, 1998):

$$g_H = 2(1.4)0.135\sqrt{\frac{u}{d}} \tag{4.3}$$

where u is the wind speed and d is the characteristic dimension defined as 0.72 times the leaf width ($d = 0.72w_l$). Factor 2 accounts for the fact that apple leaves are hypostomatous. Substituting Eqs. 4.2 and 4.3 in Eq. 4.1 and rearranging it to solve for E ($= T$) yields:

$$T = \frac{R_n - g_H C_P \Delta T}{\lambda} \tag{4.4}$$

where T is the leaf transpiration (mol m^{-2} s^{-1}), ΔT is the leaf and air temperature difference ($T_l - T_a$). The T model was assumed to represent whole canopy transpiration once leaf temperature in Eq. 4.4 has been replaced with canopy temperature (T_c).

Sensitivity analysis

Estimations of transpiration (T) from the T model (Eq. 4.4) requires measurements of canopy temperature (T_c), air temperature (T_a), relative humidity (RH), global solar radiation (R_n) and wind speed (u). To assess the effect of possible errors in the measurements of each input variable, a sensitivity analysis was carried out (Fig 4.4). For this purpose, three arbitrary weather conditions including a) a borderline cloudy, cool and humid, b) a borderline sunny, warm and dry, and c) a mild day having a condition between "a" and "b" were assumed. The values of environmental variables under each condition are presented in Table 4.1.

Table 4.1 Environmental data for two hypothetical conditions under which the sensitivity analysis of the T model was carried out.

	Weather Condition		
Parameter	Cloudy, Cool, Humid	Sunny, Warm, Dry	Mild
T_c [^{o}C]	9.6	30.0	27.0
T_a [^{o}C]	10.0	37.0	30.0
RH [%]	80.0	25.0	50.0
R_n [W m^{-2}]	200	600	400
u [m s^{-1}]	2	2	2

The independent effect of each variable on the estimation of T was assessed by assuming the other variables as constant (Blanquicet et al., 2009). The sensitivity analysis revealed that as the conditions moved from warm, sunny, and dry to cloudy, cool, and humid, T sensitivity to all of the input variables decreased. Assuming a T_c measurement accuracy of ±0.6 ^{o}C which is typical of the IRTs used (manufacturer's specification), an error of ±4% was expected on a sunny, warm and dry day. This error increased to about ±12% under the mild condition. On a cool, cloudy, and humid day, an error of only ±0.6 ^{o}C in T_c measurement yielded ±20% error in T estimations. Error/change in T_a measurement had the same effect on T as T_c.

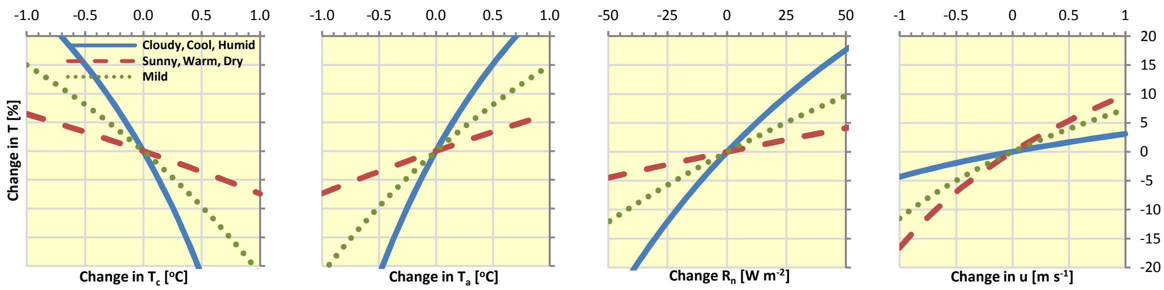

Figure 4.1 Change in T(%) in response to change in an input variable for three hypothetical weather conditions presented in Table 4.1.

On a warm, sunny and dry day, T showed small change/error of about ±5% in response to ±50 W m^{-2} change (or measurement error) in R_n. An error of ±50 W m^{-2} yielded T error of ±20% for the cool, cloudy, and humid condition and ±10% on a mild day. T behavior in response to a change in wind speed (u) was the opposite of other variables under different conditions with errors ranging from ±3% on a cool, cloudy, and humid day to about ±12% On a warm, sunny and dry day, as u changed ±1.0 m s^{-1}.

The sensitivity analysis of the T model suggests that depending on the direction of the error (i.e. negative or positive), the variables measurement errors can cancel each other or add up to one another. Total error (ε_T) can then be calculated as the following:

$$\varepsilon_T = \pm\varepsilon_c \pm\varepsilon_a \pm\varepsilon_R \pm\varepsilon_u \tag{4.5}$$

where ε_c is the measurement error in T_c, ε_a is the measurement error in T_a, ε_R is the error of R_n estimation/measurement and ε_u is the measurement error in u.

4.3.2 Field measurements

Experimental site

The field experiments were conducted in a Fuji apple orchard on the Roza Farm of the Washington State University Irrigated Agriculture Research and Extension Center near Prosser, WA, at the coordinates of latitude 46.26°N, longitude 119.74°W, and 360 m above sea level during the growing seasons of 2007, 2008 and 2013. The site was located in a semi-arid zone with almost no summer rains and an average annual precipitation of 217 mm. The site's soil was a shallow Warden Silt Loam soil (Web Soil Survey) of more than 90 cm deep (field observation).

In 2007 and 2008, the apple trees were young, well-developed and fully-irrigated while in 2013, the same apple trees bore little or no fruit (alternate bearing). During the 2007 and 2008 growing seasons, the trees were spaced 4 m (row spacing) by 2.5 m (tree spacing) apart in the orchard and irrigated by a micro-sprinkler irrigation system with water emitters of 27 L h^{-1} spaced at 2.5 m intervals. During the 2013 growing period, the same orchard was irrigated by two lines of drip tubing laterals of in-line 2.0 L h^{-1} drippers, spaced at 91.4 cm intervals along laterals.

Throughout the growing season, the quantity of irrigation water applied to the trees never allowed the soil water depletion to exceed the 50% (0.96 m) maximum allowed depletion (MAD) for apple trees (Allen et al., 1998). This was assured by taking weekly soil water content readings using a neutron probe (503DR Hydroprobe, Campbell Pacific Nuclear, Concord, CA) to a depth of 90 cm (or deeper) in all of the plots.

Meteorological measurements

Meteorological data of the 2007, 2008 and 2013 growing seasons were obtained from two standard electronic weather station (WS) nearby the apple orchard (Roza and WSU HQ, Washington Agricultural Weather Network). The data included air temperature, humidity, and wind speed at 2 m high above ground.

Measurement of canopy temperature

In 2007 and 2008, IRTs (Exergen model IRt/c.03^{TM}: Type T, Watertown, Mass.) wired to a Campbell CR21X datalogger (Campbell Scientific, Logan, UT, USA) were used to measure the surface temperature of apple trees. In 2013, canopy temperature was measured using a different model of IRT (Excergen model IRt/c.2: Type J, Watertown, Mass.). The IRTs were wired to a network of Campbell CR10 and CR10X dataloggers (Campbell Scientific, Logan, UT, USA) sending out temperature readings to a central computer wirelessly. To minimize radiation absorption by the body of the IRTs, they were shielded by white PVC fittings. The IRt/c.03^{TM} sensors were calibrated using a blackbody calibrator (BB701, Omega Engineering, Inc., Stamford, CT). The IRt/c.2 sensors were pre-calibrated; however, a checking process was conducted using the blackbody calibrator in lab. The accuracy of the thermal readings was also evaluated in the field by comparing water temperatures measured by IRTs and a thermometer. To determine proper orientation and mounting position of the IRTs, the temperature differences from sensors looking at both the north and south sides of a tree were compared with those looking at the east and west sides of a tree.

Microclimatic measurements

A portable suite of sensors was developed based on an original design by Dhillon et al. (2012) to collect microclimatological data from apple tree canopies during the growing period of 2013. The suite included two infrared thermometers (IRTs) with a 6^{o} field view (Model IRt/c.5: Type J, Exergen Co., Watertown, Mass.) to measure surface temperatures of the trunk and ground, a sonic anemometer (WindSonic, Gill Instruments Ltd., Hampshire, UK), and a combined relative humidity and temperature sensor (HMP35C, Vaisala Inc., Woburn, MA). The sensors were wired to a Campbell CR3000 datalogger (Campbell Scientific, Logan, UT, USA). During a 5 week time period (July 30 to September 4), the sensor suite was placed at 3 different locations across the orchard (C1, C2 and C3). Each time the sensor suite was installed at a height of approximately 2 m above the ground in-line with the trees (covered with foliage). The readings were recorded at 15-min intervals, 24 hour a day.

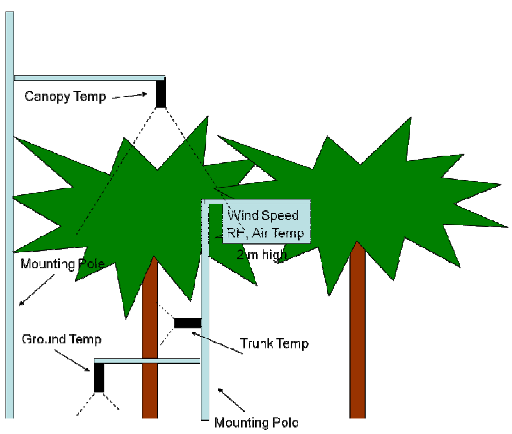

Figure 4.2 Sensor suite setup in 2013: The suite monitored three different locations of the orchard (C1, C2 and C3 where IRt/c.2 sensors were installed) one at a time. It was installed at about 2 m high within tree canopy in-line with tree rows (covered with foliage).

In addition to these data, air temperature was recorded in the field using the embedded temperature sensor of a Campbell CR21X datalogger (Campbell Scientific, Logan, UT, USA) during the growing seasons of 2007 and 2008. In 2013, air temperature was measured using three air temperature sensors (Model 109-L, Campbell Scientific, Logan, UT, USA) installed at a height of 2 m in-line with the trees (not covered with foliage) at three locations distant from each other in the orchard (AT1, AT2 and AT3). The sensors were shielded (41303-5A, Campbell

Scientific, Logan, UT, USA) and wired to Campbell CR10X dataloggers (Campbell Scientific, Logan, UT, USA). Air temperature was calculated by averaging readings from the three sensors.

The three air temperature sensors installed across the field were used to investigate spatial variability across the orchard. Wind speed, relative humidity and air temperatures collected from tree canopies were compared with the corresponding values obtained from the weather station. Ground, tree trunk and canopy IR temperatures were compared with each other. Canopy and air temperature differences were also calculated using the air temperatures from the canopy, field and weather station and were compared. The in-depth wind profile was determined by fitting the wind speed measurements (mean values regardless of wind direction) within the tree canopies and weather station to an exponential model (Cionco, 1972; Wilson et al., 1982; Campbell and Norman, 1998):

$$u(z) = u(h)exp\left[a\left(\frac{z}{h} - 1\right)\right] \tag{4.6}$$

where $u(h)$ is the wind speed at the interface of air-canopy, $u(z)$ is the wind speed at depth z within canopy and a is an attenuation coefficient for mean wind speed in apple tree canopies. The wind speed at the interface was assumed to be the same as wind speed measured at the weather station.

Measurements of stem water potential

During the growing season of 2013, stem water potential (Ψ_{stem}) was measured once per week from mid to late summer (July 31 to October 2). These measurements were taken at solar noon with a 2-hour time window (between 1:00PM and 3:00PM). For these measurements six shaded leaves from the inner, lower part of the trees canopy close to the trunk (where an IRT was mounted) were selected, enclosed in aluminum foil covered plastic envelopes and left attached to the tree for a period of time between 15 min and 60 min. The Ψ_{stem} of the leaves was then measured with a pressure bomb (Model 615, PMS Instrument Co., Albany, OR). The Ψ_{stem} measurements were made under different weather conditions including cold, humid and overcast days.

Statistical analysis

The daily values of the measurements were calculated by averaging the data of 24 hourly (mean), 6:00AM–6:00PM (daylight), 11:00AM–1:00PM (noon), 1:00PM–3:00PM (solar noon) and 1:00AM–3:00AM (after midnight, hereafter called night). Root mean square error (RMSE) was used to measure the average difference between two data sets (time series) obtained collected from different locations including within-canopy, within-orchard and weather station. Standard deviation (STD), the coefficient of variation of STD ($CV\ of\ STD$, the ratio of the standard deviation to the mean) and standard error of estimate (SEE) were also employed to calculate measurement variations and estimation errors, respectively.

4.4 Results and discussions

4.4.1 Position and orientation of IRTs

The temperature readings of the IRTs looking at both the north and south sides of a tree, and those of looking at the east and west sides of a tree were significantly different from zero (Fig. 4.3). It was concluded that either two sensors must be used to look at both sides of a tree and averaged, or a sensor must be placed such that it looks straight down on the top of the tree in a nadir position. If the sensors are oriented this way, row orientation is not critical.

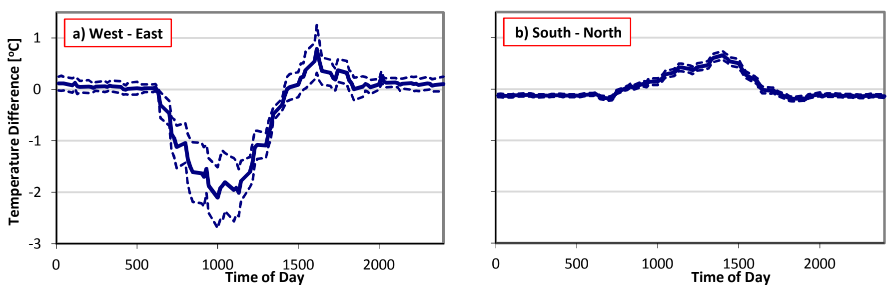

Figure 4.3 The mean temperature difference between the south and north (a, south - north) and the west and east (b) west - east) sides of the tree at different times of day. The dotted lines are the 95% confidence interval on the mean.

Based on the results, in 2007 and 2008, canopy surface temperature was monitored using a total of 12 IRTs (in 6 pairs) pointed downwards at approximately 45 degree angles at both the north and south sides of a tree (Fig 4.4). As illustrated in Fig 4.5 (a–b), no sharp, significant increase in the canopy temperatures was seen during the early-, mid- or late-seasons. This indicates that the IRT readings were not affected by the longwave radiation from the ground surface even on the early days of growing season when the foliage growth was not complete.

In 2013, canopy temperature was measured using 6 individual IRTs mounted perpendicularly above apple trees (one IRT per tree) looking at them from a distance of less than 1.0 m (Fig. 4.2). A similar mounting position and orientation to the latter setup has been successfully tried by Sepulcre-Canto et al. (2006) and Testi et al. (2008) in Olive and Pistachio trees, respectively. However, apple trees are relatively sparse and shorter compared to Olive and Pistachio trees increasing the chance of the ground being seen by the IRT.

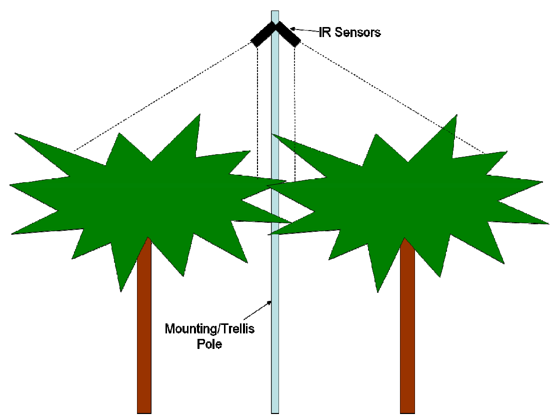

Figure 4.4 In 2007 and 2008, the IRTs were pointed downwards at approximately 45 degree angles at both the north and south sides of a tree.

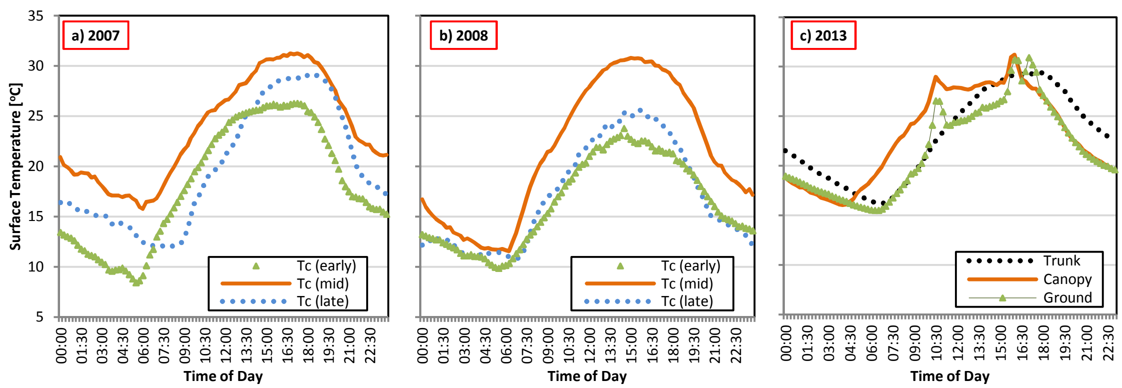

Figure 4.5 Diurnal canopy temperature changes in the growing seasons of 2007 (a) and 2008 (b). The curves represent averages of several successive days during the early- (DOY=143–153), mid- (DOY=190–200) and late-seasons (DOY=240–250). Diurnal canopy, ground and tree trunk temperature changes (c). Each value represents the average of thermal readings taken at the same time over a period of 5 weeks.

The tree trunk maintained a lower surface temperature than the canopy until solar noon when it showed higher temperatures of up to about 3^{o}C (Fig. 4.5c). The ground surface and canopy temperatures also appeared to be almost the same late in the afternoon and through the night. A sudden change in the ground temperature around 10:00AM was probably related to a direct solar radiation incident on the ground. The increase started at about 9:30AM and returned to normal at 11:00AM. A similar pattern was recognized at around 4:30PM when the ground surface was hit by direct sunlight as the sun was setting. A corresponding increase in the readings of canopy temperature occurred at the same times. It can be seen that canopy temperature readings of the IRT installed perpendicularly above the canopies was significantly affected by the longwave radiation from the ground while the readings of trunk surface temperate seemed to be unaffected by the ground longwave radiation.

4.4.2 Field variability

Air temperature

The air temperature measurements showed small variations across the orchard with an average C_v of 4.1% and STDs of 0.66^{o}C, 1.06^{o}C and 0.58^{o}C for the daily mean, solar noon and night values, respectively. The variability of 0.58^{o}C at night indicated the non-uniformity of the sensors and/or offset errors of the dataloggers while differences among the ATs at other times were caused by non-uniformity of apple tree canopies. Assuming within-field temperature differences as the only source of variability, daily average estimations of T were associated with an uncertainty of about ±4% on a sunny, warm and dry day, ±12% under the mild condition and ±20% on a cool, cloudy, and humid day.

Canopy temperature

As expected, the highest variability among individual or pairs of IRTs was seen at solar noon in all of the experimental years with 0.71^{o}C, 1.18^{o}C and 1.69^{o}C in the growing seasons of 2007, 2008 and 2013, respectively (Table 4.2). The readings at night presented the lowest variability, yet still relatively high differences of 0.40^{o}C, 0.81^{o}C and 0.74^{o}C in 2007, 2008 and 2013, respectively which was slightly higher than the expected accuracy of ±0.6^{o}C (manufacture's specification) in 2008 and 2013 and smaller in 2007.

Averaging the readings from 3 pairs of IRTs in 2007 and 2008, and 3 individual IRTs in 2013 decreased the variability to less than 0.35^{o}C at all time scales. The C_v of canopy temperature measurements among the two blocks/rows of apple tree canopies (averages of 3 individual/pairs of IRTs per block/row) and from year to year was about 4.8%. A low canopy temperature variability and small C_v indicate how by increasing the number of IRT sensors used per plot a better thermal input for the T model can be achieved. In addition, this could be an indication that, as planned, all of the trees were well-irrigated (Testi et al., 2008) and that the canopy surface viewed by the IRTs were good enough.

Table 4.2 Variability of T_c among the 6 pairs of IRTs in 2007 and 2008, and 6 individual IRTs in 2013 installed across the orchard, as well as among averages of measurements (averages of 3 individual/pairs of IRTs) for daily mean, solar noon and night values.

	Individual/Pairs of IRTs (^oC)			Averages (^oC)		
Year	Mean	Solar noon	Night	Mean	Solar noon	Night
2007	0.41	0.71	0.40	0.24	0.28	0.16
2008	0.82	1.18	0.81	0.22	0.34	0.21
2013	1.01	1.69	0.74	0.20	0.27	0.18

4.4.3 Daily changes

Comparisons of daily mean and solar noon of microclimatic measurements taken at the weather station, in the orchard and within the tree canopies (sensor suite) during the 5 weeks of the experiment in the growing season of 2013 are presented in Tables 4.3–4. Overall results indicated that, with the exception of relative humidity, the daily mean measurements of wind speed, air temperature and canopy temperature taken in the field and weather station were fairly well correlated to those taken within the canopies.

Thermal measurements

With the exception of a few days, tree canopies maintained temperature values of several degrees above the ground temperatures with average values of 23.0^{o}C compared and 21.7^{o}C for daily mean temperatures (Fig. 4.6a), and 28.6^{o}C compared to 25.1^{o}C for daily solar noon temperatures (Fig. 4.6b). The discrepancies between the ground and trunk temperatures were high on both daily mean (RMSE = 1.7^{o}C) and solar noon (RMSE = 2.0^{o}C) scales and the trunk presented higher temperatures on most days. Lower surface temperatures of the ground at all time scales could be an indication of minimal contribution to canopy temperature measurements.

Table 4.3 Comparisons of daily mean measurements taken within canopy, in the field (orchard) and those of obtained from the nearby weather station.

	$u(m\ s^{-1})$		RH(%)		$T_a(^oC)$			$T_{IR}(^oC)$		
	Canopy	WS	Canopy	WS	Canopy	WS	Field	Trunk	Ground	Canopy
Avg	0.13	1.96	57	59	22.6	22.8	23.0	23.1	21.7	23.0
STD	0.08	0.38	8	10	2.2	1.9	2.1	2.0	1.7	1.9
SEE		0.02		6.2		0.9	0.5		1.0	0.7
RMSE		1.73		7.7		0.9	0.6		1.7	0.7
R-Sqr		0.60		0.45		0.85	0.95		0.77	0.88

Table 4.4 Comparisons of daily solar noon measurements taken within canopy, in the field (orchard) and those of obtained from the nearby weather station.

	$u(m\ s^{-1})$		RH(%)		$T_a(^oC)$			$T_{IR}(^oC)$		
	Canopy	WS	Canopy	WS	Canopy	WS	Field	Trunk	Ground	Canopy
Avg	0.18	2.23	43	45	28.3	29.1	29.5	26.8	25.1	28.6
STD	0.12	0.92	6	12	2.1	2.7	2.6	1.5	1.6	2.5
SEE		0.07		5.5		1.2	1.2		1.8	1.5
RMSE		1.92		12.2		1.7	1.9		3.9	2.3
R-Sqr		0.21		0.04		0.66	0.66		0.52	0.66

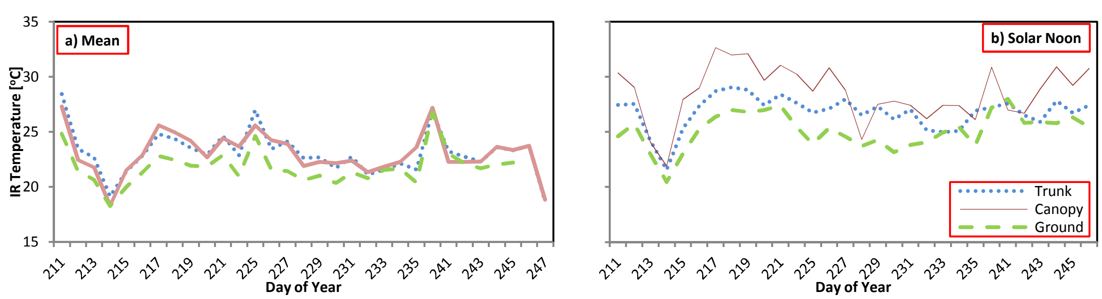

Figure 4.6 Daily mean (a) and solar noon (b) canopy, shaded ground and tree trunk temperatures for a period of 5 weeks (three separate periods each lasting two weeks).

Daily mean canopy and trunk temperatures showed high similarity on both average and amplitude with small discrepancies (RMSE of 0.7°C). The average of daily mean canopy temperatures was 23.1±2.0°C compared to a value of 23.0±1.9°C for the average of daily mean trunk temperatures. A high correlation between daily mean canopy and trunk surface temperatures (Fig 4.7a, R^2 = 0.88), allowed for canopy temperature estimations with a SEE of only 0.7°C. Considering a weaker correlation among daily solar noon values of the measurements (Fig 4.7b, R^2 = 0.77), the determination of canopy temperature from trunk temperatures resulted in a high SEE of 1.7°C.

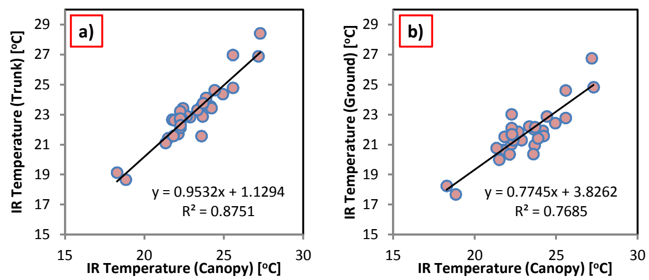

Figure 4.7 The relationship between canopy temperature, and trunk (a) and ground (b) surface temperatures for the daily mean values.

Air temperature measurements

The averages of the daily mean air temperature showed small differences with values of 22.6±2.2°C, 22.8±1.9°C and 23.0±2.1°C for the canopy, weather station and field (averages of readings across the orchard) measurements, respectively. At solar noon, weather station and field measurements presented almost similar behaviors in terms of average and amplitude of variations with values of 29.1±2.7°C and 29.5±2.6°C while canopy measurements were lower in both average (Avg = 28.3°C) and amplitude (STD = 2.1°C). There were small discrepancies between air temperature measurements in the field and within the canopies for the daily mean (RMSE = 0.6°C). The difference among the daily solar noon temperature measurements was high (RMSE = 1.9°C).

Both daily mean air temperatures of field and weather station measurements were highly correlated with those taken in the canopies with R^2 of 0.95 ($P<0.001$) and 0.85 ($P<0.001$), respectively. Daily mean estimations of canopy temperature using field or weather station data were associated with SEEs of 0.5 °C and 0.9 °C. This did not seem to have any significant improvements over a direct use of air temperature data obtained from the field or weather station as RMSEs were calculated to be 0.6 °C and 0.9 °C, respectively. It was shown that for ±0.6 °C error in air temperature measurement, the daily mean estimations of T were associated with an uncertainty of about ±4% on a sunny, warm and dry day, ±12% under the mild condition and ±20% on a cool, cloudy, and humid day.

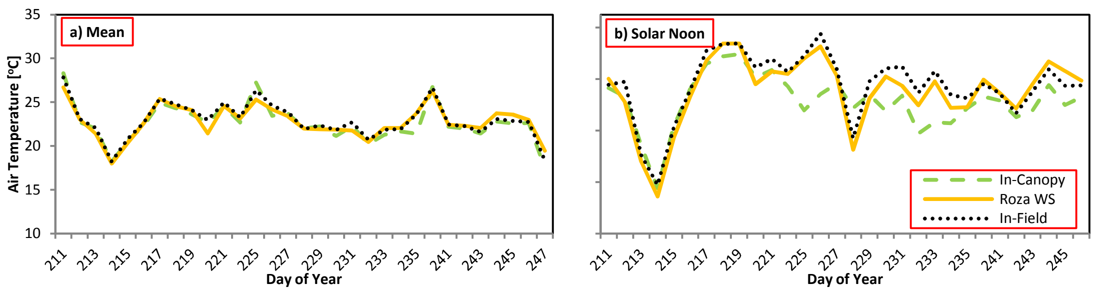

Figure 4.8 Daily changes of mean (a) and solar noon (b) air temperatures for the canopy, field and weather station measurements.

In addition to the within-canopy measurements of air temperature using the sensor suite, we collected air temperature data in the orchard in the entire growing seasons of 2007, 2008 and 2013. The highest (average) difference between air temperature measurements in the orchard and weather station occurred at solar noon in 2007 with RMSE of 6.3°C (Table 4.5) followed by RMSEs of 4.9°C and 3.9°C for daily solar noon values in 2008 and daily night measurements in 2007. There was a relatively low correlation between the measurements at the two locations at solar noon in 2007 (R^2 = 0.58, P<0.001) with a SEE of 4.2°C while daily mean values were highly correlated (R^2 = 0.93, P<0.001) with SEE of 1.6°C. In 2008, the daily mean and solar noon air temperatures in the orchard were estimated from weather station air temperature data with SEEs of 1.1°C (R^2 = 0.88, P<0.001) and 1.5°C (R^2 = 0.97, P<0.001) which were significantly better than the average differences of 1.9°C and 4.9°C, respectively.

In 2013, smaller temperature variability was observed at all time scales with RMSEs of 0.4°C, 0.8°C and 1.1°C for the mean, solar noon and night measurements. This could be attributed to lower transpiration rates of apple trees due to small fruit loads and consequently less impact on the ambient air temperature. In addition, a network of three sensors installed across the field provided a more accurate average of air temperature compared to one point measurements in 2007 and 2008. In 2013, estimations of within-orchard air temperatures from the weather station data did not show any advantage over direct use of within-orchard air temperatures (RMSE ≈ SEE). Although the differences in daily mean values were lower compared to the solar noon averages, a minimum (average) difference of about 0.8°C seen at solar noon in 2013 could easily result in T estimation errors of up to ±30%.

Table 4.5 Comparisons of T_a measurements (^oC) in the orchard and air temperature data obtained from the nearby weather station for daily, solar noon and night time values.

	Mean			Solar Noon			Night		
Year	RMSE	SEE	R-Sqr	RMSE	SEE	R-Sqr	RMSE	SEE	R-Sqr
2007	2.8	1.6	0.93	6.3	4.2	0.58	3.9	2.2	0.88
2008	1.9	1.1	0.88	4.9	1.5	0.97	1.5	1.4	0.97
2013	0.4	0.4	0.97	0.8	0.8	0.99	1.1	1.0	0.97

Relative humidity

Relative humidity does not explicitly appear in Eq. 4.4. However, through affecting the stomatal conductance it impacts canopy thermal temperature. The average difference between the RH measured within the canopies and that measured at the weather station was 7.7% and 12.2% for daily mean and solar noon measurements. In general, mean RH of apple tree canopies was higher than the weather station RH (lower D_a). This difference was more pronounced for the solar noon measurements. Both the daily mean and solar noon readings (averages) showed occasions when RH at the weather station was very high while the canopy RH was much lower (Fig. 4.9a–b).

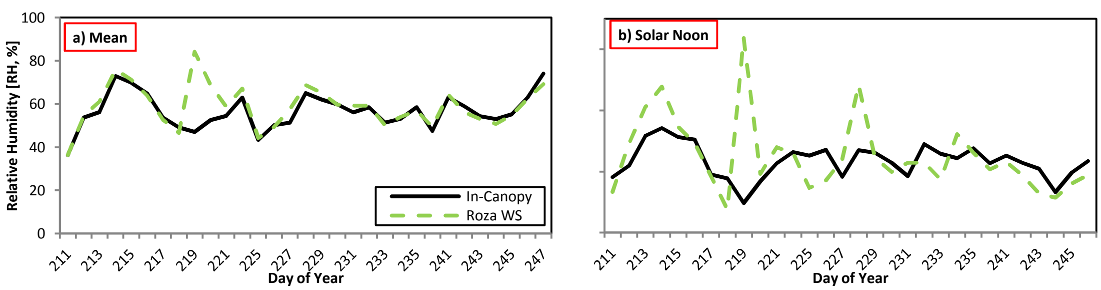

Figure 4.9 Daily mean (a) and solar noon (b) changes of relative air humidity measured within canopy and those of obtained from Roza weather station.

This could be due to sensor malfunctioning or a temporary change in the weather station microclimate. Considering that the weather station was part of an agricultural weather network installed in an irrigated field (near the orchard) a change in the weather station microclimate was more probable and could be related to a temporary increase in RH due to operating sprinklers upwind of the weather station. As a result of this, poor correlation existed between the measurements of RH at the two locations for daily means (R^2 = 0.45, P<0.001). There was no correlation at solar noon (R^2 = 0.04, p= 0.261).

Wind Speed

There was a fairly good correlation between wind speed measurements within the tree canopies and the weather station for the daily mean values (Fig. 4.10a) compared to a poor correlation for the daily solar noon measurements with R^2 of 0.21 (Fig. 4.10b, P<0.028). The difference between the daily mean measurements at the two locations was high with RMSE of 1.73 m s^{-1}, however because of a good correlation between the wind speed data obtained from the weather station and canopies (R^2 = 0.60, P<0.001), within-canopy wind speed could be estimated with a relatively small SEE of 0.02 m s^{-1} (Table 4.2).

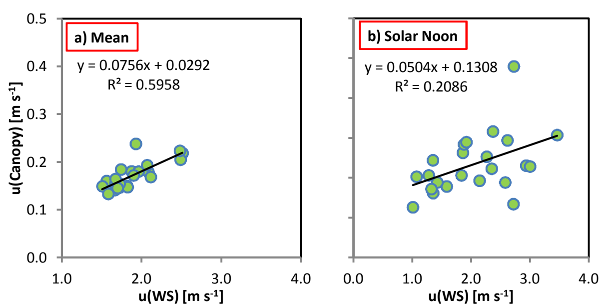

Figure 4.10 The relationship between within-canopy and weather station wind speeds for the daily mean (a, p<0.001) and solar noon (b, p=0.028) values.

The average ratio of the wind speed values measured at the center of the tree canopies (u_0) and the ones obtained from the weather station ($u_{1.5}$), regardless of relationship significance, were 0.09 and 0.09 for the diurnal and mean averages respectively, and this ratio was 0.12 for the solar noon values. It was assumed that wind speed measurements on the crown of the trees were the same as those of obtained from weather station. Considering the sensitivity of T to wind speed (Fig. 4.1), much lower within-canopy velocities of about 0.1 times the surface wind speeds meant transpiration rates of inner canopy leaves were much lower compared to the leaves at the top of the canopy. For example, the estimation of inner canopy T, when the average wind speed obtained from a nearby weather station (or at the top of the canopies) is 2 m s^{-1}, will simply lead to an error of ±20% on a warm, sunny and dry day.

The ratio of the wind speed values measured within tree canopies (u_z) and the ones obtained from the weather station ($u_h, h = 1.5\ m$) were fitted to an exponential equation (Eq. 4.6). The attenuation coefficient (average) for the apple tree canopies was calculated to be $a = 2.43$ ($a = 2.43 \pm 0.36$). No significant difference was found among the coefficient values calculated across the orchard (P = 0.922). The value of the coefficient was very close to the open canopy attenuation factor (a = 2.5; Raupach et al., 1996) indicating a similar degree of wind attenuation by apple tree foliage which was somewhat unexpected. The attenuation coefficient for apple tree canopies was relatively independent of the wind speed at the canopy surface, ($u_{1.5}$; $R^2 = 0.16$, P<0.001) and fairly correlated with the wind speed measurements within the canopies (u_0; $R^2 = 0.58$, P<0.001). The in-depth profile of wind speed from the center of the canopy to a diameter of 1.5 m at the border with the air (h = 1.5 m) is depicted in Fig 4.11.

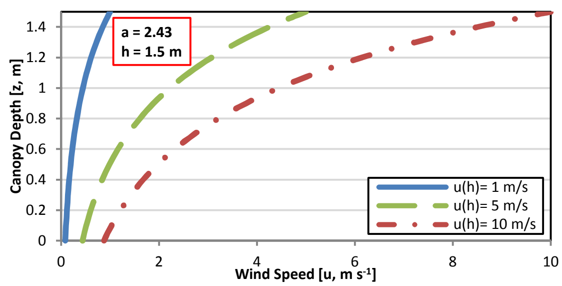

Figure 4.11 Profile of wind speed within apple tree canopies based on above canopy wind speeds, canopy depth of 2.5 m and attenuation coefficient of a = 2.43.

4.4.4 Canopy and air temperature differences

The daily mean values of canopy and air temperature differences (ΔT) were calculated using air temperature measurements at the three locations over the course of 5 weeks in the growing season of 2013. The results of this analysis are presented in Table. 4.6. The pattern of ΔT changes if air temperatures from the nearby weather station are used compared to that of ΔT calculated using within-canopy air temperature data for both the mean ($R^2 = 0.01$, p=0.663) and solar noon ($R^2 = 0.07$, p=0.166) values. A good correlation existed with the mean values of ΔT calculated using within-orchard air temperature data ($R^2 = 0.50$, p<0.001) allowing for estimations of ΔT with an error of 0.5°C. However, this improved estimations of ΔT only 0.1°C (RMSE = 0.6°C).

Table 4.6 Comparisons of the daily mean ΔT (°C) calculated using canopy temperature and air temperature measurements taken within the canopies, in the orchard and those of obtained from the nearby weather station.

	Mean			Solar Noon		
	Canopy	WS	Orchard	Canopy	WS	Orchard
Avg	0.4	0.3	0.1	0.3	-0.5	-1.0
STD	0.7	0.5	0.4	1.3	1.3	1.4
SEE		0.7	0.5		1.3	1.2
RMSE		0.9	0.6		1.7	1.9
R-Sqr		0.01	0.50		0.07	0.17

The diurnal ΔT computed using canopy temperature and air temperature measurements taken at the three locations of the weather station, orchard/field, and canopies revealed a difference in ΔT among the tree canopies monitored by individual IRTs (Fig. 4.12a–c). Two of the monitored tree canopies (C1 and C2; Fig. 4.12a–b) had more similar changing patterns while C3 (Fig. 4.12c) exhibited a completely different pattern of ΔT changes. As it can be seen in Fig. 4.12(c), two sharp rising points on the curves at about 11:30AM and 4:30PM are clearly distinguishable. As previously identified in the diurnal changes of canopies average thermal temperature (Fig. 4.5c), this was most probably the contribution of longwave radiation from the ground surface to the temperature readings of the IRT installed in the C3 canopy. The discrepancy between C1 and C2 was most probably reflecting a high degree of non-uniformity among the tree canopies in 2013.

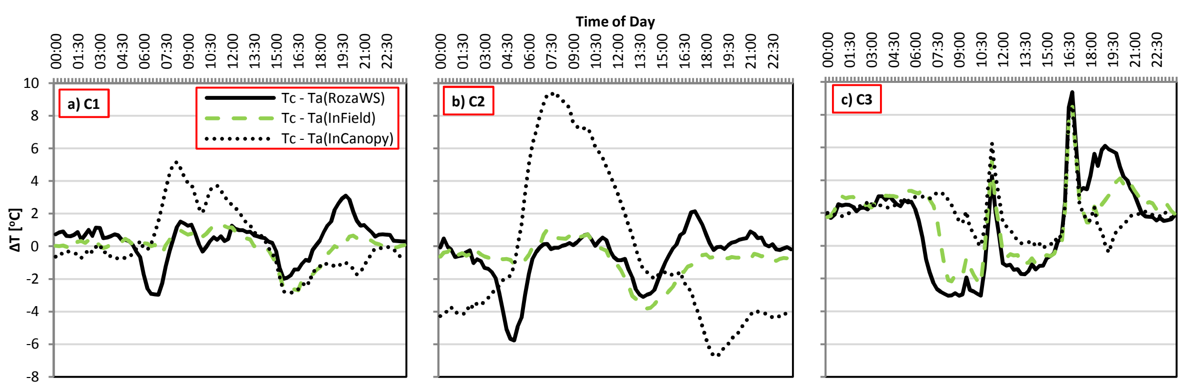

Figure 4.12 Diurnal changes of canopy and air temperature differences averaged over a period of 5 weeks.

ΔT *and* D_a

The results of linear regressions between the daily mean, daylight, noon and solar noon values of D_a, and ΔT for the time period of mid- and late-seasons in 2007, 2008 and 2013 are presented in Fig. 4.13–14. In general, the R-squared was low with values of 0.36 ($p < 0.001$) in 2007 (Fig. 4.11a1) and 0.47 ($p < 0.001$) in 2008 (Fig. 4.11b1) for the mean values, and 0.53 ($p < 0.001$) in 2007 (Fig. 4.11a2) and 0.69 ($p < 0.001$) in 2008 (Fig. 4.11b2) for the daylight ones. In 2013, the results of correlation between D_a and ΔT were better with R^2 of 0.66 (Fig. 4.11c1) for the means and 0.74 (Fig. 4.11c2) for the daylight values.

In 2007, 2008, the slopes and intercepts of the relationships were similar with -1.09 and -1.13 for the means, -1.11 and -1.37 for the daylight values, and -0.97 and -1.06 for the solar noon values. The slopes of the relationships at noon were about 60% more (negative) with values of -1.63 and -1.61 in 2007 and 2008, respectively. This was probably due to the high stomatal activity of apple trees late in the morning previously observed by Tokei and Dunkel (2005). In 2013, as a result of alternative bearing leading to less stomatal activity (Palmer et. al., 1997), the slope of the relationship at noon was the same as the slope for the mean values (-0.67 vs. -0.69). In 2013, only the slope of the relationship between the daylight values of D_a and ΔT (-0.98) was similar to the 2007 and 2008 experiments.

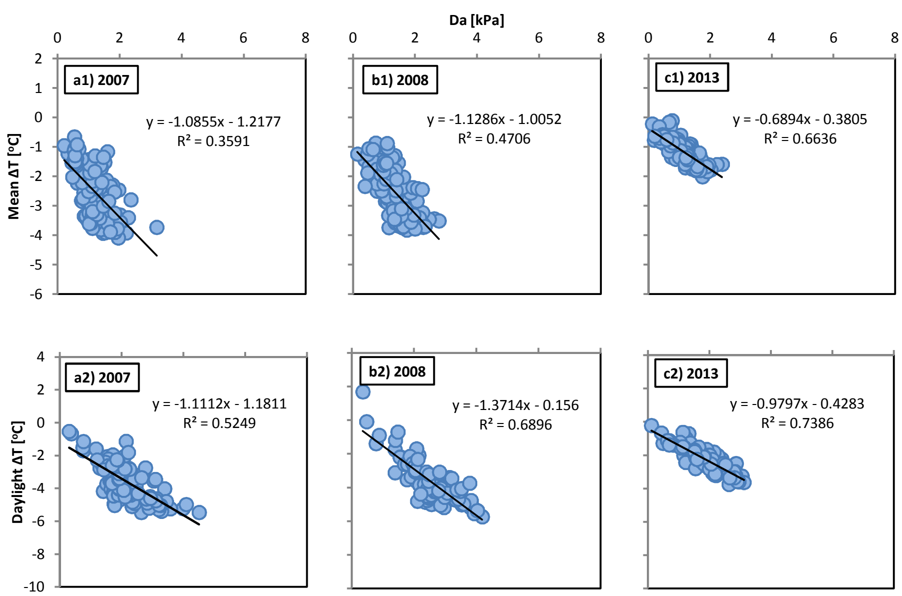

Figure 4.13 Daily mean (a1–c1) and daylight (a2–c2) values of vapor pressure deficit (D_a) versus canopy and air temperature difference (ΔT) in the growing seasons of 2007, 2008 and 2013. Cloudy days were included.

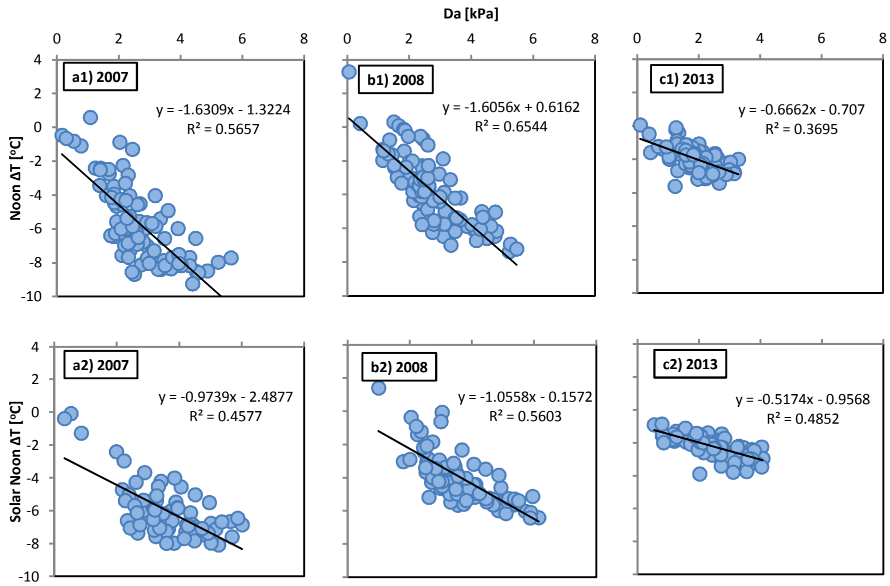

Figure 4.14 Daily noon (a1–c1) and solar noon (a2–c2) values of vapor pressure deficit (D_a) versus canopy and air temperature difference (ΔT) in the growing seasons of 2007, 2008 and 2013. Cloudy days were included.

ΔT *and solar noon* ψ_{stem}

Up to six Ψ_{stem} readings (per tree per measurement day) taken in different weather conditions were averaged to calculate the Ψ_{stem} corresponding to each IRT. The trees maintained relatively high solar noon Ψ_{stem} over the period of the experiment with fluctuations driven by the weather conditions. Considering there was no water stress, Ψ_{stem} was mainly dependent on solar radiation, air temperature and relative humidity, thus Ψ_{stem} was higher (less negative) under more humid, cooler conditions and higher (more negative) under warmer, drier conditions. During this period, solar noon Ψ_{stem} values were limited to a range with a minimum of -11.0 bar and maximum of -3.5 bar. Linear regressions between ΔT and Ψ_{stem}, once in-field air temperature data is used, yielded a fairly good correlation with $R^2 = 0.76$ (p <0.001; Fig. 4.18b) while that of air temperature obtained from the weather station resulted in weaker correlation with $R^2 = 0.58$ (p <0.001; Fig. 4.18a).

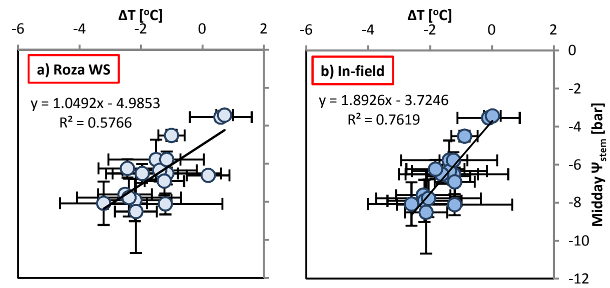

Figure 4.15 Linear relationship between solar noon ψ_{stem} and solar noon ΔT calculated using air temperature data from a weather station (a) and in-field air temperatures (b). Each ψ_{stem} value represents the average of up to six measurements. The error bars show the standard error of the mean.

4.5 Conclusions

Based on the energy budget of a single leaf, a simple model for estimating apple trees transpiration was developed. To determine the contribution of measurement errors/uncertainties in estimated T, microclimatological parameters including T_a, RH, u, T_c, and thermal temperatures of trunk and ground were measured within the canopies using a suite of different sensors and compared with those of measured across the orchard (close to the canopies) and obtained from a nearby weather station. This was done considering the fact that large tree canopies significantly impact their surrounding environment. The contribution of errors in measurements/estimation of R_n was not part of this study.

The sensitivity analysis showed that the transpiration model was fairly sensitive to wind speed measurements (±20 in T for ±1 error in u). In the application of the T model, the wind speed at the surface of the tree canopies was assumed to be the same as the wind speed obtained from a weather station, while this might be true, the crown of apple tree canopies is not a homogeneous surface. Thus, not all of the top canopy leaves are exposed to the same wind flow. Instead of using the surface wind speed, taking an "effective depth" for the measurements (or estimations) of wind speed might be a better representative of the top leaves. Moreover, wind speeds at the center of the canopies were approximately 10 times slower than those obtained from a nearby weather station (g_H of about 3.2 times less). This means transpirations from individual leaves within a canopy are highly variable with T being much lower at the center of canopy than the crown.

The required number of IRTs is a function of variability among canopies, orientation, position and field view of IRTs. The results of our experiment with perpendicularly installed sensors above apple trees showed a high variability among individual IRTs. This suggests that readings from individual IRTs cannot be trusted as the chance of the ground being seen by the sensor is high. As for the IRTs looking at canopies at 45 degree angles at the north and south sides, a pair of sensors seemed to have enough resolution. In case of high variability among the trees, the average of several pairs of IRTs can provide a better average of orchard transpiration.

Tree trunk is a relatively big component of the foliage which was expected to be in balance with the average canopy temperature. Thermal measurements revealed small differences between tree trunk surface temperature in terms of average and amplitude suggesting it as an alternative for canopy temperature measurements. Monitoring trunk temperature can decrease the chance of including longwave radiation from the ground to zero as a horizontally mounted IRT with a very narrow field of view can be used.

D_a has been proven to be linearly related to ΔT (Idso et al., 1981) in row crops and in Pistachio trees (Testi et al., 2008). This linear relationship was first explained by the theoretical approach of Jackson et al. (1981) where the intercept and slope of the relationship were mainly functions of g_H and R_n, and T_c, respectively. Since relative humidity affects apple leaves stomata (Rana et al., 2005; Dragoni et al., 2005), the relationship between D_a and ΔT was expected to be more complicated. The high similarity between the results from 2007 and 2008 when the trees were young and healthy confirmed the existence of a relationship between D_a and ΔT. Due to a stomatal response to changes in relative humidity; however, any estimations of ΔT using D_a will be associated with high errors. It was concluded that a theoretical approach which accounts for all of the factors affecting T_c needs to be developed to relate D_a to ΔT.

In general, the differences between weather station and field measurements were big enough to conclude that measurements from a nearby weather station are not a feasible alternative for within-orchard measurements. The errors were the highest at solar noon and minimum when daily mean values were used to estimate T. Except for the wind speed measurements, no significant difference was seen between the measurements taken within the canopies and in the vicinity of the canopies (within-orchard). Air temperature measurements showed the highest variability among different locations at all time scales. Therefore, it is recommended to measure air and canopy temperatures in the same spot. We suggest that air temperatures measured in the field in the vicinity of the trees be used. All of the other required meteorological parameters can be obtained from a nearby weather station.

Acknowledgments

This work was funded by the US Department of Agriculture Specialty Crop Research Initiative (USDA SCRI) grant. The authors would like to thank Clint Graf for his help in establishing the irrigation system, weed control, and pesticide applications. The authors thank Sean E. Hill, Evan Zumini and Robert Dickson for helping with a number of computer related issues, as well as Alan Kawakami and Lynn Mills for their assistance with the pressure bomb.

We also acknowledge the assistance and support of the Center for Precision and Automated Agricultural Systems (CPAAS) at Washington State University.

References

Allen, R.G., Pereira, L.S., Raes, D., Smith, M., 1998. Crop evapotranspiration: guidelines for computing crop water requirements. Irrigation and Drainage Paper No. 56. FAO, Rome, Italy, 300 pp.

Ben-Asher, J., Phene, C.J., 1992. User's guide for estimating crop evapotranspiration (ET_c) using the infrared thermometry (IRT) method. California Agricultural Technology Institute–CATI, Ben Gurion Univ. of the Negev, Israel. Available online at: http://cwi.csufresno.edu/wateright/920701.asp

Campbell, G.S., Norman, J.M., 1998. An Introduction to Environmental Biophysics. Springer-Verlag, New York, NY, USA, 286 pp.

Cionco, R., 1972. A wind-profile index for canopy flow. Boundary-Layer Meteorology, 3: 255–263.

Cohen, Y., V. Alchanatis, M. Meron, Y. Saranga, and J. Tsipris. 2005. Estimation of leaf water potential by thermal imagery and spatial analysis. J. Exp. Bot. 56(417):1843-1852.

Dhillon, R., Udompetaikul, V., Rojo, F., Roach, J., Upadhyaya, S., Slaughter, D., Lampinen, B., Shackel, K., 2012. Detection of Plant Water Stress Using Leaf Temperature Measurements for Vineyard and Nut Crops. Transactions of the ASABE, available online at: https://elibrary.asabe.org/azdez.asp?JID=5&AID=42634&CID=dall2012&T=1.

Dragoni, D., Lakso, A., Piccioni, R., 2005. Transpiration of apple trees in a humid climate using heat pulse sap flow gauges calibrated with whole-canopy gas exchange chambers. Agric. For. Meteorol., 130: 85–94.

Idso, S.B., Jackson, R.D., Pinter, P.J., Reginato, R.J., Hatfield, J.L., 1981. Normalizing the stress-degree-day parameter for environmental variability. Agric. Meteorol., 24: 45–55.

Jackson, R.D., Idso, S.B., Reginato, R.J., 1981. Canopy temperature as a crop water stress indicator. Water Resour. Res., 17: 1133–1138.

Jarvis, P.G., 1985. Coupling of transpiration to the atmosphere in horticultural crops: the omega factor. Acta Horticulturae, 171: 187–205.

Lakso, A.N., 2003. In Apples: Botany, production and uses, Water Relations of Apples, eds Ferree D.C., Warrington I.J., CABI Publishing, Wallingford, UK, pp 167–195.

Palmer, J.W., Giuliani, R., Adams, H.M., 1997. Effect of crop load on fruiting and leaf photosynthesis of 'Braeburn'/M.26 apple trees. Tree Physiology, 17: 741–746.

Rana, G., Katerji, N., Lorenzi, F., 2005. Measurement and modeling of evapotranspiration of irrigated citrus orchard under Mediterranean conditions. Agric. For. Meteorol. 128: 199–209.

Raupach, M.R., Finnigan, J.J. and Brunet, Y., 1996. Coherent eddies and turbulence in vegetation canopies: the mixing-layer analogy. Boundary-Layer Meteorology, 78: 351–382.

Sepulcre-Canto, G., Zarco-Tejada, P.J., Jimenez-Munoz, J.C., Sobrino, J.A., de Miguel, E., Villalobos, F.J., 2006. Detection of water stress in an olive orchard with thermal remote sensing imagery. Agric For Meteorol., 136: 31–44.

Taghvaeian, S., Chávez, J.L., Hansen, N.C., 2012. Infrared thermometry to estimate crop water stress index and water use of irrigated maize in northeastern Colorado. Remote Sens., 4: 3619–3637.

Testi, L., Goldhamer, D.A., Iniesta, F. & Salinas, M. 2008. Crop Water Stress Index Is a Sensitive Water Stress Indicator in Pistachio Trees. Irrigation Science, 26: 395–405.

Tanny, J., 2013. Microclimate and evapotranspiration of crops covered by agricultural screens: A review. Biosystems Engineering, 114: 26–43.

Tokei, L., Dunkel, Z., 2005. Investigation of crop canopy temperature in apple orchard. Physics and Chemistry of the Earth, 30: 249–253.

Wilson, J.D., Ward, D.P., Thurtell, G.W., Kidd, G.E., 1982. Statistics of atmospheric turbulence within and above a corn canopy. Boundary-Layer Meteorol., 24: 495–519.

CHAPTER FIVE

DEVELOPMENT OF A WIRELESS CENTRAL CONTROL SYSTEM AND AUTOMATIC ALGORITHMS FOR PRECISION IRRIGATION OF APPLE TREES

5.1 Abstract

To maximize irrigation efficiency, applied water has to be precisely adjusted to crop water use. A wireless data collection network was developed to create a site-specific irrigation water control system in a Fuji apple orchard. The work involved developing sensor nodes, base station, graphical user interface, and required scheduling algorithms to provide a fully automated irrigation system. The irrigation algorithms embraced the main categories of plant-based, soil-based and weather-based approaches including time temperature threshold (TTT), crop water stress index (CWSI), soil water potential, evapotranspiration (ET), neutron probe (NP), as well as combinations of the various approaches and conventional irrigation in the region. A comprehensive energy balance analysis of apple orchard canopies using a big leaf approach provided the base for developing lower and upper boundaries of the CWSI. A robust "adaptive" control algorithm was developed with CWSI as its core to automatically irrigate apple trees. The models used canopy temperature and meteorological data from a local weather station (i.e. relative humidity, solar radiation, wind speed, and air temperature) as inputs. Various precision irrigation methods of Fuji apple trees were compared based on the total irrigation water applied and crop water during the growing season of 2013. Statistical analysis revealed that the CWSI and midday stem water potential (Ψ_{stem}) were highly correlated ($R^2 = 0.78$). The CWSI algorithm was able to avoid over irrigation early in the season and under humid, cold weather. The total irrigation water applied by the traditional practice of applying water in the region (CNTRL) was significantly higher than all other methods (1345 mm; $P < 0.001$). Among the other methods, ET-based and soil-based (SOIL) methods resulted in the highest and lowest applied water with values of 456 mm and 214 mm, respectively. The t-test revealed that there was a significant difference between the total ET_c estimated for the season and the water use of the NP ($p = 0.021$), TTT ($p < 0.001$), and CWSI treatments ($p = 0.021$). The means of water use in the plots under the NP treatment had a higher variability compared to the TTT and CWSI treatments with standard deviation of 77 compared to 11 and 62, respectively. This could be related to a high variability among the trees of different plots. The overall performance of the control system was satisfactory.

Keywords: Wireless control system, graphical user interface, precision algorithm, irrigation scheduling

5.2 Introduction

The employment of appropriate irrigation scheduling methods can lead to increased profit and water savings for farmers, reduced environmental impacts and sustainable agriculture (Smith et al., 1996). To date, research has offered a large number of agricultural water scheduling tools including procedures to compute crop water needs and to simulate the soil water balance (Pereira, 1999). Quantitative irrigation scheduling methods may be grouped into monitoring of soil water status, calculations of soil water budget, sensing of crop stress and reference evapotranspiration (ET_r) calculations using weather data (Al-Kaisi et al., 1997; Orta et al., 2003; Jones, 2004; Ko and Piccinni, 2009; Kisekka et al., 2010). For soil water balance models, soil water in the root zone is the base used to determine when to irrigate. Leaf and stem water potentials or canopy temperature are also monitored as trigger points of irrigation for the methods based on crop status (Stegman et al., 1976; Turner, 1988; Jackson et al., 1977; Wanjura et al., 1995).

Due to advances in irrigation science, new technologies have emerged in the context of agriculture (Wiedenfeld, 2004; Kallestad et al., 2006; Farahani et al., 2007). ET-based irrigation and soil-based (sensor) irrigation are examples of such technologies which estimate actual water requirements of the crop by considering soil or weather information (Vellidis et al., 2008; McCready et al., 2009; Migliaccio et al., 2010). A considerable number of scheduling methods have been developed for automatic irrigation. These methods have been widely used by irrigation researchers; however, no user-friendly irrigation scheduling model that can be readily used by farmers for single and multiple field cases has been developed (Georgea et al., 2000).

Best et al. (1986) developed a program called WIF which used soil moisture signal to quantify the present soil moisture content. To predict the earliest irrigation, replenishing the root zone to a desired level, it combined soil signal with an estimate of plant water use in the future. Buchleiter et al. (1988) developed an irrigation scheduling program called SCHED, which was based on daily water balance calculations of the present soil moisture depletion and a future estimate of crop ET. The SCHED and WIF have been successfully used by irrigation consultants (Dockter, 1996; Salazar et al., 1996). Hess (1996) described a real-time software package of irrigation scheduling. The package included almost all of the available methods including reference ET, actual ET, soil water balance and a model of irrigation forecasting. Their evaluation of these models has shown the performance to be dependent on the accuracy of the input data measured in the field.

Automation of irrigation using soil sensors has been evaluated in a number of plants including tomato, onion and bell pepper crops (Thompson et al., 2007; Enciso et al., 2009; Zotarelli et al., 2009). Vellidis et al. (2008) developed and evaluated a real-time, smart sensor array prototype for scheduling irrigation in cotton which measured soil moisture and temperature as standard inputs.

The use of infrared temperature of plant canopies, along with a number of supplemental environmental measurements, has been an alternative approach to soil- or weather-based methods in irrigation scheduling of general crops (Cohen et al., 2005). Various thermal-based irrigation algorithms have been developed, such as crop water stress index (CWSI) and time-temperature threshold (TTT) methods. The upper and lower boundaries of the CWSI can be calculated using empirical and theoretical approaches. A theoretical CWSI which compares the canopy-air temperature differences with theoretical water stressed and non-stress base lines (WSBL and NWSBL) was first defined by Jackson et al. (1981, 1988). The most often used equations for calculating the theoretical boundaries are adapted from FAO-56 (Allen et al., 1998) which are developed for the canopies of general crops and are not suited to most tree canopy conditions.

The CWSI might be affected by many unwanted factors such as dust or passing clouds (O'Shaughnessy et al., 2012); however, in conjunction with a well developed irrigation algorithm it can be still very efficient. In order to improve the performance of the theoretical CWSI as a trigger for automatic irrigation scheduling of grain sorghum, O'Shaughnessy et al. (2012) incorporated a time threshold into the index and named it CWSI-TT. The results of their study indicated this method can be useful for automatically scheduling full or deficit irrigations of grain sorghum in a semi-arid region. Thermal methods in the form of empirical CWSI have been studied on different trees such as pistachios (Testi et al. 2008), peaches (Wang and Gartung, 2010; Paltineanu et. al. 2013), and olives (Agam et al., 2013; Berni et al., 2009, Akkuzu et al., 2013).

To date, the efforts have concentrated primarily on improving CWSI calculations by refining the empirical or theoretical methods of estimating the baselines. This is while the algorithms available are simple comparisons of the midday CWSI with a predetermined threshold, trying not to exceed it during the season. This threshold is crop and site specific and is determined for a well-watered crop grown on a lysimeter (O'Shaughnessy et al., 2012). Current irrigation scheduling algorithms work with static threshold, while in reality the threshold is a function of weather and plant conditions. In general, little information is available on the CWSI at which irrigation is needed. In addition, the CWSI value for a crop under no stress is assumed zero and for a severely stressed crop close to one

(Jackson et al., 1981). While this assumption might be true in case of homogeneous canopies of major row crops, it might not be applicable to heterogeneous tree canopies. The interference of thermal radiation from the ground with the readings of canopy temperatures, as well as the rough nature of the tree canopies can lead to smaller air-canopy temperature differences and consequently result in values of greater than zero even for well watered canopies (Fereres et al., 2012). In the case of apple trees, the canopy temperature increases as low crop loads are reached because stomatal conductance is a function of load and reduces as the load decreases (Lakso, 2003). As a result, non-water stressed baselines of apples are dependent on load and might not reach zero in case of a well-watered apple tree with no or very low load.

The TTT method (patented as “BIOTIC”) is an irrigation scheduling method developed by Wanjura et al. (1992, 1995) that relies on canopy temperature. The TTT method is an automatic method requiring a “time threshold” and a “temperature threshold.” The temperature threshold is the optimal leaf temperature for enzyme activity determined in lab and the time threshold is accumulated time above the temperature threshold for non-stressed crop in specific climate calculated using experimental or simulated data. O’Shaughnessy and Evett (2010) carried out automatic irrigation experiments using a time temperature threshold (TTT) algorithm. The results indicated that the TTT algorithm was a promising automatic method for irrigation scheduling of cotton in arid regions.

Weather parameters from a nearby weather station or a simple temperature sensor can provide the required information to predict plant water needs (i.e. ET). Frequently used ET models are the Penman-Monteith (Allen et. al, 1998) and Hargreaves (Hargreaves and Samani, 1985). Casadesus et al. (2012) proposed an approach combining a compensating mechanism based on soil or plant sensors readings (feed-back control) and an estimation of water demand by water balance method (feed-forward control). Their research suggested the use of the water balance model allows for a quick response to weather changes by predicting its effects, while at the same time the feedback mechanism can adapt the amount of water to the requirements of individual orchards by compensating for the bias of the model.

The objectives of this research were to investigate an automatic irrigation control system relying on feedbacks from field sensors such as soil moisture, air temperature and infrared temperature sensors on Fuji apple trees. The main objective here was to develop a theoretical CWSI not requiring expensive, time consuming field experiments to determine lower/upper boundaries. The goal was to develop a CWSI-based irrigation algorithm adapting to changing conditions of apple tree canopies, fruit growth (i.e. load change) and shoot growth (i.e. light interception change).

5.3 Materials and methods

5.3.1 Irrigation algorithms

Based on irrigation scheduling techniques available in the literature, and considering the extent of the project resources, the required base for implementing six different precision irrigation treatments was developed. These methods embraced most of the plant-based, soil-based and weather-based irrigation approaches and included both feed-back and closed-loop control methods including 1) a temperature-based ET equation (ET; feed-forward control), 2) soil water potential sensor (SOIL; feedback control), 3) a combination of ET and a soil moisture sensor (SL+ET; feedback-feedforward control), 4) manual irrigation scheduling using the scientifically-based method of neutron probe (NP), 5) canopy temperature signal and the TTT method (TTT; feedback control), and 6) canopy temperature signal with the crop water stress index (CWSI; feedback control). In Addition to these precision methods, a number of plots were managed using the conventional irrigation scheduling method of apple trees in the region (CNTRL).

CNTRL

This method was based on the calendar (irrigation events on specific days of week) and low, high air temperature thresholds. If the temperature was above 32.2^{o}C the amount of irrigation water was doubled. If the air temperature was below 21.1^{o}C, the trees received half of the usual amount (Appendix D: Fig. A.19).

ET

The ET method (Appendix D: Fig. A.20) was based on a simple soil water balance and daily estimations of reference ET from daily maximum and minimum temperatures using the Hargreaves method. Irrigation water depth was calculated as the following:

$$I = ET - P \tag{5.28}$$

where I is the irrigation water, and P is the precipitation. All terms are in mm. The historical weather data of 20 years and the Penamn-Monteith Eq. were used to calibrate the Hargreaves model for the region. The difference between soil water content at the beginning of the season (θ_i) and soil water content at field capacity (θ_{FC}) was added to the first irrigation event. Air temperature was measured using the sensors installed in the orchard and precipitation amount obtained from a nearby weather station.

SOIL

An irrigation scheduling algorithm was developed based on soil water tension readings from a granular matrix sensor installed at a depth of 0.3 m (one third of the root depth), the characteristic curve of the soil, as well as dry and wet thresholds of -0.8 bar and -0.3 bar, respectively (Hill et al., 2008). The field soil was assumed to be homogenous. An irrigation event was automatically scheduled whenever soil water potential exceeded the dry threshold and stopped if it reached the wet threshold (Appendix D: Fig. A.21).

SL+ET

SL+ET treatment, which was the combination of the ET and SOIL methods, used soil water tension data to correct the ET model. An irrigation event was scheduled based on estimations of ET and stopped whenever a soil tension of -0.3 bar (wet threshold) was detected (Appendix D: Fig. A.22).

NP

On a weekly basis, soil water content was measured down to a depth of 90 cm with neutron probe (503DR Hydroprobe, Campbell Pacific Nuclear, Concord, CA) and irrigation manually scheduled in the plots of the NP treatment to replace the water deficit to field capacity. Soil water content readings were also taken at the plots under CWSI and TTT methods. The installed access tubes were of sufficient depth to allow for detecting any potential deep percolation. Because of a suspicion of an impermeable layer at depths shallower than 90 cm, to avoid formation of a perched water table in the study site, and hence upward flow of water to the root zone, the water storage of soil depths down to 60 cm was used for irrigation scheduling purpose.

TTT

The required thermometry data for determining the parameters of the time-temperature-threshold (TTT) method were obtained from Peters (2007). The time threshold was determined using the experimental data collected in 2007 from the same orchard and the temperature threshold was determined in a lab in Lubbock, Texas. The determined temperature and time thresholds were 10^{o}C and 1035min. The temperature threshold seemed to be low (Table 5.1), therefore time thresholds needed to schedule irrigation at other temperature thresholds were determined and a temperature threshold of 22.2^{o}C and time threshold of 225 min were used.

Table 5.1 Time and temperature thresholds calculated from the well-watered apple tress in the growing season of 2007 (Peters, 2007).

Temperature threshold (^{o}C)	Time threshold (min)	Max daily ET (mm)	Average irrigation/Season (mm)	Total irrigation days
10	1035	9.7	1077	110

CWSI

The theoretical crop water stress index was calculated according to Jackson et al. (1981) and Idso et al. (1981):

$$CWSI = \frac{\Delta T - \Delta T_l}{\Delta T_l - \Delta T_u} \tag{5.29}$$

where ΔT is the measured difference between canopy temperature and air temperature, ΔT_l is the temperature difference for a well-watered tree canopy, and ΔT_u is the temperature difference for a non-transpiring canopy. The lower (ΔT_l) boundary of the CWSI was calculated as described in Chapter II:

$$\Delta T_l = \frac{R_n - g_T \lambda \frac{e_s(T_c) - e_a}{P_a}}{g_H C_P} \tag{5.30}$$

Where R_n is the net radiation, $e_s(T_c)$ is the saturated vapor pressure (kPa) at canopy temperature (T_c, ºC), e_a is the vapor pressure (kPa) of air, P_a is the barometric pressure (kPa), λ is the latent heat of vaporization (J mol^{-1}), g_T is the total water vapor conductance (mol m^{-2} s^{-1}), C_P is the heat capacity of air (29.17 J mol^{-1} C^{-1}), T_a is the air temperature (ºC), g_H is the boundary layer conductance to heat (mol m^{-2} s^{-1}). Because the net radiation (R_n) is a function of T_c, the ΔT_l and ΔT_u equations were linearized as described in Chapter II as the following:

$$\Delta T_l = \left(\frac{Q}{g_H C_P - n + \lambda g_T s}\right) - \left(\frac{g_T \lambda / P_a}{g_H C_P - n + \lambda g_T s}\right) D_a \tag{5.31}$$

ΔT_u was calculated by assuming that stomata are closed for a non-transpiring dry canopy ($g_T \rightarrow 0$), and replacing g_T with zero in Eq. 5.4:

$$\Delta T_u = \frac{Q}{g_H C_P - n} \tag{5.32}$$

where $R_n = Q + n\Delta T$. Q and n were defined in Chapter II by the following equations, respectively:

$$Q = 0.25\left(\alpha_S S_{gl} + \alpha_S S_{t1} + 4(\alpha_L - 1)\mathrm{L_a}\right) \tag{5.33}$$

and:

$$n = (3\alpha_L - 4)\varepsilon_a(c)\sigma \mathbf{T}_\mathrm{a}^3 \tag{5.34}$$

g_T is a series combination of boundary layer conductance to water vapor (g_v, mol m^{-2} s^{-1}) and leaf stomatal conductance to water vapor (g_s, mol m^{-2} s^{-1}):

$$g_T = \frac{1}{1/g_v + 1/g_s} \tag{5.35}$$

g_T was estimated by two different approaches: a) for a well–watered apple tree, leaf stomata tend to be wide open ($g_s \rightarrow \infty$), therefore, g_v becomes the determining factor ($g_T \rightarrow g_v$), and b) the model developed for estimating g_T in chapter II was employed:

$$g_T = b_2 \left[\frac{P_a Q}{\lambda D_a}\right] + b_0 \tag{5.36}$$

Where b_0 and b_2 are empirical coefficients. The former approach (a) was the base for scheduling irrigations in the growing season of 2013. To obtain cloudiness (c) required to estimate R_n, daily average of real-time global radiation ($\overline{S_{gl}}$, W m^{-2}) was compared with potential extraterrestrial incoming solar radiation of the same day (R_{ap}, W m^{-2}):

$$c = \begin{Bmatrix} (1 - \frac{\overline{S_{gl}}}{2Ra_{Pot}}) & if\ \overline{S_{gl}} \leq 2R_{ap} \\ 0 & otherwise \end{Bmatrix} \tag{5.37}$$

R_{ap} was calculated according to the FAO-56 bulletin (Allen et al., 1998). Factor 2 in Eq. 5.10 was added to convert the daily average solar radiation to an approximate solar noon average. Canopy temperature along with meteorological data including relative humidity, solar radiation, wind speed and air temperature were required inputs to calculate the CWSI. Real-time meteorological data of the 2013 growing season were obtained from a standard electronic weather station in the vicinity of the apple orchard (Roza, AgWeatherNet).

An irrigation scheduling algorithm which used the CWSI as its core was developed (Fig. 5.1). In this algorithm, the difference between midday CWSI ($CWSI_{Mid}$) and a base CWSI value ($CWSI_{Base}$), which is not necessarily zero, is compared with a threshold ($\Delta CWSI = CWSI_{Mid} - CWSI_{Base}$). The value of the base is determined by the plant in response to irrigations. Depending on many factors, including the errors caused by uncertainties in canopy temperature measurements and/or input weather data, in a well watered tree it might be always zero, always above it, or constantly changing.

If the algorithm calculates a negative value for the $\Delta CWSI$ then $CWSI_{Base}$ is replaced with $CWSI_{Mid}$. In this case, no irrigation is scheduled. If $CWSI_{Mid}$ is negative ($\Delta T < \Delta T_l$) it is assumed "zero" and if greater than "one" ($\Delta T > \Delta T_u$) is assumed "one." The decisions are made only if both $CWSI_{Mid}$ and $CWSI_{Base}$ have a value between "zero" and "one" ($0 < CWSI_{Mid} < 1 \; and \; 0 < CWSI_{Base} < 1$). Provided the mentioned conditions are met, in order to make an irrigation decision the $\Delta CWSI$ is compared with the threshold. If the $\Delta CWSI$ is greater than the threshold, an irrigation event will be scheduled.

The system applies some amount of water and then waits for the plant to respond. The response of plant will be reflected in a decreasing CWSI value. If the value is still bigger than the threshold, the system keeps watering until the CWSI drops below the threshold or the total amount of water applied successively exceeds 80% of the water holding capacity of the soil. At this point the base will be reset to "one." If the CWSI value goes below the current base, the base will be reset to the lower value. CWSI values below zero are assumed "zero" and values greater than "one" are treated as "one." A resulting CWSI value of "one," which is expected to happen on a humid, cloudy, or cold day, is interpreted as an uncertain condition and no comparison with the threshold or irrigation management decision is made. A base value of "one" results in no irrigation decision. The algorithm also compares the maximum air temperature with a temperature threshold value. This follows a traditional approach of farmers to not irrigate when it is too cold. In fact, the ET rate at this temperate is low enough to be neglected.

The threshold values reported in the literature for well-watered crops are site and crop specific and no reference values have been established for most tree crops; however, values close to zero (0.2-0.3) are expected to maintain crops far from being stressed. Higher thresholds are also reported in case of deficit irrigation (O'Shaughnessy et al., 2012). The adaptive nature of the presented irrigation algorithm required making changes to the traditional definition of threshold. The algorithm helped the trees reach their potential ET by providing them with water and observing their subsequent response. The algorithm needed a threshold greater than natural CWSI fluctuations (due to noises/errors) in non-stressed conditions and lower than a value causing water stress. The higher the threshold, the higher the irrigation depth had to be taken. For the purpose of this study, the control system was set for a conservative threshold of 0.2 and an irrigation depth (d) of 16.5mm (3 times the average crop ET of June and July: $d = 3 \times 5.5mm = 16.5mm$) to ensure irrigations replenished the water depleted. Before starting the main field experiment, the irrigation control system was tuned and tested using these values.

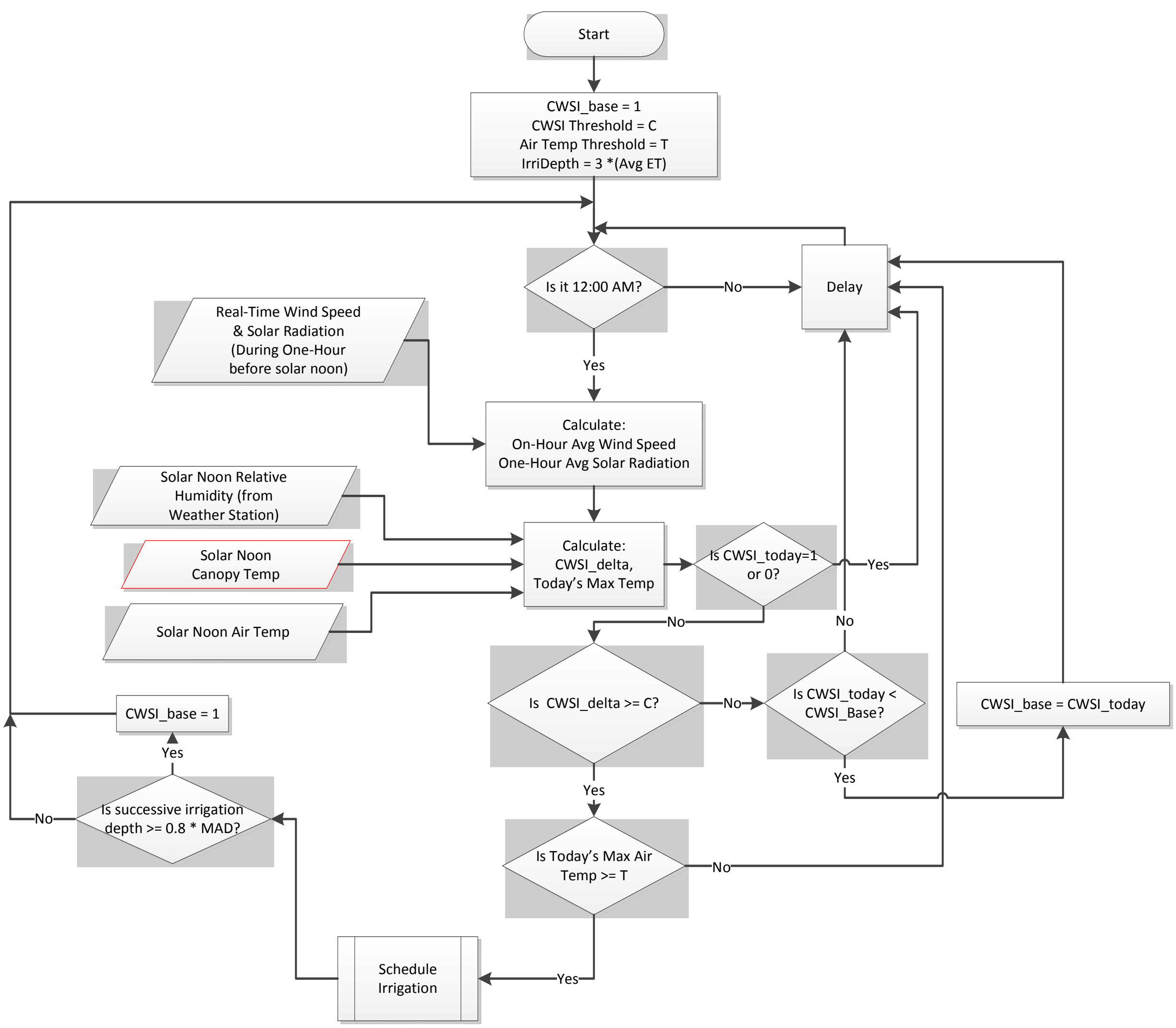

Figure 5.1 CWSI-based irrigation scheduling algorithm. Solar noon canopy and air temperatures were calculated by averaging values from 1:00PM to 3:00PM.

The control system ran different algorithms at midnight each day, based upon the input data from the same day and scheduled irrigation events (if decided) of different plots for 10:30 in the morning of next day. In case of the CWSI method, considering the low application rate of the drip irrigation system (1.1 mm h^{-1}), it took about 15 h to trickle 16.5 mm of water to the trees.

5.3.2 Development of hardware and software

A wireless central control system including hardware and software (graphical user interface) was designed and installed in a one acre drip-irrigated apple orchard at the Roza Farm, Prosser, WA (Appendix A: Fig. A.1–4). The electronic hardware of the system consisted of a centrally located RF receiver (master; RF401, Campbell Scientific, Logan, UT, USA) connected to a laptop computer and six sensor nodes (slaves) installed in the field. A sensor node was made up of CR10(X) dataloggers (Campbell Scientific, Logan, UT, USA) and all or some of the following sensors/components. Total numbers are mentioned here:

a) Six soil water potential/tension sensors (Watermark®, IRROMETER Co. Riverside, CA),
b) Three dielectric soil moisture sensors (10HS, Decagon Devices Inc., Pullman, WA)
c) Three air temperature sensors (Model 109, Campbell Scientific, Logan, UT, USA), and corresponding radiation shield (41303-5A, Campbell Scientific, Logan, UT, USA).
d) Six infrared canopy temperature sensors (Excergen model IRt/c.2: Type J, Watertown, Mass.),
e) 21 Latching solenoid valves (Irritrol, Riverside, CA) operated by L298 dual H-bridge motor drive (Robotshop Inc., Mirabel, Quebec, Canada), and
f) A radio frequency tag (RF401, Campbell Scientific, Logan, UT, USA) to transmit data to the receiver and receive control signal from the central control.
g) Six 10 W solar panels (SYP105, Instapark Co., Santa Fe Springs, CA)

The nodes took measurements from the various sensors located in each plot and reported them to the control computer located in a nearby building. This computer recorded all readings, made irrigation control decisions, and then sent signals back to the individual data-loggers which opened or closed latching solenoid valves to turn the water on and off to each block of trees. Instead of wireless communication between the field and office computers, USB modems (DataJack, Inc., Dallas, TX) were used to access the GUI in the field. This also allowed the graphical user interface (GUI) to obtain real-time weather data and send alert emails. Due to the sensitivity of the modems to high temperatures a cooling system (fan) was added to the set.

Canopy temperature was measured in real-time using individual IRTs (Excergen model IRT/c.2: Type J, Watertown, Mass.) installed perpendicularly above a tree (< 1 m high) located at the center of the six plots (small plots of 18 trees). Considering the field view of this model of IRT (35 degrees), this form of orientation and position decreased both the chance of the ground being seen by an IR sensor and the number of sensors used. Sepulcre-Canto et al. (2006) and Testi et al. (2008) used similar mounting in olive and pistachio trees, respectively. The IRT sensors were wired to a network of Campbell CR10 and CR10X dataloggers (Campbell Scientific, Logan, UT, USA) sending out temperature readings to a central computer wirelessly.

A comprehensive graphical user interface (i.e. control software) was developed in VB.Net (V.2010, Microsoft Inc., Redmond, WA) and combined with CoraScript (V.1.1.9.8, Campbell Scientific, Logan, UT, USA) to communicate with the dataloggers through LoggerNet (V.3.5, Campbell Scientific, Logan, UT, USA). The GUI was installed on a laptop computer left in the field (Appendix B: Fig. A.5–5.13). The seven irrigation scheduling algorithms including ET, SOIL, SL+ET, TTT, CWSI, NP and CTNRL were embedded into this user friendly software. The GUI gathered data from the sensor nodes, downloaded weather data from a nearby weather station, ran the models, and automatically controlled the irrigation of different blocks within the Fuji apple orchard. It also allowed for manual control of individual plots, logged sensor readings, irrigation events, errors, etc and sent emails (information, alarms, etc) to the user. The applied settings related to the irrigation treatments can be seen in Fig. 5.11–5.12 (Appendix B).

5.3.3 Application of control system

The field experiments were conducted in a Fuji apple orchard on the Roza Farm of the Washington State University Irrigated Agriculture Research and Extension Center near Prosser, WA, at the coordinates of latitude 46.26°N, longitude 119.74°W, and 360 m above sea level. The site was located in a semi-arid zone with almost no summer rains and an average annual precipitation of 217 mm. The site’s soil was a shallow Warden Silt Loam soil (Web Soil Survey) of more than 90 cm deep (field observation). The orchard was irrigated by two lines of drip tubing laterals of in-line 2.0 L h^{-1} drippers, spaced at 91.4 cm intervals along laterals. Using 3 10HS sensors, soil moisture readings were taken from 3 different locations in the orchard after irrigations to determine the field capacity (Appendix C: Fig. A.14). From these measurements, the volumetric water content at field capacity was found to be 32.5%. The permanent wilting point (PWP) was assumed to be 13.8% volumetric water content based on the soil type (Saxton and Rawls, 2006). Automatic and manual irrigation events were scheduled during May, June, July, August and September of the 2013 growing season.

The seven aforementioned irrigation treatments were evaluated in a randomized complete block design with three replications (blocks) (Fig. 5.2). In addition to automatic data gathered by the system, all of the irrigation scheduling methods were compared against each other and the traditional method of irrigating apple trees (CNTRL) over the depth of the irrigation water applied to them during the season, and three of them including NP, TTT and CWSI were also compared based on the water use. A water budget equation was used to estimate irrigation water use by apple trees in 2013 (Evett, 2002):

$$ET_{wb} = P + I + F - \Delta S \pm D - R \tag{5.38}$$

where ET_{wb} is the actual crop water use (mm), P is precipitation (mm), I is the applied irrigation depth (mm), F is lateral flux of water entering the control volume (positive) or exiting it (negative), D_p is deep percolation (mm) and R is runoff (mm). D and R were assumed to be negligible because the orchard was drip-irrigated, where no runoff or deep percolation is expected. In addition, there was no shallow water table below the root zone, thus upward flow was not a concern. F was also assumed zero because soil moisture readings were taken at the center of the plots where the effect of horizontal fluxes are negligible. ΔS is the change in soil water content (mm). It was calculated using the neuron probe readings:

$$\Delta S = \theta_f - \theta_i \tag{5.39}$$

where θ_f is the final soil water content (mm) in the end of the growing season and θ_i is the initial soil water content (mm) in the beginning of the season.

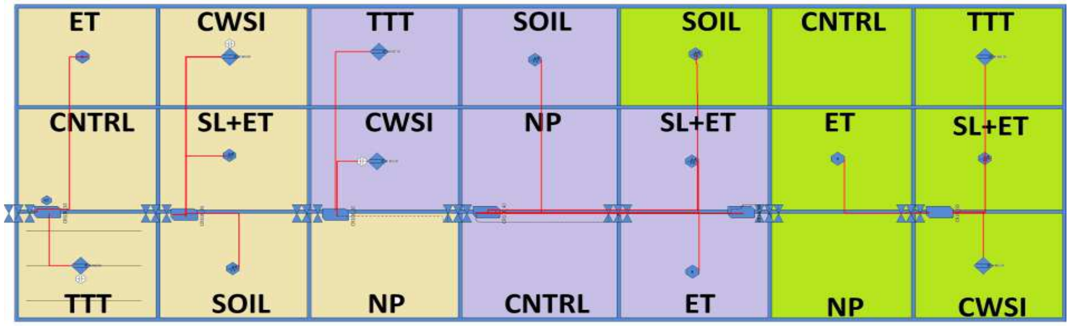

Figure 5.2 The orchard was divided into "seven" treatments and randomized in "three" blocks (21 plots). Each plot was consisting of 3 rows of 6 trees.

The statistical analysis included analysis of variance (ANOVA), using the SigmaPlot 11.0 (Systat Software Inc., San Jose, CA) to test for the differences among the crop water use, as well as applied irrigation water of the irrigation methods. To conduct multiple comparisons of the means of the irrigation treatments, the Bonferroni t-test was employed (at $p = 0.05$).

5.4 Results and discussions

5.4.1 CWSI

CWSI and Ψ_{stem}

The days on which the measurements of Ψ_{stem} took place included some unusual conditions (Table 5.1). For the purpose of irrigation scheduling, Ψ_{stem} readings made under unusually cold or overcast days should not be relied on (Mitcham and Elkins, 2007)**.** Similarly, interpretation of midday CWSI values calculated on days with unusual weather conditions needed to be carried out with caution.

Table 5.2 Ψ_{stem} measurement days with unusual weather conditions.

			Day of Year		
212	219	226	241	268	275
Cloudy day	High RH	100% Cloudy	Partially Cloudy	Cold, Partially Cloudy	Cold, Cloudy

To detect apple trees' water stress, Ψ_{stem} was measured at solar noon with a time window of about two hours (13:00-15:00). This was the time that CWSI was also expected to reflect water stress. Three Ψ_{stem} readings (per tree per measurement day) taken in different weather conditions were averaged to calculate the Ψ_{stem} corresponding to each IRT. The trees maintained relatively high solar noon Ψ_{stem} over the period of the experiment with fluctuations driven by the weather conditions. Considering there was no water stress, Ψ_{stem} was mainly dependent on solar radiation, air temperature and relative humidity, thus Ψ_{stem} was higher under more humid, cooler conditions and smaller (more negative) under warmer, drier conditions. During this period, solar noon Ψ_{stem} values were limited to a range with a minimum (average) of -11.0 bar and maximum of -3.5 bar.

Changes of midday stem water potential (ψ_{stem}) measured in the plots under the CWSI treatment during the period of irrigation (mid to late summer) followed the CWSI change very closely (Fig. 5.3). On a hot but very humid day (DOY = 219), both Ψ_{stem} and CWSI reached their lowest values at solar noon. On these days, high RH and high solar radiation were driving transpiration to opposite directions. On a very cold and overcast day (DOY = 275), both midday Ψ_{stem} and CWSI reached their highest values.

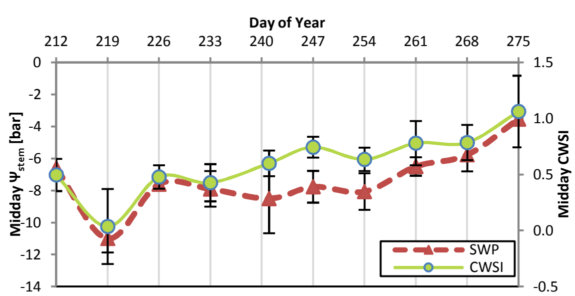

Figure 5.3 Changes of midday CWSI and SWP (ψ_{stem}). Each value represents the average of up to six measurements/predictions per treatment. The error bars show the standard error of the mean.

Linear regressions between midday CWSI and Ψ_{stem}, once total canopy conductance was estimated using the model, yielded fairly well correlations with $R^2 = 0.78$ (p <0.001; Fig. 5.4b) while the assumption of $g_T = \infty$ resulted in slightly weaker correlation with $R^2 = 0.73$ (p <0.001; Fig. 5.4a). A similar linear regression between ΔT and Ψ_{stem} in Ch. III resulted in a good correlation with $R^2 = 0.76$ (p <0.001; Fig. 4.15b) indicating that ΔT was as predictive as CWSI under the conditions of the current study.

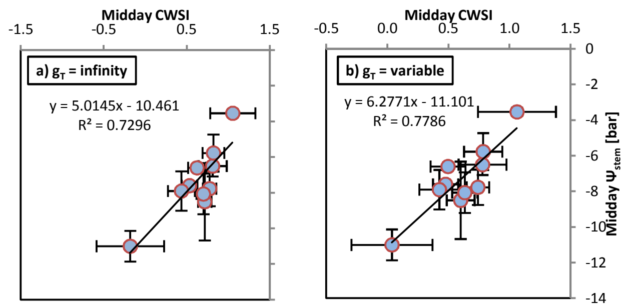

Figure 5.4 Linear relationship between solar noon ψ_{stem} and solar noon CWSI calculated by assuming $g_T = \infty$ (a) and model estimations of g_T (b). Each ψ_{stem} value represents the average of up to six measurements. The error bars show the standard error of the mean.

CWSI response to irrigations

Assuming $g_T = \infty$, early season CWSI values were calculated using meteorological and thermal data for fully-irrigated apple trees in the growing season of 2007 (Fig. 5.5a–b). The new algorithm was applied to these data after the end of the season for evaluation purpose. As illustrated, the adaptive algorithm (Fig. 5.1) has considerably decreased the number of false early-season irrigation events compared to the traditional CWSI algorithm (Appendix D: Fig. 17). Prior literature mentions one of the issues with the traditional CWSI method of scheduling irrigation is early-season over irrigation (O'Shaughnessy et al., 2012).

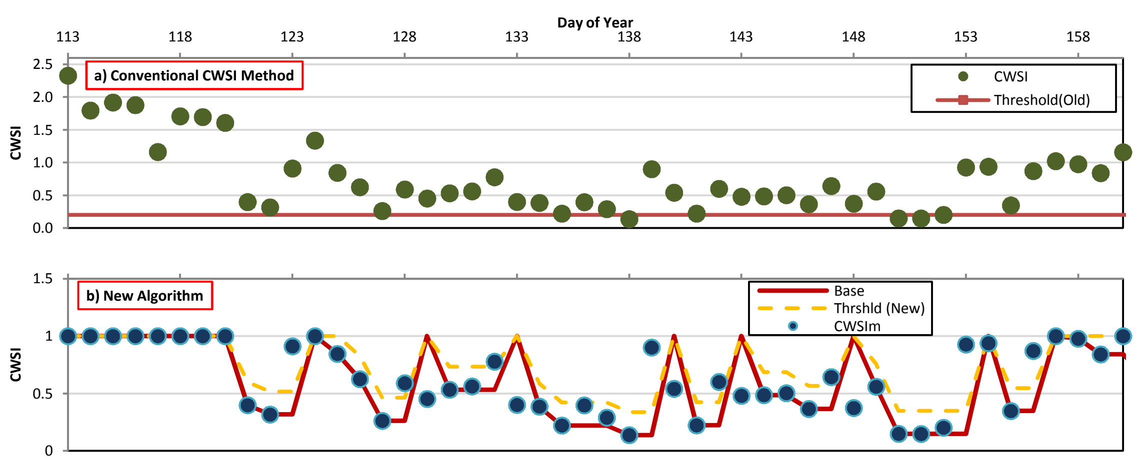

Figure 5.5 Plot of early season CWSI values calculated using meteorological and thermal data of the 2007 growing season for fully irrigated apple trees. The adaptive nature of the new algorithm (b) has resulted in considerably less numbers of false irrigation events early in the season compared to the conventional method (a).

The new algorithm adapted itself with the response of the apple trees to irrigations or rainfall and as long as the CWSI had a decreasing trend no irrigation was scheduled. Application of the new algorithm to fully-irrigated apple trees during the early-season period when the canopies are under development, and thus the ground might be seen by the IRTs, can prevent the waste of irrigation water. Daily solar noon weather data on air temperature, relative humidity, and solar radiation used for estimations of the CWSI during the irrigation period (automatic only) of 2013 (June, July, August and September) are presented in Fig. 5.6.

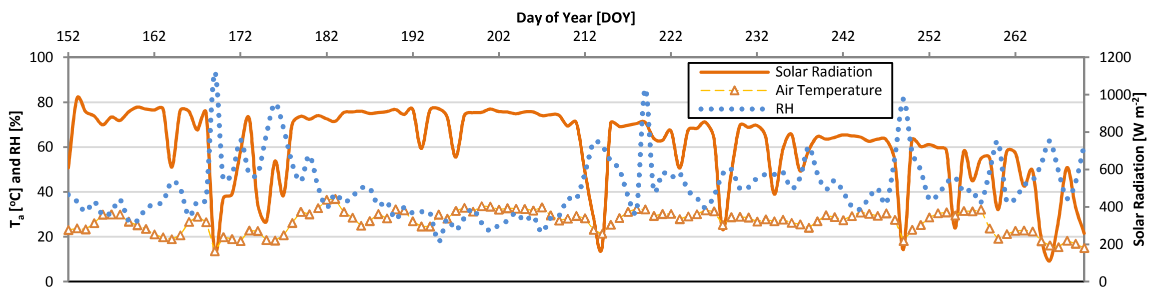

Figure 5.6 Midday changes of environmental variables including solar radiation, air temperature and relative humidity during the automatic irrigation period of 2013. The data were obtained from Roza weather station (AgWeatherNet).

The dotted circles in Fig. 5.7 indicate days on which the new irrigation algorithm detected no water stress and decided not to irrigate due to low temperature or high relative humidity, which made it impossible to detect water stress. In response to high RH, or low T_a, the CWSI was set to “one.” There is a limit on the amount of water a plant can transpire per day. Thus, a change of more than a specified value (e.g. threshold) in the midday CWSI can be related to reasons other than water stress and excluded. It can be seen in Fig. 5.7 that such a situation occurred on cool, cloudy or humid days. The present algorithm put a hold on the system after three successive irrigation events. The dotted circles in Fig. 5.8 show days on which the algorithm stopped irrigating the plot after three successive irrigation events to avoid excessive watering. Three irrigation events fulfilled 0.8 times MAD, thus after each three irrigations the base CWSI was reset to “one.” The dotted circles in Fig. 5.9 specify days on which the algorithm detected water stress and scheduled irrigation. It can be seen that CWSI dropped to values below the threshold after one or two successive irrigation events.

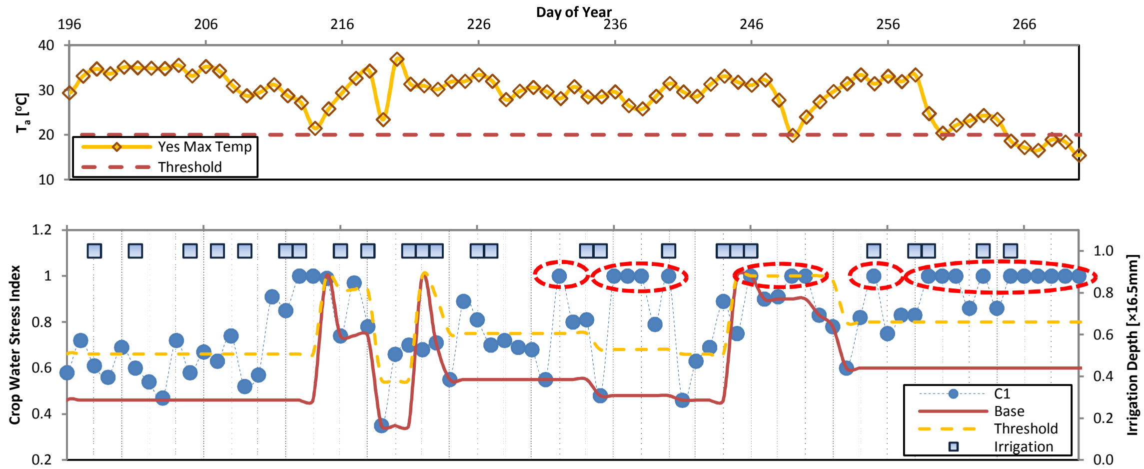

Figure 5.7 The dotted circles indicate days on which the irrigation algorithm decided not to irrigate due to low temperature (no water stress) or high relative humidity (not possible to detect water stress). In response to high RH, or Low T_a CWSI was set to "one."

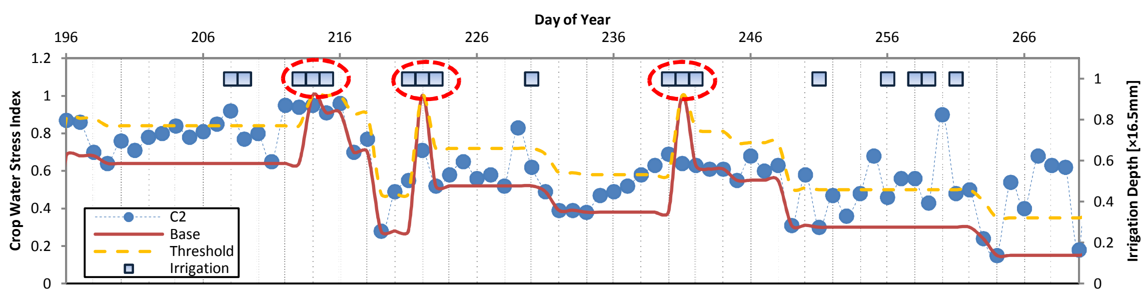

Figure 5.8 The dotted circles indicate days on which the irrigation algorithm stopped irrigating the plot after three successive irrigation events (to avoid excessive watering) and reset the base (base=1). Three irrigation events fulfilled 0.8 times MAD, thus after each three irrigations CWSI was reset to "one"

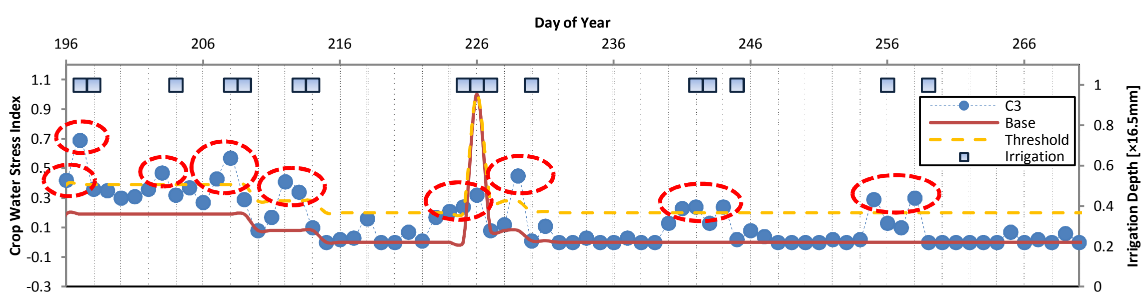

Figure 5.9 The dotted circles indicate days on which the irrigation algorithm detected water stress and scheduled irrigation. It can be seen that CWSI dropped to values below the threshold after one or two successive irrigation events.

5.4.2 Comparisons of treatments

Climate and precipitation

During the growing season of 2013, there were occasional days with overcast skies throughout the period. Rainfall from May thru September totaled 48 mm, most of which (43 mm) occurred in July. The 2013 season was a relatively warmer year compared to the 2007 growing period when the time threshold of TTT was determined with greater maximum daily temperatures and ET_r values (Table 5.2).

Table 5.3 Climatic conditions for the 2013 growing season.

Month	Max temp (^oC)	Min temp (^oC)	Min RH (%)	Max RH (%)	Total monthly precipitation (mm)	Max total solar radiation (MJ m^{-2})	Average daily ET_r^a (mm d^{-1})
May	26.3	-1.1	39.0	58.3	0.0	26.2	6.1
June	32.6	6.7	32.9	87.1	33.8	30.6	5.9
July	34.1	13.7	44.9	92.1	42.9	31.2	6.5
Aug	37.7	18.0	32.8	59.9	0.0	30.4	8.9
Sept	36.9	17.6	47.0	82.5	5.3	26.8	6.2

[a] Reference ET (ET_r) data for alfalfa from the Washington Agricultural Weather Network (AgWeatherNet).

Applied irrigation water

The difference in the mean values among the seven irrigation treatments was statistically significant (P = <0.001). The total irrigation water applied by the traditional practice of applying water in the region was significantly higher than all of the other methods (P <0.001) with a value of 1345 mm. Among the other methods, ET and SOIL resulted in the highest and lowest applied water with values of 456 mm and 214 mm, respectively (Fig. 5.10). Clearly under-irrigating the trees (visual inspection of the trees), the SOIL along with the SL+ET method (273 mm) exhibited an insufficient response to water stress. The ET method was significantly different than SOIL (P <0.001) and SL+ET (P = 0.004). All of the other methods were also significantly different than that of the SOIL method, while there was no significant difference between NP and SL+ET (p = 0.097), as well as C and SL+ET (0.069).

The under irrigation of the plots under SOIL can be explained by the fact that a soil sensor monitors only a limited volume of soil and might have not have been at a depth or place where the root systems was active. Using a feed-forward ET-based scheduling method in combination with a soil sensor did not improve irrigation scheduling as the signals to stop irrigations were probably issued as soon as the first water reached the soil surrounding the sensor. The ET method itself can lead to over or under irrigation if the estimates of crop water use are incorrect (ET model errors), the soil water content at the beginning of the season is unknown, or the application efficiency of irrigation system is lower than expected.

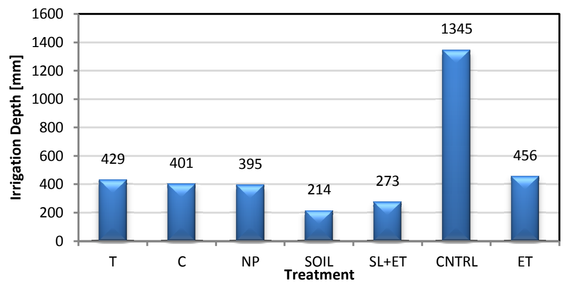

Figure 5.10 Total irrigation water applied to seven different treatments.

Crop water use

The water use of the apple trees in the TTT (T), CWSI (C) and NP treatments for the entire growing season of 2013 (DOY = 110–270) was calculated using the water budget approach (Fig. 11a–b). The difference in the mean values among the TTT, CWSI, NP and ET_c methods was statistically significant ($P = 0.280$). A multiple comparison procedure (t-test) revealed that there was a significant difference between the estimated ET and the crop water use of the NP treatment, T treatment, and the CWSI treatment ($p < 0.05$; Table 4) while there was no significant difference among the thermal treatments (i.e. TTT, CWSI) and the NP treatment ($P < 0.001$).

The means of crop water use in the NP and TTT treatments were almost the same with 483 mm for TTT compared to 488 mm for NP. The mean of crop water use in the CWSI treatment was slightly higher with a value of 541 mm. The t-test revealed that there was a significant difference between the total ET_c estimated for the season and the water use of the NP ($p = 0.021$), TTT ($p < 0.001$), and CWSI treatments ($p = 0.021$). Fig. 11 (a) shows the means of water use in the plots under the NP treatment had a higher variability compared to the TTT and CWSI treatments with standard deviation of 77 compared to 11 and 62, respectively. This could be related to a high variability among the trees of different plots.

Table 5.4 Comparisons of applied irrigation water of the irrigation treatments using the Bonferroni t-test for significant differences among means.

Comparison	Diff of Means	t	P	P<0.050
CNTRL vs. SOIL	1131	32.381	<0.001	Yes
CNTRL vs. SL+ET	1072	30.69	<0.001	Yes
CNTRL vs. NP	951	27.218	<0.001	Yes
CNTRL vs. CWSI	944	27.034	<0.001	Yes
CNTRL vs. TTT	916	26.215	<0.001	Yes
CNTRL vs. ET	890	25.456	<0.001	Yes
ET vs. SOIL	242	6.925	<0.001	Yes
ET vs. SL+ET	183	5.234	0.004	Yes
ET vs. NP	62	1.762	1	No
ET vs. CWSI	55	1.577	1	No
ET vs. TTT	27	0.759	1	No
TTT vs. SOIL	215	6.165	0.001	Yes
TTT vs. SL+ET	156	4.475	0.016	Yes
TTT vs. NP	35	1.003	1	No
TTT vs. CWSI	29	0.818	1	No
CWSI vs. SOIL	187	5.347	0.004	Yes
CWSI vs. SL+ET	128	3.656	0.069	No
CWSI vs. NP	7	0.185	1	No
NP vs. SOIL	180	5.163	0.005	Yes
NP vs. SL+ET	121	3.472	0.097	No
SL+ET vs. SOIL	59	1.691	1	No

As depicted in Fig. 5.12, the soil water depletion of the plots under NP, CWSI and TTT treatments was never allowed to exceed the 50% maximum allowed depletion (MAD) for apple trees (Allen et al., 1998). There was also no sign of over irrigation. This illustrates the CWSI and TTT methods of scheduling irrigation properly responded to water stress of the apple trees under the treatments and these methods competed well with the scientifically method of irrigation (i.e. NP).

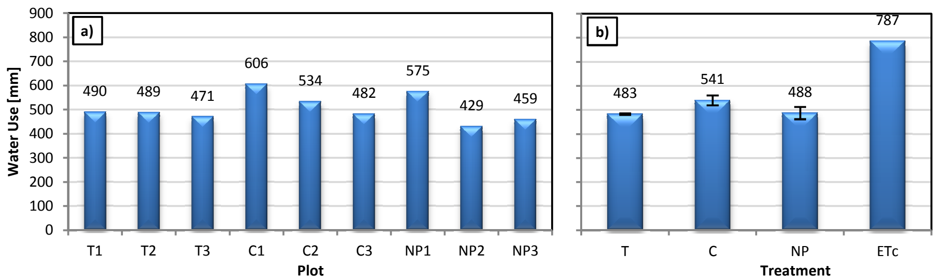

Figure 5.11 Water use of the irrigation treatments. Each value represents the average of three measurements per treatment. The error bars show the standard error of the mean. The weekly soil moisture readings were used to calculate the total water use of the season.

Table 5.5 Comparisons of crop water use of three irrigation treatments and predicted ET for significant differences among the means.

Comparison	Diff of Means	P	Significant (P<0.050)?
ETc vs. NP	246	0.021	Yes
ETc vs. TTT	304	0.000	Yes
ETc vs. CWSI	246	0.021	Yes
CWSI vs. NP	53	0.178	No
CWSI vs. TTT	57	0.204	No
TTT vs. NP	5	0.923	No

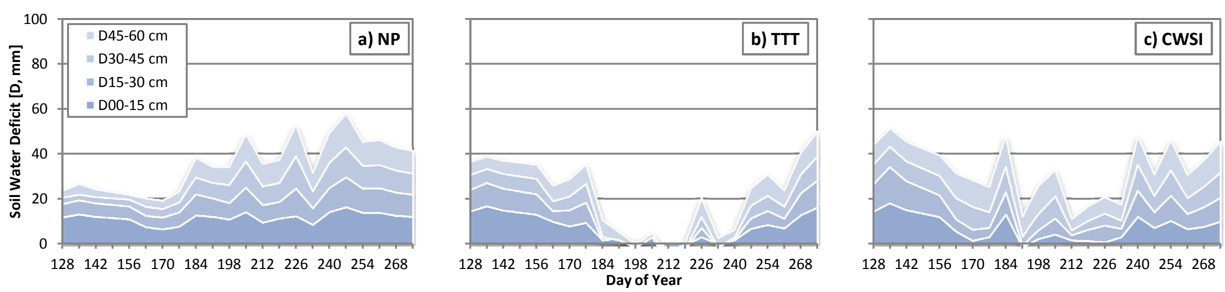

Figure 5.12 Average volumetric soil water content of the NP (a), TTT (b) nad CWSI (c) treatments measured down to the depth of 60cm using the neutron probe (DOY = 128–275). The total water deficit in all of the plots of irrigated using the CWSI and TTT automatic algorithms, as well as NP has maintained below the maximum allowed depletion of 96cm ( )).

5.5 Conclusions

Seven irrigation scheduling algorithms including automatic (TTT, CWSI, SOIL, SOIL+ET, ET) and manual (NP and CNTRL) methods were developed. The base for these methods, except for the CWSI, was already available. CWSI values were calculated using the theoretical models of the NWSBL and WSBLs previously developed in Chapter II. The algorithms were embedded into a computer software (e.g. GUI) controlling the hardware (i.e. the sensor nodes, solenoid valves, etc) installed in the orchard. Although, the NP method was manual, weekly readings of soil water content were fed into the GUI to automatically turn on/off the valves. Another model was also developed which automatically irrigated the plots under CNTRL based on the calendar days and the temperature thresholds. The overall performance of the control system was satisfactory.

In the 2013 growing season, the irrigation methods were tested in a one acre orchard of Fuji apple trees. The crop water use of plots irrigated using CWSI and TTT was also compared with those irrigated using the scientific-based irrigation method of neutron probe and crop ET estimated using the P-M model corrected by crop coefficient. The CWSI algorithm drastically decreased early season over-irrigation, yielded significantly fewer false irrigation signals on cloudy, humid, or cold days and adapted to changing conditions of apple trees (i.e. shoot and fruit growth). In addition, the theoretical CWSI was highly correlated to midday Ψ_{stem}. The CWSI irrigation algorithm introduced here avoided over-irrigation at the beginning of the growing season because no irrigation was scheduled on the cold days of early season and/or when the CWSI had a decreasing trend. No irrigation occurred on cold, humid, or cloudy days or at the absence of wind as the CWSI value was either “1” or “0” on these days. The adaptive nature of the algorithm, through the use of a dynamic lower, non-stressed boundary, allowed monitoring the real-time water demand of the trees, avoiding wrong stress signals caused by wind effect, shoot growth, etc. It was minimally sensitive to different sources of error including temporary atmospheric conditions (i.e. dust, passing clouds, etc), IR sensor installation and measurement errors, apple tree architecture and model errors. While the crop water stress index was developed for apple trees the adaptive control algorithm is independent of crop or irrigation method.

In the current study, the treatments were compared solely based on the irrigation water applied and crop water use. In future studies, the treatments can be compared based on decreased water and labor costs, as well as decreased losses of water and nutrients to deep percolation. In the event of future experiments, it is anticipated the methods relying on the sensing of canopy temperature will result in more water savings, compared to other irrigation scheduling methods. While this is an initial step toward implementing variable rate irrigation practices on apple trees, it has the potential to improve water use efficiency, which leads to increased production, reduced production costs, reduced pumping energy requirements, and improved quality.

Acknowledgments

This research was funded by the US Department of Agriculture Specialty Crop Research Initiative (USDA SCRI) grant. The authors would like to thank Clint Graf for his help in establishing the irrigation system, weed control, and pesticide applications. The authors thank Sean E. Hill and Robert Dickson for helping with a number of computer software related issues, as well as Alan Kawakami and Lynn Mills for their assistance with the pressure bomb. The authors also acknowledge the help of Dr. Melba Salazar with the statistical analysis.

References

Agam, N., Cohen, Y., Berni, J.A.J., Alchanatis, V., Kool, D., Dag, A., Yermiyahu, U., Ben-Gal, A., 2013. An insight to the performance of crop water stress index for olive trees, Agricultural Water Management, 118: 79–86.

Akkuzu, E., Kaya, Ü., Çamoglu, G., Mengü, G.P., Aşık, Ş., 2013. Determination of crop water stress index (CWSI) and irrigation timing on olive trees using a handheld infrared thermometer. Journal of Irrigation and Drainage Engineering-ASCE, 139: 728–737.

Allen, R.G., Pereira, L.S., Raes, D., Smith, M., 1998. Crop evapotranspiration: guidelines for computing crop water requirements. Irrigation and Drainage Paper No. 56. FAO, Rome, Italy, 300 pp.

Al-Kaisi, M.M., Berrada, A., Stack, M., 1997. Evaluation of irrigation scheduling program and spring wheat yield response in southwestern Colorado. Agricultural Water Management 34, 137–148.

Best, K.R., James, L.G., Ley, T.W., 1986. An interactive computer model for forecasting irrigations: A project completion report submitted to state of Washington Water Research Center and US Department of the Interior.

Berni, J.A.J., Zarco-Tejada, P.J., Sepulcre-Cantó, G., Fereres, E., Villalobos, F., 2009. Mapping canopy conductance and CWSI in olive orchards using high resolution thermal remote sensing imagery. Remote Sensing of Environment, 113: 2380–2388.

Buchleiter, G.W., Duke, H.R., Heermann, D.F., 1988. User's guide for USDA-ARS irrigation scheduling program SCHED. USDA-Agricultural Research Service Agricultural Engineering Research Center, Colorado State University, Fort Collins, CO.

Casadesus, J., Mata, M., Marsal, J., Girona, J., 2012. A general algorithm for automated scheduling of drip irrigation in tree crops. Computers and Electronics in Agriculture 83, 11–20.

Campbell, G.S., Norman, J.M., 1998. An Introduction to Environmental Biophysics. Springer-Verlag, New York, NY, USA, 286 pp.

Cohen, Y., V. Alchanatis, M. Meron, Y. Saranga, and J. Tsipris. 2005. Estimation of leaf water potential by thermal imagery and spatial analysis. J. Exp. Bot. 56(417):1843–1852.

Dockter, D.T., 1996. AgriMet—The Pacific Northwest Cooperative Agricultural Weather Station Network. In: Camp, C.R., Sadler, E.J., Yoder, R.E. (Eds.), Evapotranspiration and Irrigation Scheduling. Proceedings of the International Conference. ASAE, San Antonio, pp. 75–80.

Enciso, J., Wiedenfeld, B., Jifon, J., Nelson, S., 2009. Onion yield and quality response to two irrigation scheduling strategies. Scientia Horticulturae 120, 301–305.

Farahani, H.J., Howell, T.A., Shuttleworth, W.J., Bausch, W.C., 2007. Evapotranspiration: progress in measurement and modeling in agriculture. Trans. ASABE 50, 1627–1638.

Fereres, E., Goldhamer, D., Sadras, V.O., 2012. In Crop yield response to water of fruit trees and vines: guidelines. Steduto, P., Hsiao, T.C., Fereres, E. and Raes, D. (eds.). Ch. 4, pp 246–295.

Georgea, B.A., Shendeb, S.A., Raghuwanshi, N.S., 2000. Development and testing of an irrigation scheduling model. Agricultural Water Management 46, 121–136.

Hargreaves, G.H., Samani, Z.A., 1985. Reference crop evapotranspiration from temperature. Appl. Eng. Agric. 1(2), 96–99.

Hess, T., 1996. A microcomputer scheduling program for supplementary irrigation. Computers and Electronics in Agriculture 15, 233–243.

Hill, R.W., Black, B., Cardon, G., 2008. Orchard Irrigation: Apple. Utah Ag. Exp. Stn. Res. Utah State University, Logan UT. Available on the Web at http://extension.usu.edu/files/publications/publication/Horticulture_Fruit_2008-01pr.pdf

Jackson, R.D., Reginato, R.J., Idso, S.B., 1977. Wheat canopy temperatures: a practical tool for evaluating water requirements. Water Resources Res. 13, 651–656.

Jackson, R.D., Idso, S.B., R.J.E., Reginato, Pinter, P.J., 1981. Canopy temperature as a crop water stress indicator. Water Resources Res. 17, 1133-1138.

Jackson, R.D., Kustas, W.P.E., Choudhury, B.J., 1988. A reexamination of the crop water stress index. Irrigation Science 9, 309-317.

Jones, H., 2004. Irrigation scheduling: advantages and pitfalls of plant-based methods. J. Exp. Bot. 55, 2427–2436.

Kallestad, J.C., Sammis, T.W., Mexal, J.G., White, J., 2006. Monitoring and management of pecan orchard irrigation: a case study. HortTechnology 16, 667–673.

Kisekka, I., Migliaccio, K.W., Dukes, M.D., Schaffer, B., Crane, J.H., 2010. Real-time evapotranspiration-based irrigation scheduling and physiological response in a carambola (Averhoha carambola) orchard. Applied Engineering in Agriculture 26, 373–380.

Ko, J., Piccinni, G., 2009. Corn yield responses under crop evapotranspiration-based irrigation management. Agricultural Water Management 96, 799–808.

McCready, M.S., Dukes, M.D., Miller, G.L., 2009. Water conservation potential of smart irrigation controllers on St. Augustine grass. Agricultural Water Management 96, 1623–1632.

Migliaccio, K.W., Schaffer, B., Crane, J.H., Davies, F.S., 2010. Plant response to evapotranspiration and soil water sensor irrigation scheduling methods for papaya production in south Florida. Agricultural Water Management 97, 1452–1460.

Mitcham, E., Elkins, R., 2007. Pear Production and Handling Manual. 215 pp.

Orta, A.H., Erdem, Y., Erdem, T., 2003. Crop water stress index for watermelon. Scientia Horticulturae 98, 121–130.

O'Shaughnessy, S.A., Evett, S.R., 2010. Canopy temperature based system effectively schedules and controls center pivot irrigation of cotton. Agricultural Water Management 97, 1310–1316.

O'Shaughnessy, S.A., Evett, S.R., Colaizzi, P.D., Howell, T.A., 2012. A crop water stress index and time threshold for automatic irrigation scheduling of grain sorghum. Agricultural Water Management 107, 122–132.

Paltineanu, C., Septar, L., Moale, C., 2013. Crop Water Stress in Peach Orchards and Relationships with Soil Moisture Content in a Chernozem of Dobrogea. J. Irrig. Drain Eng., 139(1), 20–25.

Peters, R.T., 2007. Irrigation automation using infrared temperature sensors. WTFRC Project #TR-06-606, Washington State University, Pullman, WA. Available on the Web at http://jenny.tfrec.wsu.edu/wtfrc/PDFfinalReports/2007FinalReports/Peters07Tech.pdf

Pereira, L.S., 1999. Higher performance through combined improvements in irrigation methods and scheduling: a discussion. Agricultural Water Management 40, 153–169.

Salazar, L.J., Thompson, K.R., Crane, K., 1996. Computerized irrigation scheduling in the San Luis Valley of Colorado. In: Evapotranspiration and Irrigation Scheduling, C.R. Camp, E.J. Sadler, and R.E. Yoder (Eds.) Proceedings of the International Conference. ASAE pp. 75-80.

Saxton, K.E., Rawls, W.J., 2006. Soil water characteristic estimates by texture and organic matter for hydrologic solutions. Soil Science Society of America Journal, 70, 1569–1578.

Sepulcre-Canto, G., Zarco-Tejada, P.J., Jimenez-Munoz, J.C., Sobrino, J.A., de Miguel, E., Villalobos, F.J., 2006. Detection of water stress in an olive orchard with thermal remote sensing imagery. Agric For Meteorol., 136: 31–44.

Smith, M., Pereira, L.S., Beregena, J., Itier, B., Goussard, J., Ragab, R., Tollefson, L. Van Hoffwegen, P. (Eds.), 1996. Irrigation Scheduling: From Theory to Practice. FAO Water Report 8, ICID and FAO, Rome.

Stegman, E.C., Schiele, L.H., Bauer, A., 1976. Plant water stress criteria for irrigation scheduling. Trans. ASAE 19, 850–855.

Testi, L., Goldhamer, D.A., Iniesta, F. & Salinas, M. 2008. Crop Water Stress Index Is a Sensitive Water Stress Indicator in Pistachio Trees. Irrigation Science, 26: 395–405.

Thompson, R.B., Gallardo, M., Valdez, L.C., Fernandez, M.D., 2007. Using plant water status to define threshold values for irrigation management of vegetable crops using soil moisture sensors. Agricultural Water Management 88, 147–158.

Turner, N.C., 1988. Measurement of plant water status by the pressure chamber technique. Irrigation Science 9, 289–308.

Vellidis, G., Tucker, M., Perry, C., Kvien, C. Bednarz, C., 2008. A real-time wireless smart sensor array for scheduling irrigation. Computers and Electronics in Agriculture 61, 44–50.

Wanjura, D.F., Upchurch, D.R., Mahan J.R., 1992. Automated irrigation based on threshold canopy temperature. Trans. ASAE 35(1):153–159

Wanjura, D.F., Upchurch, D.R., Mahan, J.R., 1995. Control irrigation scheduling using temperature-time thresholds. Trans. ASAE 38, 403–409.

Wiedenfeld, B., 2004. Scheduling water application on drip irrigated sugarcane. Agricultural Water Management 64, 169–181.

Wang, D., Gartung, J., 2010. Infrared canopy temperature of early-ripening peach trees under postharvest deficit irrigation, Agricultural Water Management, 97(11): 1787-1794.

Zotarelli, L., Scholberg, J.M., Dukes, M.D., Mu˜noz-Carpena, R., 2009. Tomato yield, biomass accumulation, root distribution and irrigation water use efficiency on a sandy soil, as affected by nitrogen rate and irrigation scheduling. Agricultural Water Management 96, 23–34.

CHAPTER SIX

GENERAL CONCLUSIONS

In the present research, the following models were developed and validated in an apple orchard of Fuji in the Roza Farm, at the Washington State University, Irrigated Agriculture Research and Extension Center in Prosser, WA:

1- Canopy conductance (Chapter II)

Since alfalfa/grass mainly respond to net radiation, in the P-M approach a constant value of 0.6 mol m^{-2} s^{-1} is assumed for the "big leaf" stomatal conductance (Allen et al., 1998). To account for the response of apple leaves stomas to the bulk air relative humidity, in the present approach, a simple model with theoretical basis dependent merely on radiation and vapor pressure deficit was developed:

$$g_T = b_2 \left[\frac{P_a Q}{\lambda D_a}\right] + b_0 \qquad (6.40)$$

where Q is defined by the following equation:

$$Q = 0.25\left(\alpha_S S_{gl} + \alpha_S S_{t1} + 4(\alpha_L - 1)\mathrm{L_a}\right) \qquad (6.41)$$

In case of well-irrigated, young apple trees, this model only requires determination of one empirical coefficient (i.e. b_2). In the studied orchard, b_0 was zero and b_2 showed to be fairly constant with slight variations from plot to plot and from year to year.

2- Potential canopy and air temperature difference (Chapter II)

D_a has been proven to be linearly related to ΔT (Idso et al., 1981) in row crops and in Pistachio trees (Testi et al., 2008). This linear relationship was first explained by the theoretical approach of Jackson et al. (1981) where the intercept and slope of the relationship were mainly functions of g_H and R_n, and T_c, respectively. Since relative humidity affects apple leaves stomata (Rana et al., 2005; Dragoni et al., 2005), the relationship between D_a and ΔT was expected to be more complicated. The high similarity between the results from 2007 and 2008 when the trees were young and healthy confirmed the existence of a relationship between D_a and ΔT. Due to stomatal response to change in relative humidity; however, any estimations of ΔT using D_a

will be associated with high errors. It was concluded that a theoretical approach which accounts for all of the factors affecting T_c is to be developed to relate D_a to ΔT. The following equation is the result of this modeling effort:

$$\Delta T_p = \left(\frac{Q}{g_H C_P - n + \lambda g_T s}\right) - \left(\frac{g_T \lambda / P_a}{g_H C_P - n + \lambda g_T s}\right) D_a \tag{6.42}$$

where $R_n = Q + n\Delta T_m$. n is defined by the following equation:

$$n = (3\alpha_L - 4)\varepsilon_a(c)\sigma \mathbf{T}_a^3 \tag{6.43}$$

Climatic parameters and canopy conductance (g_T) were the only required inputs to the ΔT_p model. Once used to calculate the CWSI, the present NWSBL model can be used for fully automating of apple orchards. Considering the response of apple trees to the bulk air relative humidity, the advantages of the NWSBL and T_p models will be more pronounced if used in more humid areas compared to Eastern Washington.

3- Potential transpiration (Chapter II)

Eq. 6.5 relates transpiration to bulk air vapor pressure deficit (D_a) and presents a theoretical method for estimating potential transpiration of apple trees.

$$T = \frac{(1-\beta)}{\lambda} Q + \frac{\lambda g_T \beta}{P_a} D_a \tag{6.44}$$

During the 2007, 2008 and 2013 growing seasons, this transpiration model along with these IR measurements, in-field air temperature sensors, and local meteorological data from a nearby weather station were used to estimate potential transpiration of apple trees. The T_p model presented here adequately described the transpiration of apple trees under real field conditions.

4- Actual transpiration (Chapter III)

Similar to the potential transpiration model, the actual transpiration of apple trees was modeled based on the energy budget of a single leaf. It mainly relied on the difference between the thermal temperature of the canopies and air temperature, formulated in ΔT_m as an indicator of stomatal enclosure, to estimate real-time water use of the apple trees:

$$T = \left(\frac{Q}{\lambda}\right) - \left(\frac{g_H C_P - n}{\lambda}\right)\Delta T_m \tag{6.45}$$

The overall results of the experiments with Fuji apple trees showed that actual canopy transpiration can be reliably estimated by the means of infrared thermometery.

There were some sources of uncertainty in modeling light and thermal energy interceptions by apple trees. A tree canopy is comprised of unknown number of shaded and sunlit leaves, and shoot growth constantly changes light interception pattern. Apple trees have discontinuous canopies. They can have various forms of architecture and their leaves are of different shapes, sizes and orientations. Moreover, the T-model was basically derived for light interception conditions at solar noon. This introduced some errors in estimations of T when used for times other than solar noon in hourly or smaller time scales. Another approximation was introduced into the model by the temperature across the upper half of the canopy being assumed uniform and equal to the average temperature measured with the IRTs.

The sensitivity analysis showed that the T-model was fairly sensitive to wind speed measurements. In the application of the T-model, the wind speed at the surface of the tree canopies was assumed to be the same as wind speed obtained from a weather station, while this might be true the crown of apple tree canopies is not a homogeneous surface. Thus, not all of the top canopy leaves are exposed to the same wind flow. Instead of using the surface wind speed, taking an "effective depth" for the measurements (or estimations) of wind speed might be a better representative of the top leaves. Moreover, wind speeds at the center of the canopies showed to be approximately 10 times slower than those of obtained from a nearby weather station (g_H of about 3.2 times less). This means transpirations from individual leaves within a canopy are highly variable with T being much lower at the center of canopy than the crown.

Required number of IRTs is a function of variability among canopies, orientation, position and field view of IRT. The results of our experiment with perpendicularly installed sensors above apple trees showed a high variability among individual IRTs. This suggests that readings from individual IRTs cannot be trusted as the chance of the ground being seen by the sensor is high. As for the IRTs looking at canopies at 45 degree angles at the north and south sides, a pair of sensors seemed to have enough resolution. In case of high variability among the trees, average of several pairs of IRTs can provide a better average of orchard transpiration.

In general, the differences between weather station and field measurements were big enough to conclude that measurements from a nearby weather station are not a feasible alternative for within-orchard measurements. The errors were the highest at solar noon and minimum when daily mean values were used to estimate T. Except for the wind speed measurements, no significant difference was seen between the measurements taken within the canopies and in the vicinity of the canopies (within-orchard). Air temperature measurements showed the highest variability among different locations at all time scales.

In the 2013 growing season, seven irrigation methods were tested in a orchard of Fuji apple trees. The crop water use of plots irrigated using CWSI and TTT was also compared with those of irrigated using the scientific-based irrigation method of neutron probe and crop ET estimated using the P-M model corrected by crop coefficient. The CWSI algorithm drastically decreased early season over-irrigation, yielded a lot less false irrigation signals on cloudy, humid, cold days and adapted to changing conditions of apple trees (i.e. shoot and fruit growth). In addition, the theoretical CWSI was highly correlated to midday Ψ_{stem}. The CWSI irrigation algorithm introduced here avoided over-irrigation at the beginning of the growing season because no irrigation was scheduled on the cold days of early season and/or when the CWSI had a decreasing trend. The adaptive nature of the algorithm through the use of a dynamic lower, non-stressed boundary allowed for following the real-time water demand of the trees avoiding wrong stress signals caused by wind effect, shoot growth etc. It was minimally sensitive to different sources of error including temporary atmospheric conditions (i.e. dust, passing clouds etc), IR sensor installation and measurement errors, apple tree architecture and model errors. While the CWSI was developed for apple trees the adaptive control algorithm is independent of crop or irrigation method.

Significant Findings

- Infrared thermometry can be used for estimating real-time water use of apple trees.
- Readings from individual IRTs installed perpendicularly above canopies cannot be trusted as the chance of the ground being seen by the sensor is high. As for the IRTs looking at canopies at 45 degree angles at the north and south sides, a pair of sensors seemed to have enough resolution. In case of high variability among the trees, average of several pairs of IRTs can provide a better average of orchard transpiration.
- Canopy temperature correlates very well with trunk surface temperature on a daily scale. Measurements of trunk surface temperature can be an alternative to canopy temperature monitoring and a promising method for automation of irrigation in apple trees.
- Maximum transpiration of apple trees occurred in the morning.

While this is an initial step toward implementing variable rate irrigation practices on apple trees, it has the potential to improve water use efficiency, which leads to increased production, reduced production costs, reduced pumping energy requirements, and improved quality.

CHAPTER SEVEN

SUGGESTIONS FOR FUTURE STUDIES

In 2013, the average stomatal conductance was maintained low by the trees in response to low fruit loads which resulted in the empirical coefficients being different than the rest of the years. This has to be accounted for in estimations of transpiration at post-harvest times because reduction in crop loads can decrease the stomatal conductance and consequently transpiration of apple trees (Auzmendi et al., 2011; Girona et al., 2011). To formulate this phenomenon, in future studies the relationship between the conductance and apple fruit loads needs to be established.

The proposed T-model can provide a basis for a fully automated system of irrigating apple orchards as real-time water use can be computed in any time scale. Precision irrigation scheduling of small areas within larger fields or even individual trees is another possibility. There may also be a hope for replacing IRT sensors with satellite IR pictures for estimating transpiration of larger orchards. The conventional use of crop coefficient and reference ET can be then replaced by the present approach.

Although the overall performance of the T-model was satisfactory, net radiation (daylight average) estimations on some days were sometimes small negative values close to zero, while net radiation is expected to be positive during the daytime (Allen et al., 1998). A source of error was the simplicity of the approach used here to calculate cloud cover and sky emissivity. If better accuracy is desired more advanced approaches for estimating incoming longwave radiation can be adapted from Flerchinger et al. (2009).

Tree trunk is relatively big component of the foliage which was expected to be in balance with average canopy temperature. Thermal measurements revealed small difference between tree trunk surface temperature in terms of average and amplitude suggesting it as an alternative for canopy temperature measurements. Monitoring trunk temperature can decrease the chance of including longwave radiation from the ground to zero as a horizontally mounted IRT with a very narrow field of view can be used.

In the current study, the treatments were compared just based on the irrigation water applied and crop water use. In future studies, the treatments can be compared based on decreased water and labor costs, decreased losses of water and nutrients to deep percolation as well. Other suggestions can be summarized as the following:

- One interesting finding of this study was that the peak transpiration in apple trees occurred in the morning rather than the solar noon which was in agreement with previous studies. In order to detect water stress, it is suggested that apple trees be monitored during morning hours.
- The main focus of this research was well-watered, non-stressed apple trees. In future studies, it might be a good idea to investigate the applicability of developed models in apple trees under water deficit.
- Here we compared our transpiration models (i.e. T and T_p) against the P-M model (i.e. ET_r and ET_c). The performance of the models and their components can be further investigated using lysimeter (Auzmendi et al., 2011) or sap flow measurements (Dragoni et al., 2005; Nicolasa et al., 2005).
- Based on the results of the present study, it is recommended that air and canopy temperatures be measured in the same spot. All of the other required meteorological parameters can be obtained from a nearby weather station.

APPENDIX A: HARDWARE SETUP IN THE FIELD

Figure A.1 Different hardware components of the irrigation control system.

Figure A.2 The USB modems (USB Modem, DataJack, Inc.) were employed to access the central control computer in the field. A 3G model was first used; however, after it stopped working it was replaced with a 4G model by the company. Due to the sensitivity of the modems to high temperatures a cooling system (fan) was added to the set.

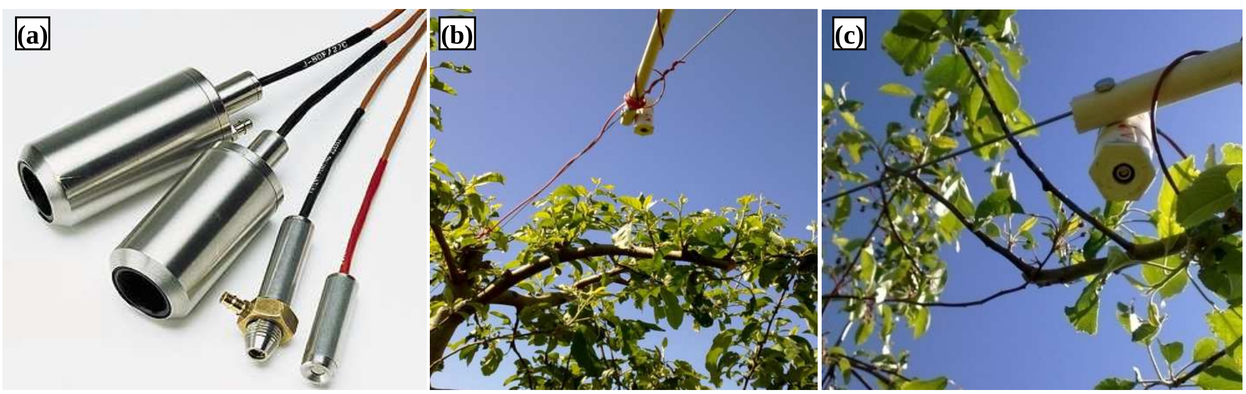

Figure A.3 IRTs used to remotely measure leaf temperature (a). Sensor setup in the field (b) and c) in-line with tree rows. IRT sensors were shielded by PVC pipes from radiation. Later on the IRT sensors were also wrapped in aluminum foil.

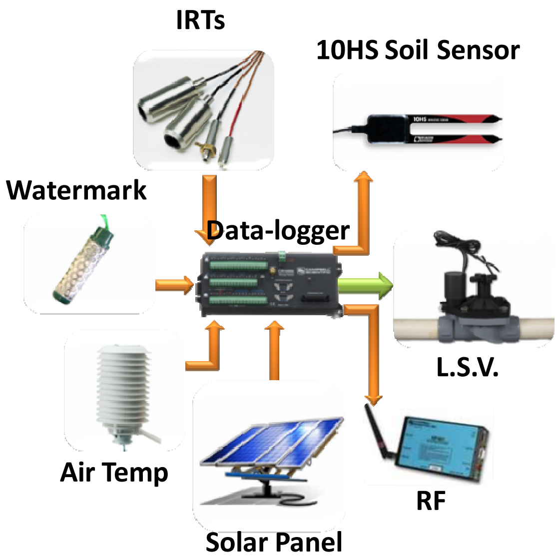

Figure A.4 A typical wireless node, hooked-up sensors and central control computer.

APPENDIX B: GRAPHICAL USER INTERFACE

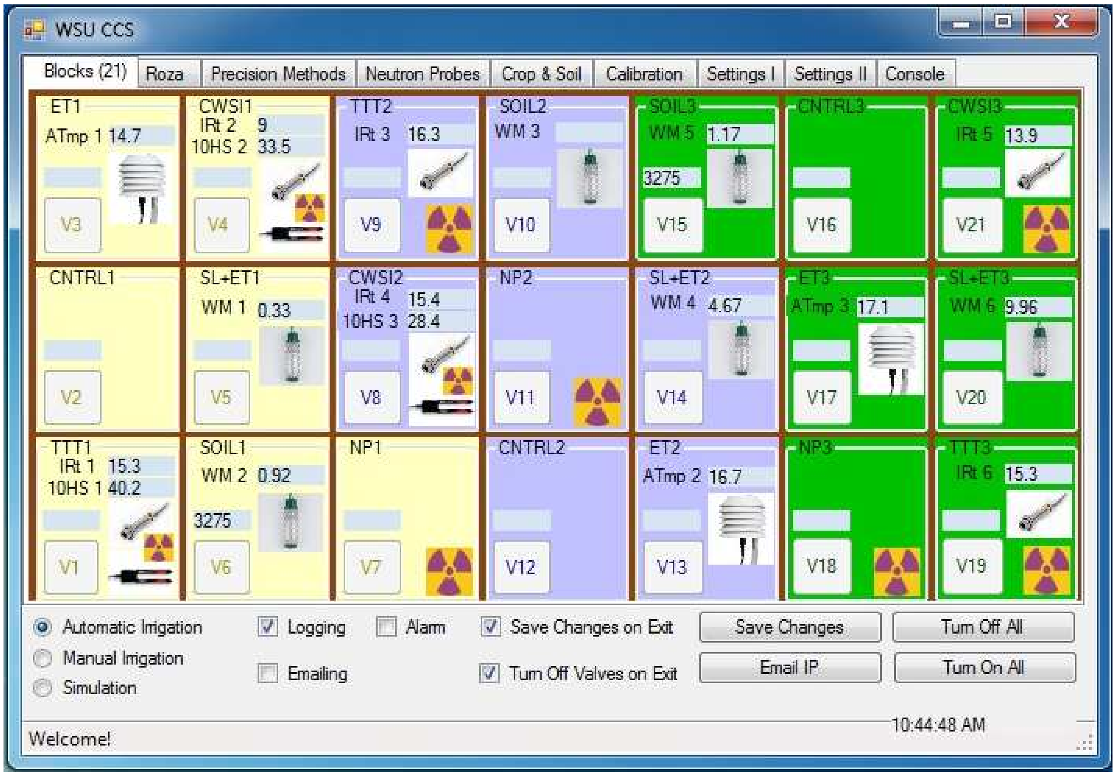

Figure A.5 "Blocks" tab of the Graphical user interface.

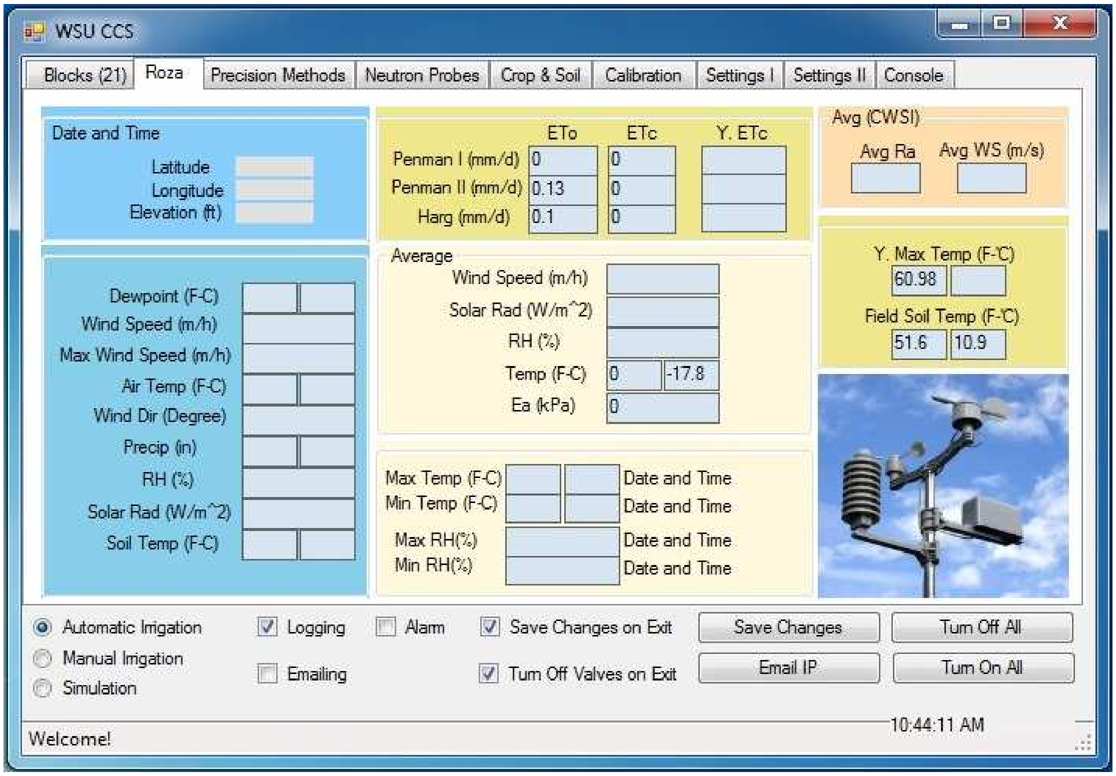

Figure A.6 "Weather station (Roza)" tab of the Graphical user interface.

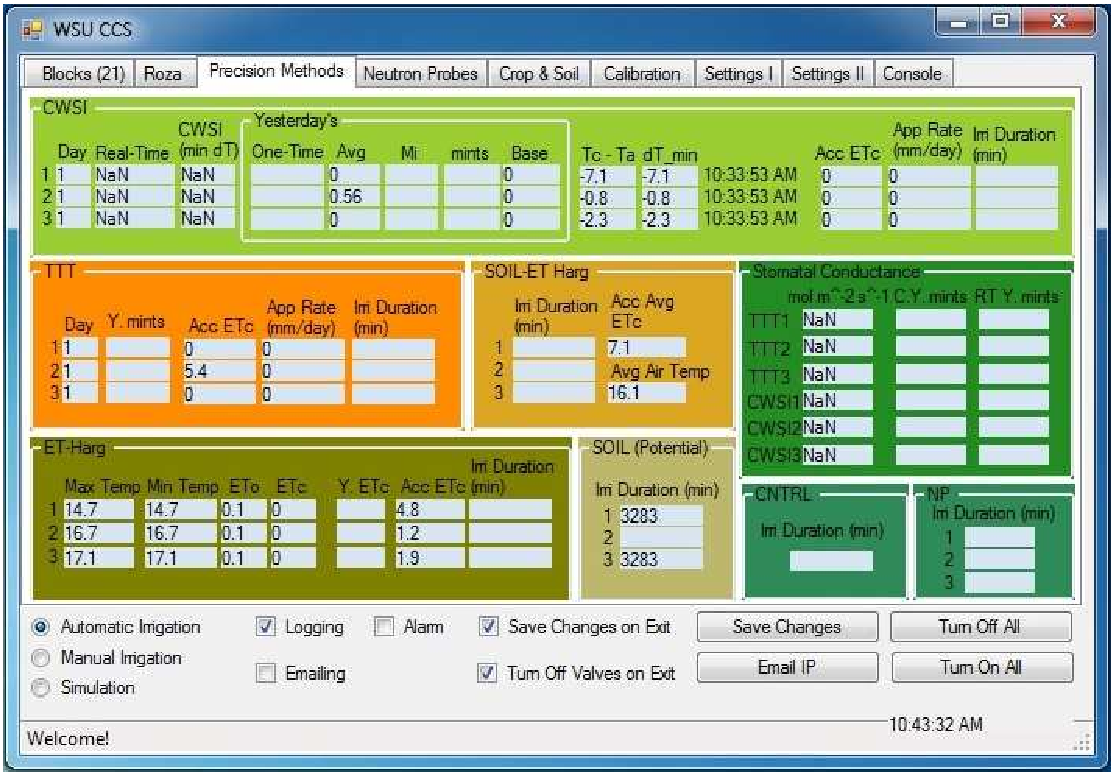

Figure A.7 "Precision Methods" tab of the Graphical user interface.

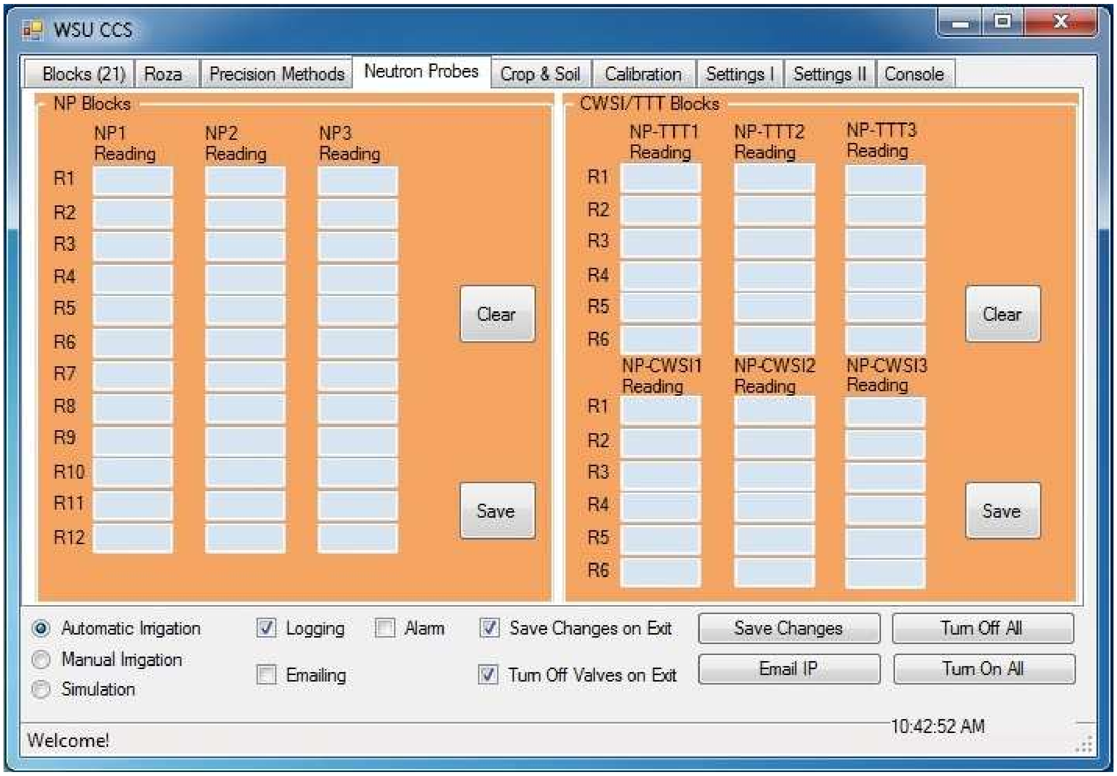

Figure A.8 "Neutron Probes" tab of the Graphical user interface.

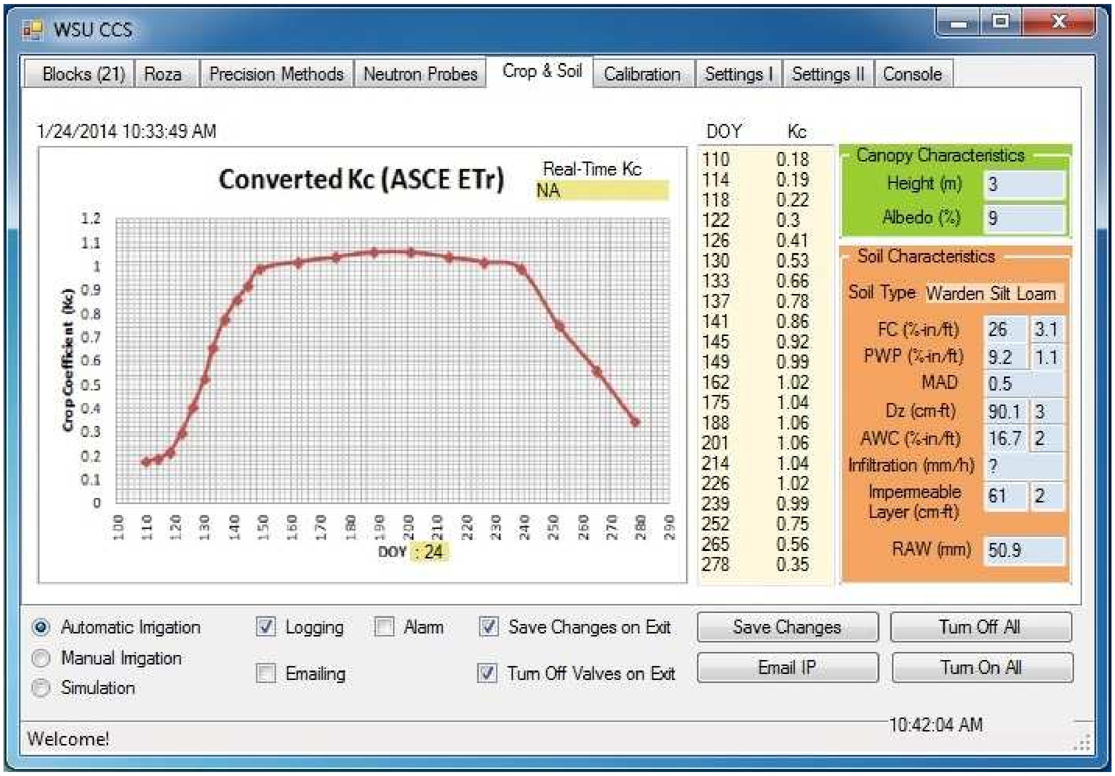

Figure A.9 "Neutron Probes" tab of the Graphical user interface.

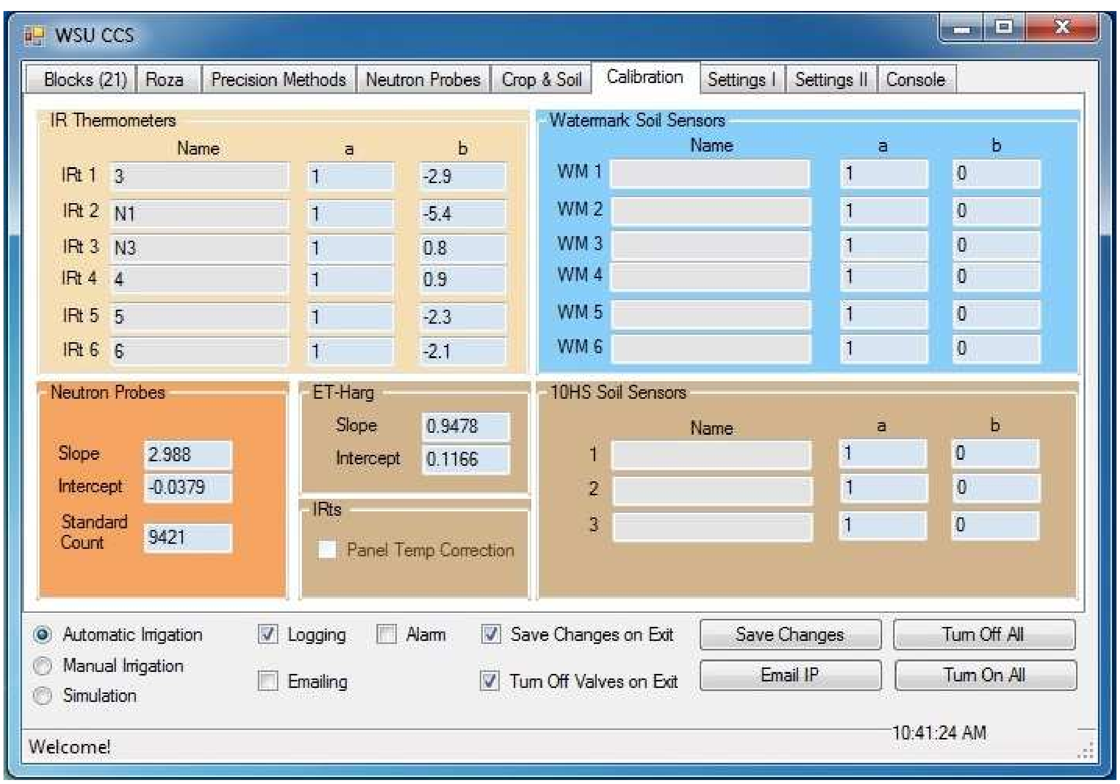

Figure A.10 "Calibration" tab of the Graphical user interface.

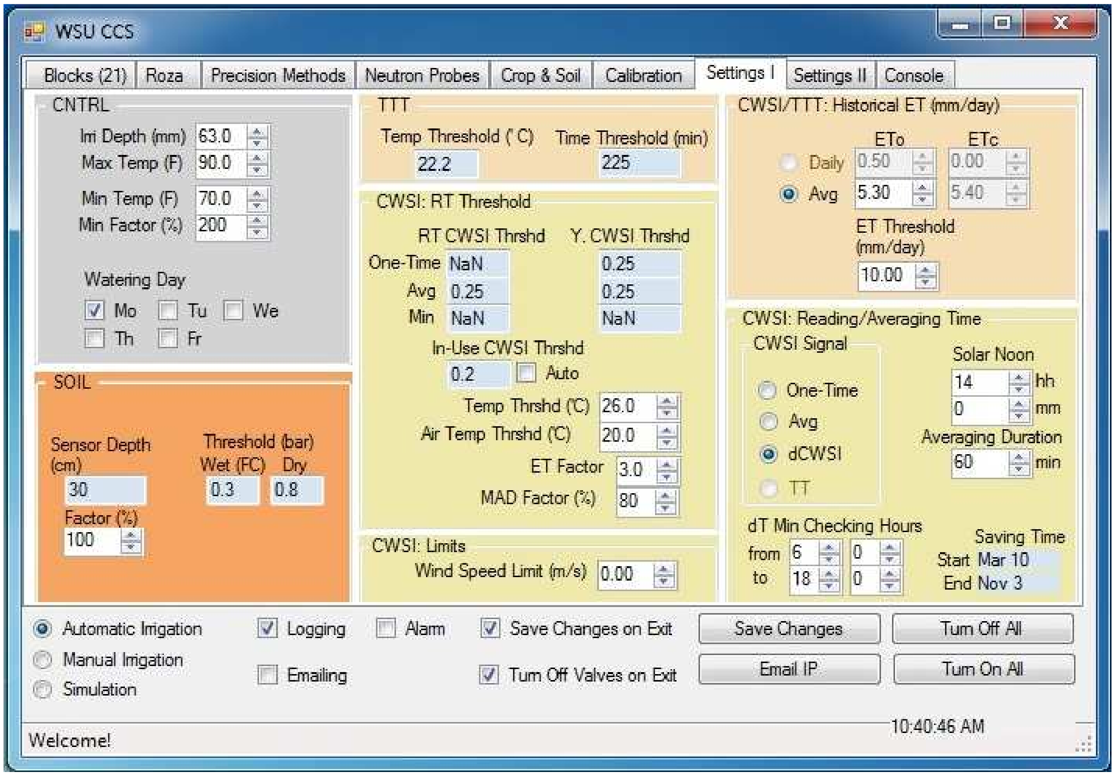

Figure A.11 "Settings I" tab of the Graphical user interface.

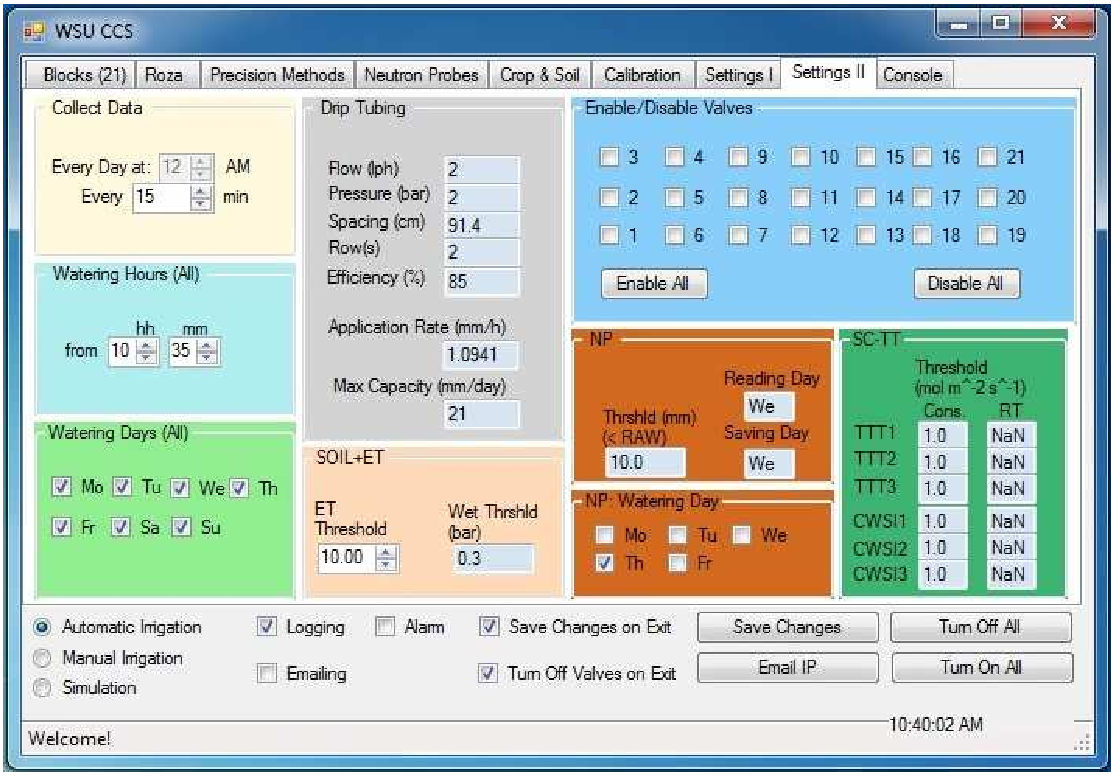

Figure A.12 "Settings II" tab of the Graphical user interface.

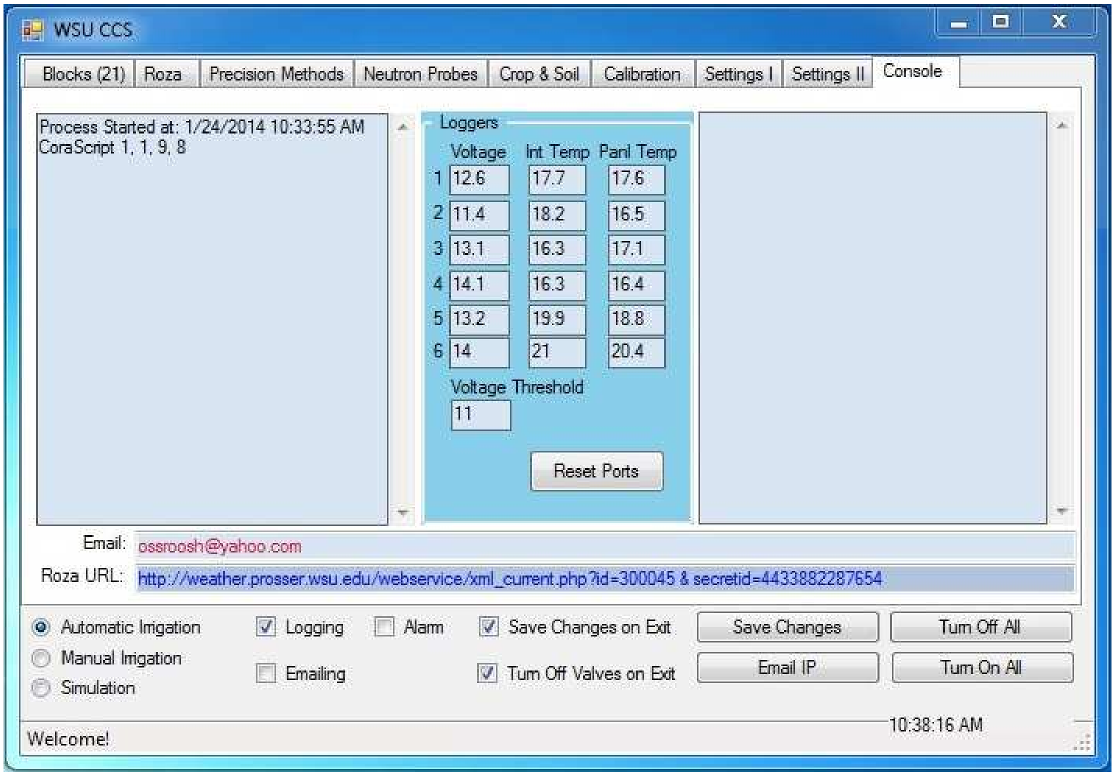

Figure A.13 "Console" tab of the Graphical user interface.

APPENDIX C: SENSOR READINGS

Soil water content (10HS sensors)

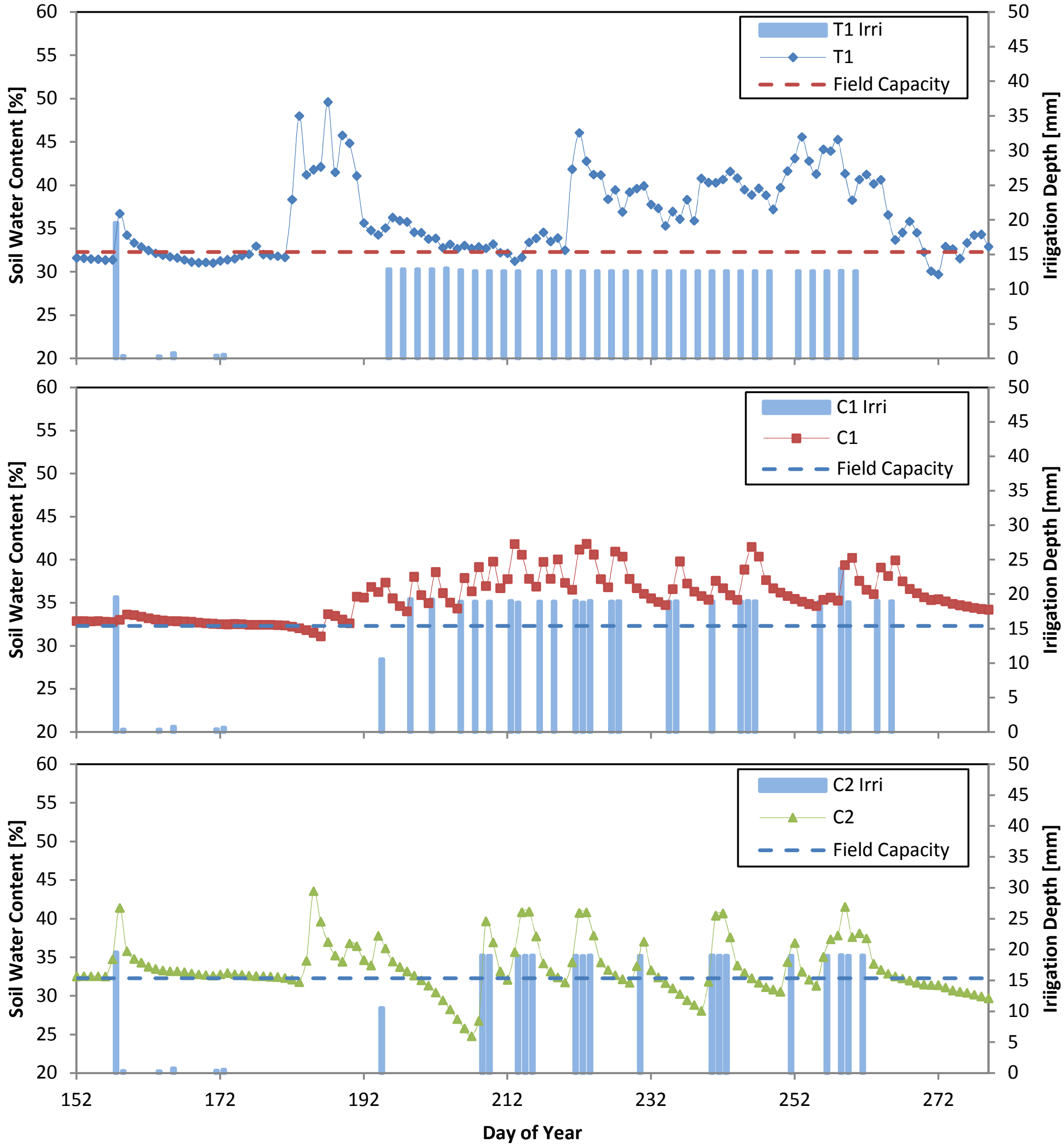

Figure A.14 Plots of soil moisture data collected using the 10HS soil moisture sensors (Decagon Devices Inc., Pullman, WA).

Soil water potential (SL+ET treatment)

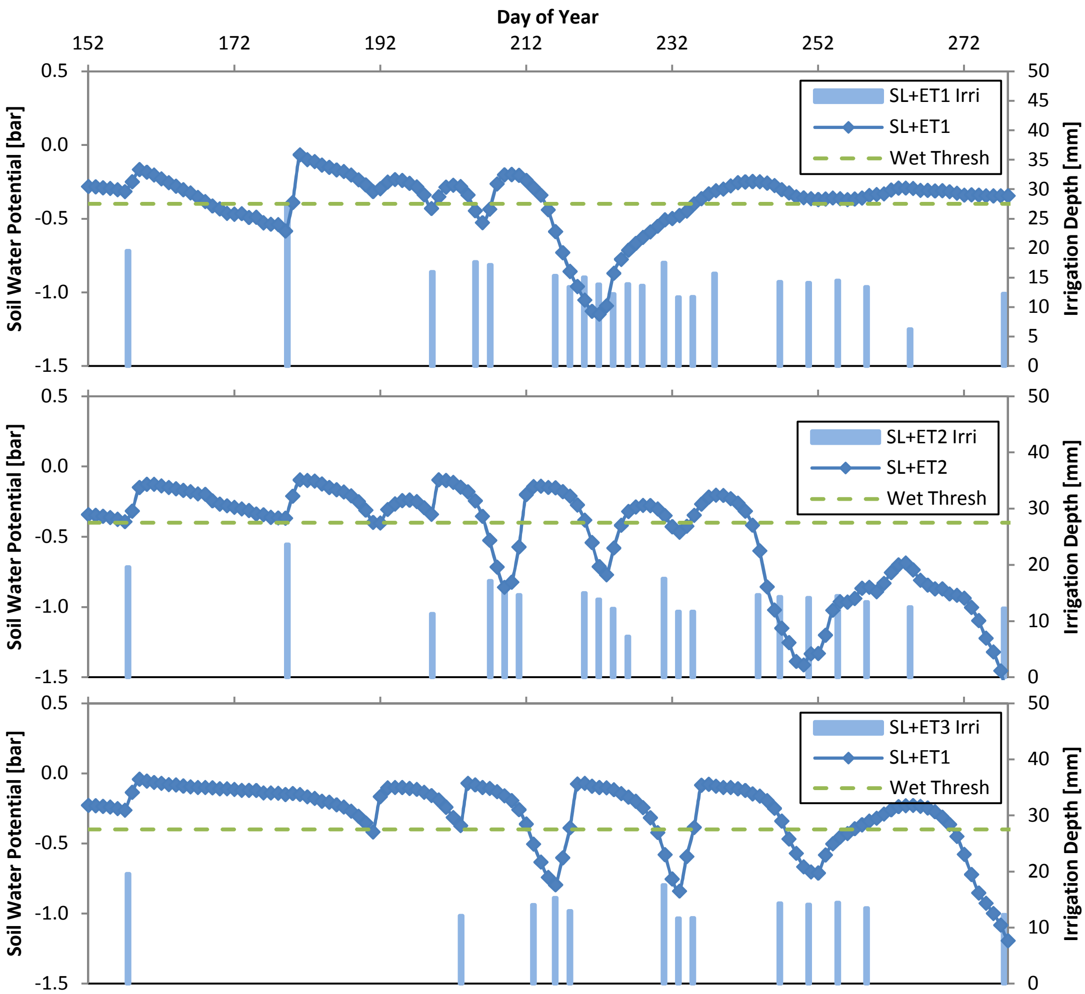

Figure A.15 Plots of soil water potential collected at three plots ("SL+ET" treatment) using Watermark sensors.

Soil water potential (SOIL treatment)

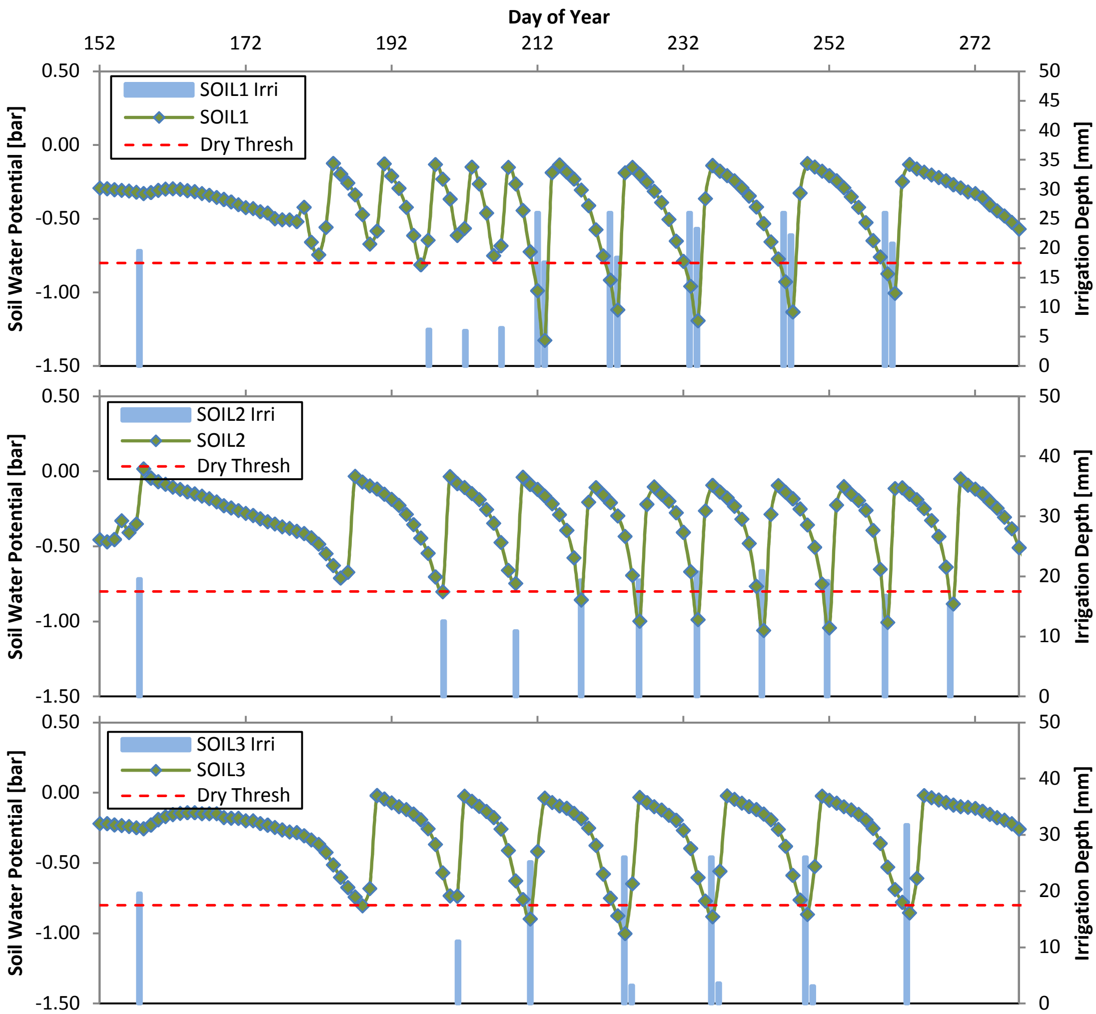

Figure A.16 Plots of soil water potential monitored at three plots (Treatment "SOIL") using Watermark sensors.

APPENDIX D: ALGORITHMS

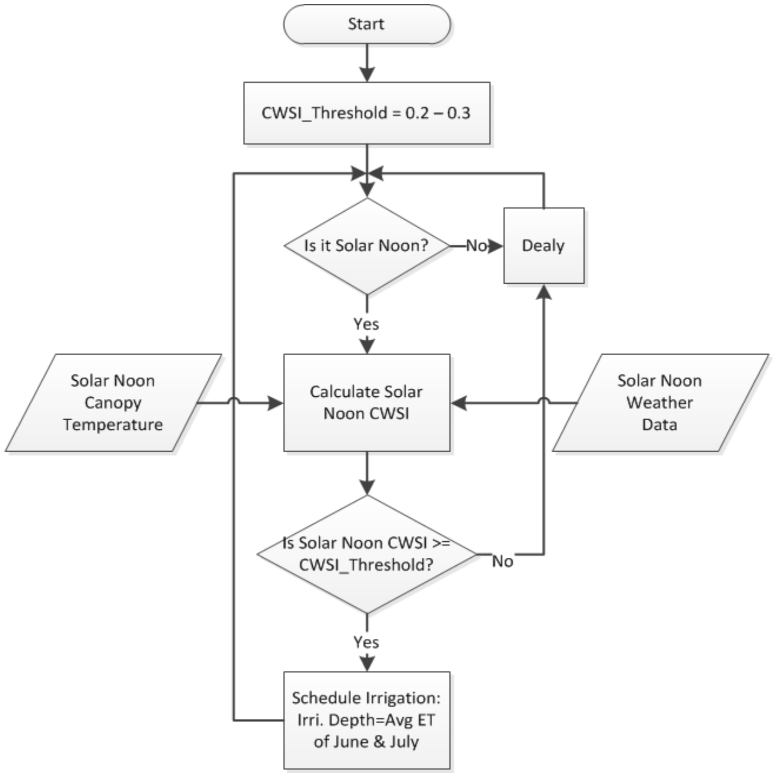

Figure A.17 Conventional CWSI algorithm.

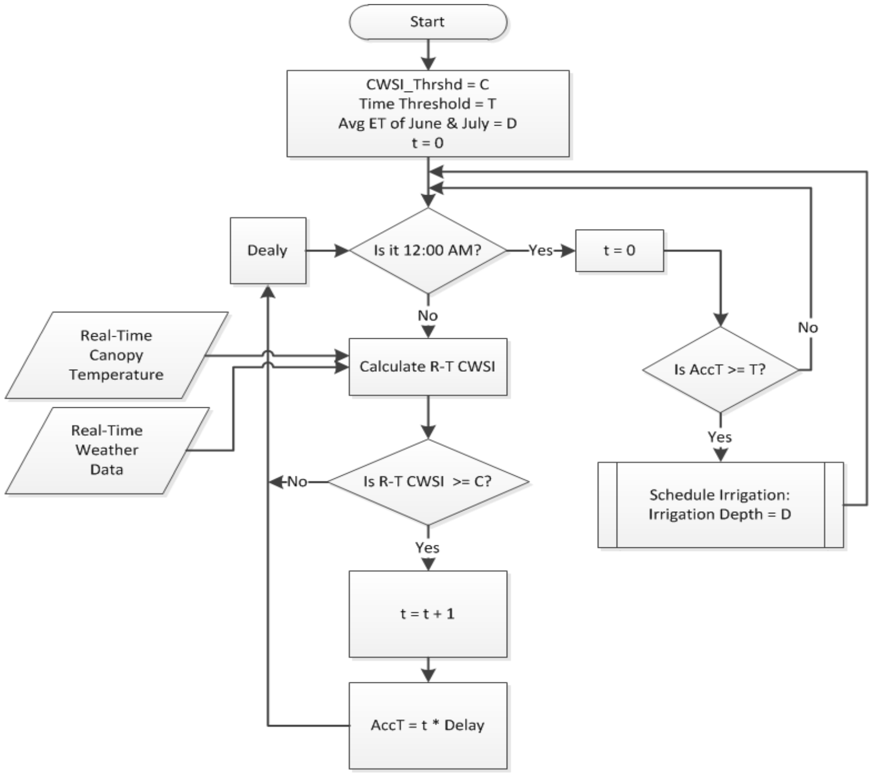

Figure A.18 CWSI-TT algorithm developed by O'Shaughnessy et al. (2012).

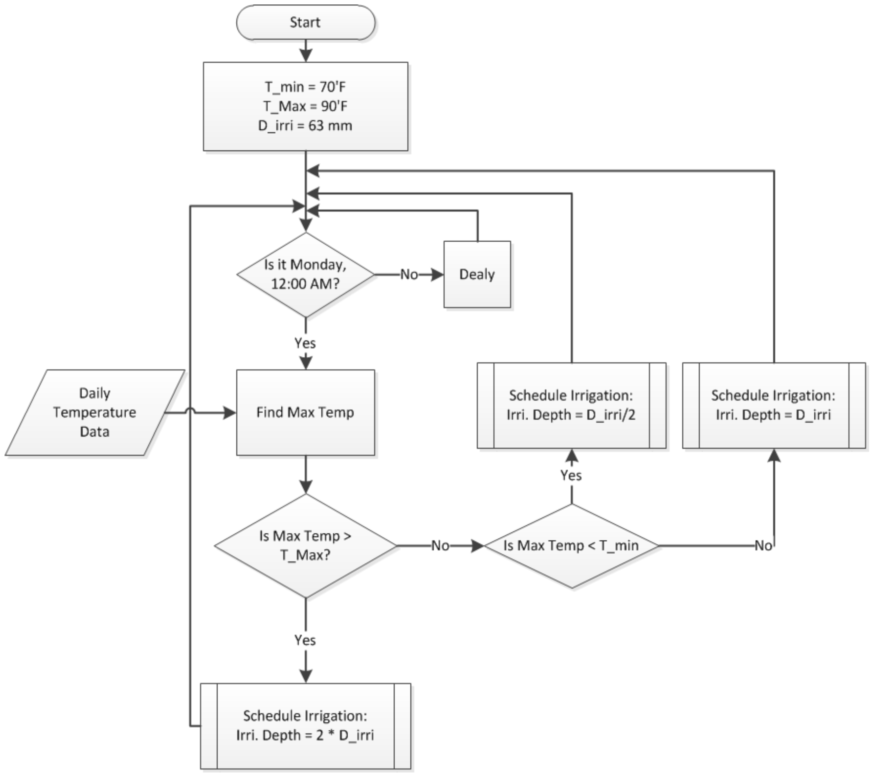

Figure A.19 Traditional irrigation scheduling algorithm (CNTRL).

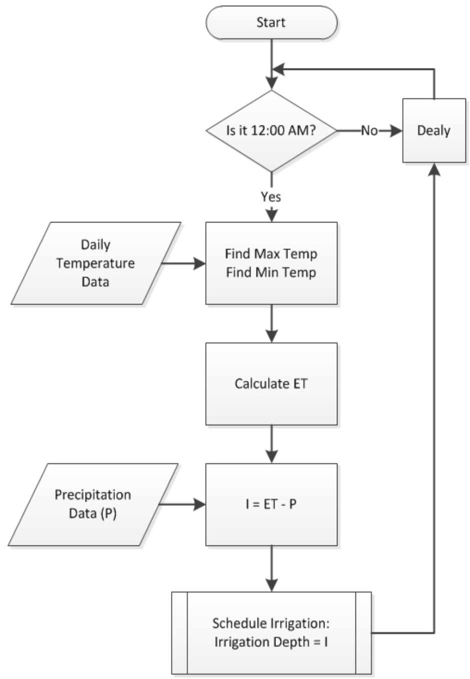

Figure A.20 Temperature-based ET control.

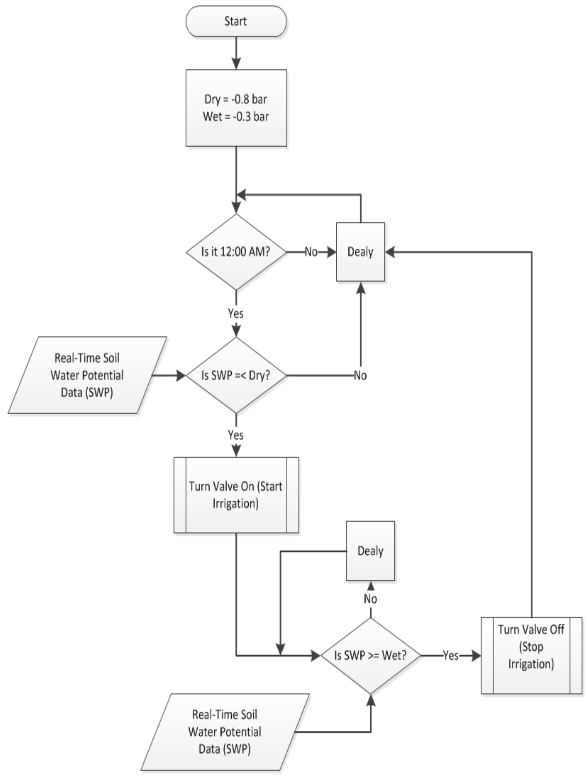

Figure A.21 Soil moisture-based irrigation scheduling algorithm (SOIL).

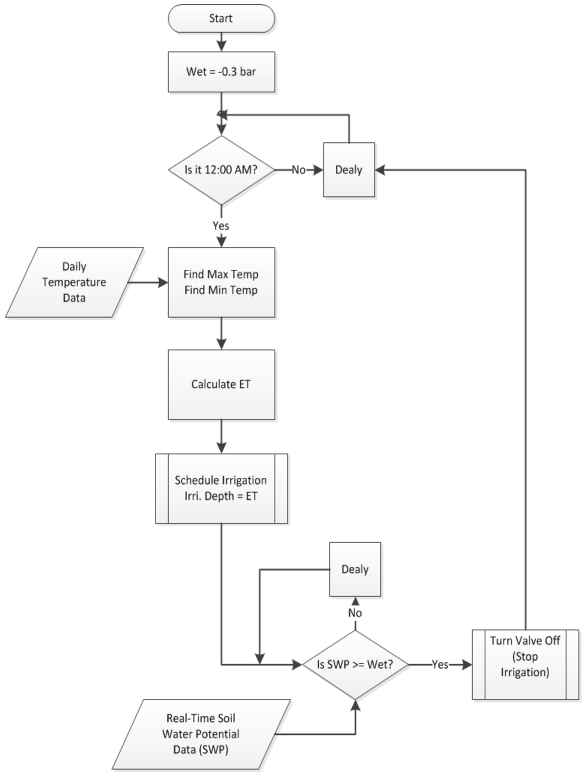

Figure A.22 Combined soil moisture and ET irrigation scheduling algorithm (SL+ET).

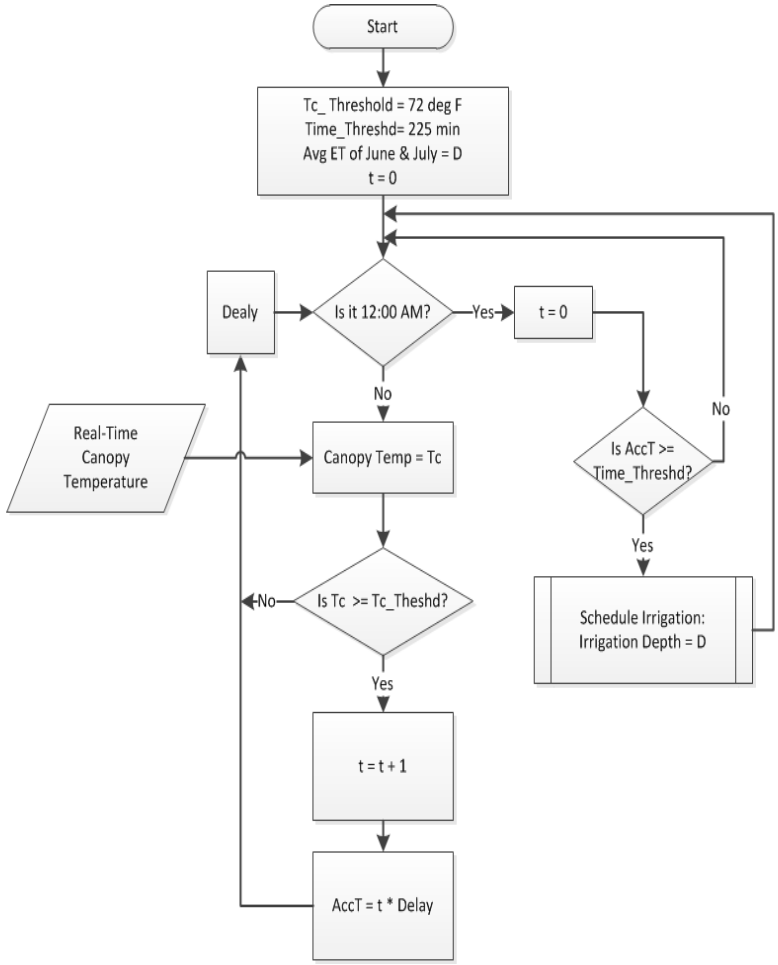

Figure A.23 Time-temperature-threshold irrigation scheduling algorithm (TTT)